TÜRKİYE VE DÜNYADA MATEMATİK

Editör: Prof.Dr. Zehra YÜCEDAĞ

yaz
yayınları

Türkiye ve Dünyada Matematik

Editör

Prof.Dr. Zehra YÜCEDAĞ

yaz yayınları

2025

yaz yayınları

Türkiye ve Dünyada Matematik

Editör: Prof.Dr. Zehra YÜCEDAĞ

E_ISBN 978-625-8678-16-1

Aralık 2025 – Afyonkarahisar

Dizgi/Mizanpaj: YAZ Yayınları

Kapak Tasarım: YAZ Yayınları

YAZ Yayınları. Yayıncı Sertifika No: 73086

M.İhtisas OSB Mah. 4A Cad. No:3/3
İscehisar/AFYONKARAHİSAR

www.yazyayinlari.com

yazyayinlari@gmail.com

İÇİNDEKİLER

NULL MAGNETIC CURVES ON 3D SEMI-RIEMANNIAN MANIFOLDS IN THE CONTEXT OF KILLING VECTOR FIELDS

Fatma ALMAZ[1]

1. INTRODUCTION

3-dimensional semi-Riemannian geometry, a broad branch of differential geometry, arises by relaxing the requirement that the metric tensor be positive definite. This plays a vital role in modeling physical systems, particularly the space-time geometry of general relativity. Unlike classical Riemannian geometry, vectors on semi-Riemannian manifolds can have space-like, time-like, or null (light-like) characteristics, significantly affecting the internal structure of the manifold and the dynamics on it.

This study focuses on the study of null magnetic curves on a 3-dimensional semi-Riemannian manifold defined by an adapted frame consisting of two null vectors and a time-like vector. This particular choice of frame allows for a more in-depth analysis of the specific metric and topological properties of space. Magnetic curves are non-geodesic curves that represent the motion of a charged particle placed in a magnetic field and are derived from the Lorentz force equations. A null curve means that the norm of its tangent vector is zero, suggesting that these curves have a character similar to the trajectories of massless particles moving at the speed of light.

[1] Assist. Prof. Dr, Batman University, Faculty of Arts and Sciences, Department of Mathematics, ORCID: 0000-0002-1060-7813.

Null magnetic curves are of great interest in both differential geometry and theoretical physics, particularly in understanding high-energy astrophysical phenomena and cosmological models. The study of such curves illuminates the behaviour of the Lorentz force equations in degenerate metric spaces and also provides important information on how magnetic fields interact with the curvature of spacetime. This introductory section will discuss the theoretical basis of null magnetic curves, the importance of the frenet frame structure in 3-dimensional semi-Riemannian space, and the fundamental concepts necessary for characterizing these curves. The ultimate goal is to develop new insights into the dynamics of these complex systems by elucidating the existence of these special curves, their geometric properties, and their relationship to the structure of the magnetic field.

Studies on magnetic curves in Lightike cone space have been done by the authors in references (Almaz & Kulahci, 2018, 2020, 2021). Some mathematical results have been obtained by the authors in reference (Drut-Romaniuc & Munteano, 2011) on magnetic curves corresponding to killing magnetic fields, some results on contact magnetic flow in 3D Sasakian manifolds and magnetic vortex filament flows are given in references ((Barros & Romero, 2007), (Cabrerizo & Gomez, 2009)).

2. PRELIMINARIES

Let (M^3, g) be a real $3D$ semi-Riemannian manifold of index $q = 1$ and for a smooth null curve $\gamma(t) = \left(x^0(t), x^1(t), x^2(t)\right)$; $t \in I \subset \mathbb{R}$ in M^3 the tangent vector field of γ satisfies

$$\zeta = \frac{d\gamma}{dt} = (\frac{dx^0}{dt}, \frac{dx^1}{dt}, \frac{dx^2}{dt}); g(\zeta, \zeta) = 0; g_{ij} \frac{dx^i}{dt} \frac{dx^j}{dt} = 0,$$

where $g_{ij} = g(\partial_i, \partial_j)$ and $i, j \in \{0,1,2\}$. $T\gamma$ is the tangent bundle of γ and $T\gamma$ is defined as follows (see (O'Neill, 1983))

$$T\gamma^{\perp} = \cup_{P\in\gamma} T_P\gamma^{\perp}; T_P\gamma^{\perp} = \{P \in T_PM : g(W_P, \zeta_P) = 0\},$$

where ζ_P is null vector tangent of γ at any $P \in \gamma(t)$, $T\gamma^{\perp}$ is a vector bundle of γ of rank 2. Hence, the tangent bundle $T\gamma$ is a vector subbundle of $T\gamma^{\perp}$, of rank 1 and this implies that $T\gamma^{\perp}$ is not complementary to $T\gamma$ in $TM|_{\gamma}$, according to the classical non-degeneracy theory, there must be a vector bundle complementary to $T\gamma$ in the TM, this bundle will play the role of the normal bundle $T\gamma^{\perp}$.

Theorem 1. Let γ be a null curve of a semi-Riemannian manifold (M, g) and S(Tγ$^{\perp}$) a screen vector bundle of γ. Then, there exists a unique vector bundle E of rank 1 of the curve γ, such that over each coordinate neighbourhood V ⊂ γ, there exists a unique partition N ∈ Γ(E$|_{V}$) satisfying the following equation

$$g(\frac{d\gamma}{dt}, N) = 1, g(N, N) = g(N, X) = 0, \forall X \in \Gamma(S(T\gamma^{\perp})|_V, \quad (2.2)$$

for the null transversal bundles E and N of γ and $\left\{\frac{d\gamma}{dt}, N\right\}$ is a null basis of $\Gamma((T\gamma \oplus E)|_V)$, which is

$$TM|_{\gamma} = (T\gamma \oplus E) \perp S(T\gamma^{\perp}),$$

((Duggal & Bejancu, 1996), (O'Neill, 1983)).

Let γ be a null curve of an $3D$ semi-Riemannian manifold (M^2, g) of index 2 and N be the null vector field. For $\frac{d\gamma}{dt} = \zeta$ and the Levi-Civita connection ∇ on M^2, and from $g(\zeta, \zeta) = 0$ and $g(\zeta, N) = 1$ one has $g(\nabla_{\zeta}\zeta, \zeta) = 0$, $g(\nabla_{\zeta}\zeta, N) = -g(\zeta, \nabla_{\zeta}N) = h$, where h is a smooth function. The null Frenet equations are written as

$$\nabla_\zeta \zeta = h\zeta + k_1 W$$

$$\nabla_\zeta N = -hN + k_2 W \tag{2.1}$$

$$\nabla_\zeta W = k_2 \zeta + k_1 N,$$

where $\{h, k_1, k_2\}$ are curvature functions of γ, $W \in \Gamma(S(T\gamma^\perp))$ and $g(W, W) = -1$. Then, for screen vector bundle $S(T\gamma^\perp)$, Frenet frame on M along γ can be written as $\{\zeta, N, W\}$, ((Graves & Nomizu, 1978), (Ikawa, 1985)).

The Lorentz force of magnetic field F on M is described to be a skew symetric operator Φ given by

$$g(\Phi(X), Y) = F(X, Y), \forall X, Y \in \varkappa(M) \tag{2.2}$$

and the mixed product of the vector fields İs given as

$$g(X \times Y, Z) = dv_g(X, Y, Z), \forall X, Y, Z \in \varkappa(M). \tag{2.3}$$

The magnetic trajectories of F are curves γ on M^3 which satisfy the Lorentz equation

$$\nabla_\zeta \zeta = \Phi(\zeta). \tag{2.4}$$

Let F be a Killing vector field on M^3 which is $F_v = \iota_v dv_g$, where ι is denoted the inner product. In this context, the Lorentz force of the F_v is given as

$$\Phi(X) = \mathrm{F} \times X \tag{2.5}$$

and Lorentz force equation is defined as

$$\nabla_\zeta \zeta = \mathrm{F} \times \zeta. \tag{2.6}$$

Proposition 1. Let γ be a curve in a 3D semi Riemannian Manifold and F be a vector field along the curve γ. The, for a variation of a in the direction of F, a map $\Gamma: \mathrm{I} \times (-\varepsilon, \varepsilon) \to \mathrm{M}$

which satisfies

$$\Gamma(s,0)=\gamma(s),\left(\frac{\partial\Gamma}{\partial s}(s,t)\right)=F(s). \tag{2.7}$$

Then, for the curvature function $\kappa(s,t)$ of the γ, the following expressions are provided

$$F(v)=\left(\frac{\partial v}{\partial t}(s,t)\right)_{t=0}=g(\nabla_{\zeta}F,\zeta)v \tag{2.8}$$

$$F(\kappa)=\left(\frac{\partial\kappa}{\partial t}(s,t)\right)_{t=0}=g\left(\nabla_{\zeta}^{2}F,N\right)-2\kappa g\left(\nabla_{\zeta}F,\zeta\right)+g(R(F,\zeta)\zeta,N) \tag{2.9}$$

where

$$v(s,t)=\left\|\frac{\partial\Gamma}{\partial s}(s,t)\right\|, \tag{2.10}$$

(Barros, Cabrerizo & Gomez, 2009).

Proposition 2. Let $F(s)$ be the restriction to γ of a Killing vector field. In this case, the following expression for F is satisfied

$$F(v)=F(\kappa)=0, \tag{2.11}$$

(Barros, Cabrerizo & Gomez, 2009).

3. THE NULL MAGNETIC CURVES IN 3D SEMI-RIEMANNIAN MANIFOLD

In this section, by consider the null magnetic curves whose Frenet frame is made up of two null vectors ζ and N, W is timelike vector. and some characterizations of the null helices are expressed according to the null frenet frame in $3D$ semi-Riemannian nanifold of index 2.

The following theorems were tried to be expressed.

Definition 1. Let γ be a null curve in 3D semi-Riemannian Manifold and with the Frenet apparatus $\{\zeta, N, W, h, k_1, k_2\}$ and let F be a magnetic vector field along null curve γ on M_2^3. If the Lorentz force equation given below, expressed for null N-magnetic vector field γ, the null curve γ is called an N-magnetic curve, is satisfied

$$\nabla_\zeta N = \Phi_N(N) = F_N \times N. \tag{3.1}$$

Theorem 2. Let γ be a null N-magnetic curve in 3D semi-Riemannian Manifold and with the Frenet apparatus $\{\zeta, N, W, h, k_1, k_2\}$. Then, the Lorentz force in the Frenet frame is given as

$$\begin{bmatrix} \Phi_N(\zeta) \\ \Phi_N(N) \\ \Phi_N(W) \end{bmatrix} = \begin{bmatrix} h & 0 & -\Theta_1 \\ 0 & -h & -k_2 \\ k_2 & \Theta_1 & 0 \end{bmatrix} \begin{bmatrix} \zeta \\ N \\ W \end{bmatrix}, \tag{3.2}$$

where $\Theta_1 = g(\Phi_N(W), \zeta)$.

Proof. Let γ be a null N-magnetic curve in (M_2^3, g) with the Frenet apparatus $\{\zeta, N, W, h, k_1, k_2\}$. Then,

$$\Phi_N(\zeta) = \lambda_1\zeta + \lambda_2 N + \lambda_3 W$$

and from (3.1) and (2.2), one gets

$$\lambda_1 = g(\Phi_N(\zeta), N) = F(\zeta, N) = -F(N, \zeta) = -g(\Phi(N), \zeta) = h$$

$$\lambda_2 = g(\Phi_N(\zeta), \zeta) = 0$$

$$\lambda_3 = -g(\Phi_N(\zeta), W) = -\Theta_1.$$

Thus, one writes

$$\Phi_N(\zeta) = h\zeta - \Theta_1 W.$$

Similarly, the Lorentz force functions $\Phi_N(N)$ and $\Phi_N(W)$ can be calculated that

$$\Phi_N(N) = -hN - k_2 W; \Phi_N(W) = k_2\zeta + \Theta_1 N.$$

Theorem 3. Let γ be null N-magnetic trajectory of a magnetic field F_N in 3D semi-Riemannian Manifold with the Frenet apparatus $\{\zeta, N, W, h, k_1, k_2\}$ if and only if F_N is satisfied

$$F_N(s) = \frac{c(s)}{h(s)}(-k_2(s)\zeta(s) + \Theta_1(s)N(s) + h(s)W(s)). \quad (3.3)$$

Proof. Let γ be null N-magnetic trajectory of a magnetic field F_N. In a 3D semi-Riemannian manifold, the vector product of two time-like vectors usually produces a space-like vector that is orthogonal to both time-like vectors with respect to the metric tensor. If null vectors are linearly dependent, their vector product yields the zero vector. If null vectors are linearly independent, their vector product generally produces a space-like vector. This resulting vector is orthogonal to both null vectors with respect to the metric tensor. Let's prove the theorem using the case of linear dependence. Then, by using (2.5) and theorem 2, from $F_N = a\zeta + bN + cW$, where $a, b, c \in C^\infty$ one obtains

$$F_N = \frac{c}{h}(-k_2\zeta + \Theta_1 N + hW),$$

where

$$h\zeta - \Theta_1 W = cN_1;\ -hN - k_2 W = cN_2;$$
$$k_2\zeta + \Theta_1 N = -aN_1 - bN_2, \quad (3.4)$$

where N_1, N_2 are spacelike vector fields.

Theorem 4. Let F_N be a Killing vector field 3D semi-Riemannian Manifold with the Frenet apparatus $\{\zeta, N, W, h, k_1, k_2\}$ for the null N −magnetic curve γ. Then, the following equations are satisfied for the given null N −magnetic curve

$$\Theta_1 = \frac{-h}{c(s)} e^{\int h ds} \left\{ \int c(s) k_1 e^{\int h ds} ds \right\},$$

$$-((fk_2)')' - (fk_2)'h + ((fh)' - fk_1k_2 + fk_2\Theta_1) = 0,$$

where $f = \frac{c}{h}, c \in C^{\infty}$.

Proof. For a null magnetic vector field F_N in (M^3, g), from (3.3) and by differentiating of (3.3) with respect to parameter s, one gets

$$\nabla_{\zeta} F_N = (-f'k_2 + fl_1)\zeta + (f'\Theta_1 + fl_2)N + (f'h + fl_3)W, \quad (3.5)$$

where

$$f = \frac{c}{h}; l_1 = -k_2'; l_2 = \Theta_1' - h\Theta_1 + hk_1;$$
$$l_3 = -k_1k_2 + k_2\Theta_1 + h'. \quad (3.6)$$

By differentiating of (3.5) with respect to s and from (2.1), one gets

$$\nabla_{\zeta}^2 F_N = \begin{pmatrix} m_1' + m_1 h \\ +m_3 k_2 \end{pmatrix} \zeta + \begin{pmatrix} m_2' - m_2 h \\ +m_3 k_1 \end{pmatrix} N + \begin{pmatrix} m_3' + m_2 k_2 \\ +m_1 k_1 \end{pmatrix} W \quad (3.7)$$

where

$$m_1 = -f'k_2 + fl_1; m_2 = f'\Theta_1 + fl_2; m_3 = f'h + fl_3$$

and from (2.8), (2.9) and (2.11), $F_N(v) = 0$, one has

$$f'\Theta_1 + fl_2 = 0 \Rightarrow \left(\frac{c}{h}\right)' \Theta_1 + \frac{c}{h}(\Theta_1' - h\Theta_1) = 0 \qquad (3.8)$$

and

$$\Theta_1 = \frac{-h(s)}{c(s)} e^{\int h ds}\left\{\int c(s)k_1 e^{\int h ds} ds\right\} \qquad (3.9)$$

and from $F_N(\kappa) = 0$, one obtains

$$(-f'k_2 + fl_1)' + (-f'k_2 + fl_1)h + (f'h + fl_3)k_2 + g(R(F,\zeta)\zeta, N) = 0$$

from C is constant curvature $g(R(F_N,\zeta)\zeta, N) = Cg(F_N, N) = 0$, one gets

$$(-f'k_2 + fl_1)' + (-f'k_2 + fl_1)h + (f'h + fl_3)k_2 = 0$$

and

$$-((fk_2)')' - (fk_2)'h + ((fh)' - fk_1k_2 + fk_2\Theta_1) = 0. \quad (3.10)$$

Definition 2. Let γ be null curve in 3D semi-Riemannian Manifold and with the Frenet apparatus $\{\zeta, N, W, h, k_1, k_2\}$ and let F be a magnetic vector field along the curve γ on M_2^3. If the Lorentz force equation given below, expressed for null $W-$magnetic vector field, the curve γ is called null $W-$magnetic curve, is satisfied

$$\nabla_\zeta W = \Phi_W(W) = F_W \times W. \qquad (3.11)$$

Theorem 5. Let γ be null W-magnetic curve in 3D semi-Riemannian Manifold and with the Frenet apparatus $\{\zeta, N, W, h, k_1, k_2\}$. Then, the Lorentz force in the Frenet frame is given as

$$\begin{bmatrix} \Phi_W(\zeta) \\ \Phi_W(N) \\ \Phi_W(W) \end{bmatrix} = \begin{bmatrix} \Theta_2 & 0 & -k_1 \\ 0 & -\Theta_2 & -k_2 \\ k_2 & k_1 & 0 \end{bmatrix} \begin{bmatrix} \zeta \\ N \\ W \end{bmatrix}, \qquad (3.12)$$

where $\Theta_2 = g(\Phi_W(\zeta), N)$.

Proof. Let γ be a null W-magnetic curve in (M_2^3, g) with the Frenet apparatus $\{\zeta, N, W, h, k_1, k_2\}$. Then,

$$\Phi_W(\zeta) = \eta_1\zeta + \eta_2 N + \eta_3 W$$

and from (3.11) and (2.2), one gets

$$\eta_1 = g(\Phi_W(\zeta), N) = \Theta_2; \eta_2 = g(\Phi_W(\zeta), \zeta) = 0;$$

$$\eta_3 = -g(\Phi_W(\zeta), W) = -k_1,$$

one writes

$$\Phi_W(\zeta) = \Theta_2\zeta - k_1 W.$$

Similarly, the Lorentz force functions $\Phi_W(N)$ and $\Phi_W(W)$ can be calculated that

$$\Phi_W(N) = -\Theta_2 N - k_2 W; \Phi_W(W) = k_2\zeta + k_1 N.$$

Theorem 6. Let γ be a null W-magnetic trajectory of a magnetic field F_W in 3D semi-Riemannian Manifold with the Frenet apparatus $\{\zeta, N, W, h, k_1, k_2\}$ if and only if F_W is satisfied

$$F_W(s) = \frac{z(s)}{\Theta_2(s)}(k_2(s)\zeta(s) - k_1(s)N(s) + \Theta_2(s)W(s)). \quad (3.13)$$

Proof. Let γ be null W-magnetic trajectory of a magnetic field F_W. Then, the vector product of two time-like vectors produces a space-like vector that is orthogonal to both time-like vectors, since null vectors product yields the zero vector, by using (2.5) and theorem 5, from $F = x\zeta + yN + zW$, where $x, y, z \in C^\infty$ one obtains

$$F_W = \frac{z}{\Theta_2}(k_2\zeta - k_1 N + \Theta_2 W),$$

where

$$\Theta_2\zeta + k_1 W = zN_1^*, -\Theta_2 N - k_2 W = zN_2^*;$$
$$k_2\zeta + k_1 N = -xN_1^* - yN_2^*, \qquad (3.14)$$

where N_1^*, N_2^* are spacelike vector fields.

Theorem 7. Let F_W be a Killing vector field 3D semi-Riemannian Manifold with the Frenet apparatus $\{\zeta, N, W, h, k_1, k_2\}$ for the null N-magnetic curve γ. Then, the following equations are satisfied for the given null W-magnetic curve

$$\big(-(gk_1)' + k_1 g(h + \Theta_2)\big)' - \big(-(gk_1)' + k_1 g(h + \Theta_2)\big)h + (g\Theta_2)'k_1 = 0$$

$$\big((gk_2)' + k_2 g(h + \Theta_2)' + h\big(-(gk_1)' + k_1 g(h + \Theta_2)\big) + k_2(g\Theta_2)'\big) = 0,$$

where $g = \frac{z}{\Theta_2}, z \in C^\infty$.

Proof. For a null magnetic vector field F_W in (M^3, g), by differentiating of (3.13) according to parameter s, one gets

$$\nabla_\zeta F_W = \big((gk_2)' + k_2 g(h + \Theta_2)\big)\zeta + \big(-(gk_1)' + k_1 g(h + \Theta_2)\big)N + (g\Theta_2)'W \qquad (3.15)$$

where

$$g = \frac{z}{\Theta_2}. \qquad (3.16)$$

By differentiating of (3.15) with respect to s and from (2.1), one has

$$\nabla_\zeta^2 F = \big((gk_2)' + k_2 g(h + \Theta_2)' + h\big(-(gk_1)' + k_1 g(h + \Theta_2)\big) + k_2(g\Theta_2)'\big)\zeta$$

$$+\left(\left(-(gk_1)' + k_1 g(h + \Theta_2)\right)' - \left(-(gk_1)' + k_1 g(h + \Theta_2)\right)h + (g\Theta_2)'k_1\right)N + \left(\begin{pmatrix}((f\Theta_2)')' + \left(-(gk_1)' + k_1 g(h + \Theta_2)\right)k_2 \\ +\begin{pmatrix}(gk_2)' + k_2 g(h + \Theta_2)' \\ +h\left(-(gk_1)' + k_1 g(h + \Theta_2)\right) + k_2(g\Theta_2)'\end{pmatrix}k_1\end{pmatrix}W$$

and from (2.8), (2.9) and (2.11), $F_W(v) = 0$, one has

$$\left(-(gk_1)' + k_1 g(h + \Theta_2)\right)' - \left(-(gk_1)' + k_1 g(h + \Theta_2)\right)h + (g\Theta_2)'k_1 = 0 \tag{3.17}$$

and from $F_W(\kappa) = 0$, one obtains

$$\left((gk_2)' + k_2 g(h + \Theta_2)' + h\left(-(gk_1)' + k_1 g(h + \Theta_2)\right) + k_2(f\Theta_2)'\right) + g(R(F, \zeta)\zeta, N) = 0,$$

from C is constant curvature $g(R(F_W, \zeta)\zeta, N) = Cg(F_W, N) = 0$, one gets

$$(gk_2)' + k_2 g(h + \Theta_2)' + h\left(-(gk_1)' + k_1 g(h + \Theta_2)\right) + k_2(g\Theta_2)' = 0. \tag{3.18}$$

4. CONCLUSION

In this study, we consider the interactions between null magnetic curves and Killing vector fields on defined 3-dimensional semi-Riemannian manifolds. Null magnetic curves represent light-like trajectories under the influence of the Lorentz force, while Killing vector fields characterize the isometries of the manifold, i.e., metric tensor-preserving symmetries. Our findings demonstrate that the geometric and kinematic behavior of null magnetic curves in this particular space is directly related to the existence and structure of Killing vector fields. In

particular, the influence of a Killing vector field on the null magnetic curve provides important clues to the existence of conserved magnitudes of the curve and, consequently, to the integrability of the equations of motion. The results provide a valuable framework for the application of these manifolds in physical models and point to new directions for future research.

REFERENCES

Almaz, F., & Külahcı, MA. (2018). On x-magnetic surfaces generated by trajectory of x-magnetic curves in null cone. *General Letters in Mathematics*, 5(2), 84-92.

Almaz, F., & Kulahci, MA. (2021). A survey on magnetic curves in 2-dimensional lightlike cone. *Malaya Journal of Matematik*, 7(3), 477-485.

Almaz, F., & Kulahci MA. (2020). A Different Interpretation on Magnetic Surfaces Generated by Special Magnetic Curve in $Q^2 \subset E_1^3$. *Adıyaman University Journal of Science*, 10(2), 524-547.

Barros, M., & Romero, A. (2007). Magnetic vortices. EPL, 77.

Barros, M., Cabrerizo, JL., Fernandez, M., Romero, A. (2007). Magnetic vortex filament flows. *Journal of Mathematical Physics*, 48(8).

Cabrerizo, JL., Fernandes, M., Gomez, JS. (2009). The contact magnetic flow in 3D Sasakian manifolds. *J. Phys. A. Math. Theo.*, 42(19), 195-201.

Drut-Romaniuc, SL. & Munteanu MI. (2011). Magnetic curves corresponding to Killing magnetic fields in E^3. *J. Math. Phys.* 52.

Duggal, KL. & Bejancu, A. (1996). *Lightlike submanifolds of semi-Riemannian manifolds and applications*, Kluwer Academic Publishers, Dordrecht, 364, 52-76.

Graves, L. & Nomizu, K. (1978). Isometric immersions of Lorentzian space forms, *Math. Ann.*, 233, 125-136.

Ikawa, T. (1985). On curves and submanifolds in an indefinite-Riemannian manifold, *Tsukuba J. Math*., 9(2), 353-371.

O'Neill, B. (1983). *Semi-Riemannian Geometry with applications to relativity*, Academic Press, NewYork.

ON q-LEONARDO SPLIT QUATERNION POLYNOMIALS

Ali ATASOY[1]

1. INTRODUCTION

Quantum calculus (q-calculus) has garnered significant scholarly attention, demonstrating broad applicability in pure mathematics (e.g., combinatorics, special functions) and applied fields, including fractal analysis, multifractal measures, and the entropy formulations of chaotic dynamical systems. The present study introduces the concept of quantum split quaternion polynomials, establishing their fundamental properties and associated identities.

Integer sequences represent a cornerstone of mathematical inquiry and remain an active research domain. Canonical examples, particularly the Fibonacci and Lucas sequences, are considered foundational. This status is attributable to their complex structural characteristics, profound interconnections with diverse mathematical fields, and extensive applicability in disciplines ranging from biology and physics to statistics and computer science.

Classical studies on Fibonacci and Lucas numbers form the foundational background of many modern recursive structures. Early works such as A Primer for the Fibonacci Numbers provide a comprehensive introduction to these sequences and their mathematical behavior (Bicknell, Hoggatt, & Verner, 1972). Koshy's well-known monograph further expands

[1] Asst. Prof. Dr., Kırıkkale University, Keskin Vocational School, ORCID: 0000-0002-1894-7695.

this framework with formal properties and applications in various mathematical domains (Koshy, 2001). More recent contributions examine number theoretic representations, showing that integers can be expressed through combinations of Fibonacci and Lucas numbers (Park, Cho, Cho, Cho, & Park, 2020). Classical references, including those by Vajda (1989) and by Verner and Hoggatt (1969), detail the connections between these sequences and the golden ratio. Extensions of these ideas to hypercomplex systems were advanced by Halıcı (2012) through the study of Fibonacci quaternions. Foundational sequence generalizations were introduced in a series of works by Horadam (1961, 1963, 1965), who developed generalized Fibonacci sequences, explored their complex analogues, and established fundamental structural properties that continue to influence contemporary recursive sequence theory.

The recursive formulations of the Fibonacci and Lucas sequences are given by the following relations:

$$\mathrm{F}_n = \mathrm{F}_{n-1} + \mathrm{F}_{n-2}\ ;\ \mathrm{F}_0 = 0, \mathrm{F}_1 = 1,$$

$$\mathrm{L}_{n+2} = \mathrm{L}_{n+1} + \mathrm{L}_n\ ; \mathrm{L}_0 = 2, \mathrm{L}_1 = 1.$$

The Fibonacci and Lucas sequences can be expressed explicitly through their well-known Binet formulas.

$$\mathrm{F}_n = \frac{\varphi^n - \psi^n}{\varphi - \psi},\ \mathrm{L}_n = \varphi^n + \psi^n. \qquad (1.1)$$

For $n \geq 2$, Fibonacci polynomials are given as follows:

$$\mathrm{F}_n(x) = x\mathrm{F}_{n-1}(x) + \mathrm{F}_{n-2}(x)\ ;\ \mathrm{F}_0(x) = 0, \mathrm{F}_1(x) = 1.$$

Recent advancements in Leonardo number theory have expanded the classical framework into new algebraic and analytic domains. A modern treatment of the Leonardo sequence, incorporating dual vector and dual angle representations, has been proposed by Babadağ and Atasoy (2024), offering an enriched geometric interpretation of these numbers. The structural

properties of Leonardo sequences were further addressed in several studies, including those by Catarino and Borges (2019) and by Alp and Koçer (2021), who investigated combinatorial and arithmetic behaviors of the sequence. Extended generalizations, such as those presented by Shannon and Deveci (2022), highlight the adaptability of Leonardo-type recursions to broader number-theoretic contexts. Complex-valued extensions of Leonardo numbers were explored by Karataş (2022), providing insights into their behavior within complex algebraic structures. Complementary to these contributions, Shattuck (2022) offered combinatorial proofs for generalized Leonardo identities, thereby strengthening the theoretical foundations of Leonardo number analysis.

The Leonardo number sequence Le_n is defined through the recurrence relation

$$\mathrm{Le}_n = \mathrm{Le}_{n-1} + \mathrm{Le}_{n-2} + 1$$

starting with the terms $\mathrm{Le}_0 = \mathrm{Le}_1 = 1$. Then,

$$\mathrm{Le}_n - \mathrm{Le}_{n+1} = \mathrm{Le}_{n-1} + \mathrm{Le}_{n-2} + 1 - \mathrm{Le}_n - \mathrm{Le}_{n-1} - 1$$
$$\mathrm{Le}_{n+1} = 2\mathrm{Le}_n - \mathrm{Le}_{n-2}$$

(Mangueira, Vieira, Alves, & Catarino, 2022).

For $n \geq 3$, Leonardo polynomials are given as follows:

$$\mathrm{Le}_n(x) = 2x\mathrm{Le}_{n-1}(x) - \mathrm{Le}_{n-3}(x)$$

where $\mathrm{Le}_0(x) = \mathrm{Le}_1(x) = 1$ and $\mathrm{Le}_2(x) = 3$.

Leonardo numbers are explicitly defined by Binet's formulas:

$$\mathrm{Le}_n = 2\mathrm{F}_{n+1} - 1 = \frac{2\varphi^{n+1} - 2\psi^{n+1}}{\varphi - \psi} - 1, \quad n \geq 0. \qquad (1.2)$$

The study of special number sequences and polynomial structures has led to significant advances in discrete mathematics, particularly through identities and summation formulas derived using generating functions. These constructions play a central

role in mathematical physics, modeling, and analytic number theory (Nallı & Haukkanen, 2009; Horadam, 1996). Within this context, Lee and Asci expanded classical recursive systems by establishing fundamental properties of the (p,q)-Fibonacci and (p,q)-Lucas polynomials (Lee & Asci, 2012). Catarino subsequently introduced $h(x)$-Fibonacci quaternion polynomials, linking special sequences to quaternionic algebra (Catarino, 2015). More recently, Zhang, Khan, and Kızılateş analyzed (p,q)-Fibonacci and (p,q)-Lucas polynomials associated with Changhee numbers, further broadening the algebraic framework of generalized Fibonacci-type structures (Zhang, Khan, & Kızılateş, 2023).

Further developments in generalized Fibonacci-type structures have emerged through the integration of quantum calculus and its extensions. Zhang and friends offered an advanced treatment of (p,q)-Fibonacci and (p,q)-Lucas polynomials associated with Changhee numbers, providing new insights into their algebraic and combinatorial behavior (Zhang, Khan, & Kızılateş, 2023). Parallel contributions by Babadağ explored quantum-calculus-based approaches to dual and hyper-dual number sequences, demonstrating the applicability of q-analogue methods to broader algebraic systems (Babadağ, 2023a; Babadağ, 2023b). Foundational work on quantum calculus by Kac and Cheung (2002) established the theoretical framework upon which many recent generalizations depend, while the analysis of quantum integers by Le Stum and Quirós further clarified structural properties relevant to sequence theory (Le Stum & Quirós, 2015). Akkuş and Kızılaslan (2019) argued that the quantum calculus approach provides novel methods for quaternion analysis. Additional extensions of quantum-calculus-based recursive systems, including dual bicomplex Fibonacci and Lucas numbers, were introduced by Kome and friends, marking another significant step in the integration of quantum operators

with hypercomplex number systems (Kome, Kome, & Catarino, 2022).

For arbitrary integers n and m, we introduce the function

$$[n]_q = \frac{1-q^n}{1-q} = 1 + q + \cdots + q^{n-1}$$

and

$$\begin{aligned} [m+n]_q &= [m]_q + q^m[n]_q, \\ [mn]_q &= [m]_q[n]_{q^m}. \end{aligned}$$

If we take $q = \frac{\psi}{\varphi}$ in (1.1) and (1.2), we can write q-integer form respectively as:

$$\mathrm{F}_n(\varphi; q) = \varphi^{n-1}[n]_q = \varphi^n \frac{1-q^n}{\varphi - \varphi q},$$

$$\mathrm{L}_n(\varphi; q) = \varphi^n \frac{[2n]_q}{[n]_q} = \varphi^n \frac{1-q^{2n}}{1-q^n}$$

and

$$\mathrm{Le}_n(\varphi; q) = 2\varphi^n[n+1]_q - 1 = 2\varphi^{n+1}\frac{1-q^{n+1}}{\varphi - \varphi q} - 1$$

(Akkuş & Kızılaslan, 2019).

A split quaternion may be described as an ordered quadruple given by

$$\gamma = \gamma_0 + \gamma_1 i_1 + \gamma_2 i_2 + \gamma_3 i_3$$

with $\gamma_0, \gamma_1, \gamma_2, \gamma_3 \in \mathbb{R}$ ($\mathbb{R}$ denotes the set of real numbers) and split quatenionic units i_1, i_2, i_3 satisfy

$$i_1^2 = -i_2^2 = -i_3^2 = -1,\ i_1 i_2 = -i_2 i_1 = i_3,\ i_2 i_3 = -i_1. \quad (1.3)$$

Addition and multiplication operations are defined as follows:

$$\gamma + \delta = (S_\gamma + S_\delta) + (V_\gamma + V_\delta),$$
$$\gamma\delta = S_\gamma S_\delta + \langle V_\gamma, V_\delta \rangle + S_\gamma V_\gamma + S_\delta V_\delta + V_\gamma \times V_\delta,$$

where γ and δ are split quaternions (Atasoy, Ata, Yaylı, & Kemer, 2017).

2. q-LEONARDO SPLIT QUATERNIONS

The scope of this section encompasses the definition of the q-Leonardo and q-Lucas split quaternions, followed by the presentation of their key structural characteristics and associated algebraic identities.

The associated q-Leonardo split quaternion polynomial sequences are introduced herein, and their fundamental properties are subjected to rigorous examination.

Definition 2.1. The n^{th} q-Fibonacci split quaternions and the q-Lucas split quaternions are defined as follows:

$$\mathcal{F}_n(\varphi; q) = \mathrm{F}_n(\varphi; q) + \mathrm{F}_{n+1}(\varphi; q)i_1 + \mathrm{F}_{n+2}(\varphi; q)i_2 + \mathrm{F}_{n+3}(\varphi; q)i_3,$$
$$\mathcal{L}_n(\varphi; q) = \mathrm{L}_n(\varphi; q) + \mathrm{L}_{n+1}(\varphi; q)i_1 + \mathrm{L}_{n+2}(\varphi; q)i_2 + \mathrm{L}_{n+3}(\varphi; q)i_3$$

where i_1, i_2 and i_3 are the imaginary basis elements whose products follow the multiplication rule stated in (1.3).

The Binet formulas of these quaternions

$$\mathcal{F}_n(\varphi; q) = \left(\frac{\varphi^{n+1}\underline{\varphi} - (\varphi q)^{n+1}\underline{\beta}}{\varphi - \varphi q} \right),$$

$$\mathcal{L}_n(\varphi; q) = \varphi^n \underline{\varphi} + (\varphi q)^n \underline{\beta}$$

where $\underline{\varphi} = 1 + \varphi i_1 + \varphi^2 i_2 + \varphi^3 i_3$ and $\underline{\beta} = 1 + (\varphi q)i_1 + (\varphi q)^2 i_2 + (\varphi q)^3 i_3$.

Definition 2.2. The n^{th} q-Leonardo split quaternion sequences is defined by

$$\begin{aligned}\mathcal{L}e_n(\varphi;q) &= \mathrm{L}e_n(\varphi;q) + \mathrm{L}e_{n+1}(\varphi;q)i_1 + \mathrm{L}e_{n+2}(\varphi;q)i_2 \\ &\quad + \mathrm{L}e_{n+3}(\varphi;q)i_3 \\ &= 2\varphi^{n+1}\frac{1-q^{n+1}}{\varphi-\varphi q} + 2\varphi^{n+2}\frac{1-q^{n+2}}{\varphi-\varphi q}i_1 \\ &\quad + 2\varphi^{n+3}\frac{1-q^{n+3}}{\varphi-\varphi q}i_2 + 2\varphi^{n+4}\frac{1-q^{n+4}}{\varphi-\varphi q}i_3 \\ &\quad - (1+i_1+i_2+i_3) \qquad (2.1)\end{aligned}$$

or equivalent

$$\begin{aligned}\mathcal{L}e_n(\varphi;q) &= 2\big(\varphi^n[n+1]_q + \varphi^{n+1}[n+2]_q i_1 + \varphi^{n+2}[n+3]_q i_2 \\ &\quad + \varphi^{n+3}[n+4]_q i_3\big) - (1+i_1+i_2+i_3). \qquad (2.2)\end{aligned}$$

Theorem 2.1. The Binet-like formula for the n^{th} q-Leonardo split quaternions are

$$\mathcal{L}e_n(\varphi;q) = 2\mathcal{F}_n(\varphi;q) - \mathcal{A} = 2\left(\frac{\varphi^{n+1}\underline{\varphi} - (\varphi q)^{n+1}\underline{\beta}}{\varphi-\varphi q}\right) - \mathcal{A} \qquad (2.3)$$

or equivalent

$$\mathcal{L}e_n(\varphi;q) = 2\left(\varphi^n[n]_q\underline{\varphi} + (\varphi q)^n\underline{\psi}\right) - \mathcal{A}$$

where,

$\mathcal{A} = 1 + i_1 + i_2 + i_3$,

$\underline{\varphi} = 1 + \varphi i_1 + \varphi^2 i_2 + \varphi^3 i_3$,

$\underline{\psi} = 1 + \varphi[2]_q i_1 + \varphi^2[3]_q i_2 + \varphi^3[4]_q i_3$,

$\underline{\beta} = 1 + (\varphi q)i_1 + (\varphi q)^2 i_2 + (\varphi q)^3 i_3$.

Proof. Using equations (2.1) and (2.2) and carrying out the corresponding computations, we obtain

$$\begin{aligned}\mathcal{L}e_n(\varphi;q) &= \mathrm{L}e_n(\varphi;q) + \mathrm{L}e_{n+1}(\varphi;q)i_1 + \mathrm{L}e_{n+2}(\varphi;q)i_2 \\ &\quad + \mathrm{L}e_{n+3}(\varphi;q)i_3 \\ &= 2\varphi^{n+1}\frac{1-q^{n+1}}{\varphi-\varphi q} + 2\varphi^{n+2}\frac{1-q^{n+2}}{\varphi-\varphi q}i_1 \\ &\quad + 2\varphi^{n+3}\frac{1-q^{n+3}}{\varphi-\varphi q}i_2 + 2\varphi^{n+4}\frac{1-q^{n+4}}{\varphi-\varphi q}i_3 \\ &\quad - (1+i_1+i_2+i_3) \\ &= 2\frac{\varphi^{n+1}}{\varphi-\varphi q}(1+\varphi i_1+\varphi^2 i_2+\varphi^3 i_3) \\ &\quad - 2\frac{(\varphi q)^{n+1}}{\varphi-\varphi q}(1+(\varphi q)i_1+(\varphi q)^2 i_2+(\varphi q)^3 i_3) \\ &= 2\left(\frac{\varphi^{n+1}\underline{\varphi}-(\varphi q)^{n+1}\underline{\beta}}{\varphi-\varphi q}\right) - \mathcal{A}\end{aligned}$$

or equivalent

$$\begin{aligned}\mathcal{L}e_n(\varphi;q) &= \mathrm{L}e_n(\varphi;q) + \mathrm{L}e_{n+1}(\varphi;q)i_1 + \mathrm{L}e_{n+2}(\varphi;q)i_2 \\ &\quad + \mathrm{L}e_{n+3}(\varphi;q)i_3 \\ &= 2\big(\varphi^n[n+1]_q + \varphi^{n+1}[n+2]_q i_1 \\ &\quad + \varphi^{n+2}[n+3]_q i_2 + \varphi^{n+3}[n+4]_q i_3\big) \\ &= 2\varphi^n\big([n]_q + q^n\big) + 2\varphi^{n+1}\big([n]_q + q^n[2]\big)i_1 \\ &\quad + 2\varphi^{n+2}\big([n]_q + q^n[3]\big)i_2 + 2\varphi^{n+3} \\ &= 2\varphi^n[n]_q(1+\varphi i_1+\varphi^2 i_2+\varphi^3 i_2) \\ &\quad + 2\varphi^n q^n\big(1+\varphi[2]_q i_1+\varphi^2[3]_q i_2+\varphi^3[4]_q i_3\big) \\ &= 2\left(\varphi^n[n]_q\underline{\varphi} + (\varphi q)^n\underline{\psi}\right) - \mathcal{A}\end{aligned}$$

To illustrate, take the case where $n = 0$ in (2.3). We will have

$$\mathcal{L}e_0(\varphi;q) = 2\frac{\varphi - q\overline{\beta}}{(1-q)} - (1 + i_1 + i_2 + i_3)$$
$$= 2\frac{1 + \varphi i_1 + \varphi^2 i_2 + \varphi^3 i_3 - q(1 + (\varphi q)i_1 + (\varphi q)^2 i_2 + (\varphi q)^3 i_3)}{(1-q)}$$
$$- \mathcal{A}$$
$$= 2\frac{(1-q) + \varphi i_1(1-q^2) + \varphi^2 i_2(1-q^3) + \varphi^3 i_3(1-q^4)}{(1-q)} - \mathcal{A}$$
$$= 2(1 + \varphi[2]i_1 + \varphi^2[3]i_2 + \varphi^3[4]i_3) - \mathcal{A}.$$

3. q-LEONARDO SPLIT QUATERNION POLYNAMIALS

This section introduces the formal definition of the q-Leonardo split quaternion polynomial. Following this, we establish the Binet formula and the generating functions associated with this class of polynomials, and present several key results concerning the behavior of the derived sequences.

Definition 3.1. For complex polynomials $\alpha = \alpha(x)$ and $\mu = \mu(x)$, the q-Leonardo polynomial $\mathrm{L}e_n(x)$ is introduced using the recurrence relation

$$\mathrm{L}e_n(x) = 2\alpha \mathrm{L}e_{n-1}(x) - \mu \mathrm{L}e_{n-3}(x) \tag{3.1}$$

with the initial conditions $\mathrm{Le}_0(x) = \mathrm{L}e_1(x) = 1, \mathrm{L}e_2(x) = 3$ and $\mathrm{L}e_3(x) = 6\alpha - \mu,\ \mathrm{L}e_4(x) = 12\alpha^2 - 2\alpha\mu - \mu, \cdots$

The Binet formula of the q-Leonardo polynomial can now be obtained.

Theorem 3.1. Let $t_1 = t_1(x), t_2 = t_2(x), t_3 = t_3(x)$ be the roots of the characteristic equation roots of

$$t^3 - 2\alpha t^2 + \mu = 0$$

in (3.1) where $t = t(x)$. Then, for $n \geq 0$, the Binet formula for q-Leonardo polynomials $\mathrm{L}e_n(x)$ is

$$\mathrm{L}e_n(x) = \rho(x)\mathrm{t}_1^n(x) + \tau(x)\mathrm{t}_2^n(x) + \omega(x)\mathrm{t}_3^n(x)$$

where $\rho = \rho(x), \tau = \tau(x), \omega = \omega(x)$ and

$$\rho = \frac{3 - t_2 - t_3 + t_2t_3}{(t_1 - t_2)(t_1 - t_3)},$$

$$\tau = \frac{3 - t_1 - t_3 + t_1t_3}{(t_2 - t_1)(t_2 - t_3)},$$

$$\omega = \frac{3 - t_1 - t_2 + t_1t_2}{(t_3 - t_1)(t_3 - t_2)}.$$

Proof. The proof can be obtained by mathematical calculations for $n = 0, n = 1, n = 2$.

Definition 3.2. The q-Leonardo split quaternion polynomial $\mathcal{L}e_n(x)$ is recursively defined as follows:

$$\mathcal{L}e_n(x) = \mathrm{L}e_n(x) + \mathrm{L}e_{n+1}(x)i_1 + \mathrm{L}e_{n+2}(x)i_2 + \mathrm{L}e_{n+3}(x)i_3.$$

The initial values for the q-Leonardo quaternion polynomials $\mathcal{L}e_n(x)$ are are given by:

$$\begin{aligned}\mathcal{L}e_0(x) &= \mathrm{L}e_0(x) + \mathrm{L}e_1(x)i_1 + \mathrm{L}e_2(x)i_2 + \mathrm{L}e_3(x)i_3\\ &= 1 + i_1 + 3i_2 + \big(6\alpha(x) - \mu(x)\big)i_3,\end{aligned}$$

$$\begin{aligned}\mathcal{L}e_1(x) &= \mathrm{L}e_1(x) + \mathrm{L}e_2(x)i_1 + \mathrm{L}e_3(x)i_2 + \mathrm{L}e_4(x)i_3\\ &= 1 + 3i_1 + \big(6\alpha(x) - \mu(x)\big)i_2\\ &\quad + \big(12\alpha^2(x) - 2\alpha(x)\mu(x) - \mu(x)\big)i_3\end{aligned}$$

where the imaginary units i_1, i_2 and i_3 adhere to the multiplication rule described in (1.3).

Theorem 3.2. Consider $\mathcal{L}_e G(t)$ as the generating function of the q-Leonardo split quaternion polynomial $\mathcal{L}e_n(x)$, which is defined by:

$$\mathcal{L}_e G(t) = \frac{\mathcal{L}e_0(x) + [\mathcal{L}e_1(x) - 2\alpha\mathcal{L}e_0(x)]t + [\mathcal{L}e_2(x) - 2\alpha\mathcal{L}e_1(x)]t^2}{1 - 2\alpha t + t^3}.$$

Proof. The generating function of the q-Leonardo split quaternion polynomials $\mathcal{L}e_n(x)$, denoted by $\mathcal{L}_e G(t)$, is given by the series $\sum_{n=0}^{\infty} \mathcal{L}\, e_n(x)t^n$. For $n \geq 3$, we write

$$\mathcal{L}e_n(x) - 2\alpha\mathcal{L}e_{n-1}(x) + \mu\mathcal{L}e_{n-3}(x) = 0$$

$$\sum_{n=3}^{\infty} \mathcal{L}\, e_n(x)t^n - 2\alpha \sum_{n=3}^{\infty} \mathcal{L}\, e_{n-1}(x)t^n + \mu \sum_{n=3}^{\infty} \mathcal{L}\, e_{n-3}(x)t^n = 0$$

$$\sum_{n=0}^{\infty} \mathcal{L}\, e_n(x)t^n - \mathcal{L}e_0(x) - \mathcal{L}e_1(x)\mathrm{t} - \mathcal{L}e_2(x)t^2 - 2\alpha t\left(\sum_{n=0}^{\infty} \mathcal{L}\, e_n(x)t^n - \mathcal{L}e_0(x) - \mathcal{L}e_1(x)\mathrm{t}\right) + \mu t^3 \sum_{n=0}^{\infty} \mathcal{L}\, e_n(x)t^n = 0.$$

Then,

$$\mathcal{L}_e G(t) - \mathcal{L}e_0(x) - \mathcal{L}e_1(x)\mathrm{t} - \mathcal{L}e_2(x)t^2 - 2\alpha t\left(\mathcal{L}_e G(t) - \mathcal{L}e_0(x) - \mathcal{L}e_1(x)\mathrm{t}\right) + \mu t^3 \mathcal{L}_e G(t) = 0.$$

In the last equality, if we make the necessary calculations, we find the result as:

$$\mathcal{L}_e G(t) = \frac{\mathcal{L}e_0(x) + [\mathcal{L}e_1(x) - 2\alpha\mathcal{L}e_0(x)]t + [\mathcal{L}e_2(x) - 2\alpha\mathcal{L}e_1(x)]t^2}{1 - 2\alpha t + \mu t^3}.$$

The proof is completed.

Theorem 3.3. The Binet-like formula for the q-Leonardo split quaternion polynomial $\mathcal{L}e_n(x)$ is

$$\mathcal{L}e_n(x) = \rho\mathrm{t}_1^n Q_1(x) + \tau\mathrm{t}_2^n Q_2(x) + \omega\mathrm{t}_3^n Q_2(x)$$

where $Q_1(x) = +t_1 i_1 + \mathrm{t}_1^2 i_2 + \mathrm{t}_1^3 i_3$, $Q_2(x) = 1 + t_2 i_1 + \mathrm{t}_2^2 i_2 + \mathrm{t}_2^3 i_3, Q_2(x) = 1 + t_3 i_1 + \mathrm{t}_3^2 i_2 + \mathrm{t}_3^3 i_3$.

Proof. Based on Theorem 3.1, the proof can be readily established by applying the Binet formula for the q-Leonardo split quaternion polynomial. For $n \geq 0$,

$$\begin{aligned}
\mathcal{L}e_n(x) = \mathrm{L}e_n(x) + \mathrm{L}e_{n+1}(x)i_1 + \mathrm{L}e_{n+2}(x)i_2 + \mathrm{L}e_{n+3}(x)i_3 \\
&= \rho \mathrm{t}_1^n + \tau \mathrm{t}_2^n + \omega \mathrm{t}_3^n \\
&+ (\rho \mathrm{t}_1^{n+1} + \tau \mathrm{t}_2^{n+1} + \omega \mathrm{t}_3^{n+1}) i_1 \\
&+ (\rho \mathrm{t}_1^{n+2} + \tau \mathrm{t}_2^{n+2} + \omega \mathrm{t}_3^{n+2}) i_2 \\
&+ (\rho \mathrm{t}_1^{n+3} + \tau \mathrm{t}_2^{n+3} + \omega \mathrm{t}_3^{n+3}) i_3 \\
&= \rho \mathrm{t}_1^n (1 + t_1 i_1 + \mathrm{t}_1^2 i_2 + \mathrm{t}_1^3 i_3) \\
&+ \tau \mathrm{t}_2^n (1 + t_2 i_1 + \mathrm{t}_2^2 i_2 + \mathrm{t}_2^3 i_3) \\
&+ \omega \mathrm{t}_3^n (1 + t_3 i_1 + \mathrm{t}_3^2 i_2 + \mathrm{t}_3^3 i_3) \\
&= \rho \mathrm{t}_1^n Q_1(x) + \tau \mathrm{t}_2^n Q_2(x) + \omega \mathrm{t}_3^n Q_2(x).
\end{aligned}$$

4. CONCLUSIONS

In this study, split quaternion sequences are introduced using notations from quantum calculus. We introduce a novel class of q-Leonardo split quaternion polynomial sequences and explore a range of their properties. This representation obtain a new perspective on the structure of q-Leonardo split quaternions and give a deeper understanding of their geometric and algebraic interpretations and transformations.

REFERENCES

Akkuş, I., & Kızılaslan, G. (2019). Quaternions: Quantum calculus approach with applications. *Kuwait Journal of Science, 46(4),* 1-13.

Alp, Y., & Koçer, E. G. (2021). Some properties of Leonardo numbers. *Konuralp Journal of Mathematics, 9,* 183–189.

Atasoy, A., Ata, E., Yaylı, Y., & Kemer, Y. (2017). A new polar representation for split and dual split quaternions. *Advances in Applied Clifford Algebras, 27,* 2307–2319.

Babadağ, F. (2023). Quantum calculus approach to the dual number sequences. In *Research on Science and Mathematics–III* (pp. 49–60). Özgür Publications.

Babadağ, F. (2023). Quantum calculus approach to the hyper dual number sequences. In *Science in Theory and Practice* (pp. 57–71). Yaz Publications.

Babadağ, F., & Atasoy, A. (2024). A new approach to Leonardo number sequences with the dual vector and dual angle representation. *AIMS Mathematics, 9,* 14062–14074.

Bicknell, M., Hoggatt, J. R., & Verner, E. (1972). *A primer for the Fibonacci numbers*. Santa Clara, CA: The Fibonacci Association.

Catarino, P. (2015). A note on h(x)-Fibonacci quaternion polynomials. *Chaos, Solitons & Fractals, 77,* 1–5.

Catarino, P., & Borges, A. (2019). On Leonardo numbers. *Acta Mathematica Universitatis Comenianae, 89,* 75–86.

Halıcı, S. (2012). On Fibonacci quaternions. *Advances in Applied Clifford Algebras, 22,* 321–327.

Horadam, A. F. (1961). A generalized Fibonacci sequence. *The American Mathematical Monthly, 68,* 455–459.

Horadam, A. F. (1963). Complex Fibonacci numbers and Fibonacci quaternions. *The American Mathematical Monthly, 70*, 289–291.

Horadam, A. F. (1965). Basic properties of a certain generalized sequence of numbers. *Fibonacci Quarterly, 3*, 161–176.

Horadam, A. F. (1996). Extension of a synthesis for a class of polynomial sequences. *Fibonacci Quarterly, 34*, 68–74.

Kac, V., & Cheung, P. (2002). *Quantum calculus*. New York, NY: Springer.

Karataş, A. (2022). On complex Leonardo numbers. *Notes on Number Theory and Discrete Mathematics, 28*, 458–465.

Kome, S., Kome, C., & Catarino, P. (2022). Quantum calculus approach to the dual bicomplex Fibonacci and Lucas numbers. *Journal of Mathematical Extensions, 6*, 1–17.

Koshy, T. (2001). *Fibonacci and Lucas numbers with applications*. New York, NY: Wiley-Interscience.

Lee, G., & Asci, M. (2012). Some properties of the (p, q)-Fibonacci and (p, q)-Lucas polynomials. *Journal of Applied Mathematics, 2012*, Article ID 264842.

Le Stum, B., & Quirós, A. (2015). On quantum integers and rationals. *Contemporary Mathematics, 649*, 107–130.

Mangueira, M. C. S., Vieira, R. P. M., Alves, F. R. V., & Catarino, P. M. M. C. (2022). Leonardo's bivariate and complex polynomials. *Notes on Number Theory and Discrete Mathematics, 28(1),* 115-123.

Nallı, A., & Haukkanen, P. (2009). On generalized Fibonacci and Lucas polynomials. *Chaos, Solitons & Fractals, 42*, 3179–3186.

Park, H., Cho, B., Cho, D., Cho, Y. D., & Park, J. (2020). Representation of integers as sums of Fibonacci and Lucas numbers. *Symmetry, 12*, 1625.

Shannon, A., & Deveci, O. (2022). A note on generalized and extended Leonardo sequences. *Notes on Number Theory and Discrete Mathematics, 28*, 109–114.

Shattuck, M. (2022). Combinatorial proofs of identities for the generalized Leonardo numbers. *Notes on Number Theory and Discrete Mathematics, 28*, 778–790.

Vajda, S. (1989). *Fibonacci and Lucas numbers and the golden section*. Chichester, England: Ellis Horwood.

Verner, E., & Hoggatt, J. (1969). *Fibonacci and Lucas numbers*. Santa Clara, CA: The Fibonacci Association.

Zhang, C., Khan, W. A., & Kızılateş, C. (2023). On (p, q)-Fibonacci and (p, q)-Lucas polynomials associated with Changhee numbers and their properties. *Symmetry, 15*, 851.

DİFERANSİYEL MAHREMİYET VE MODERN UYGULAMALARI

Muhammed HASDEMİR[1]

1. GİRİŞ

Büyük Veri çağında bireysel mahremiyetin korunması, geleneksel anonimleştirme yöntemlerinin yetersiz kalması nedeniyle kritik bir zorluk haline gelmiştir. Diferansiyel Mahremiyet (DP), bu soruna matematiksel olarak kanıtlanabilir garantiler sunarak modern veri analizi için altın standarttır.

Bu bölümde, Merkezi DP modelinde kullanılan Laplace Mekanizması için gizlilik–fayda dengesini nicel olarak karakterize eden bir analiz çerçevesi sunulmaktadır. Sayma sorguları için mekanizmanın varyans ve Ortalama Mutlak Hata (MAE) açısından teorik davranışı türetilmekte, ardından kurgusal bir veri seti üzerinde gerçekleştirilen 5000 tekrarlı simülasyonlarla doğrulanmaktadır.

Farklı gizlilik (ε) değerleri boyunca elde edilen sonuçlar, (ε) ile hata metrikleri arasındaki ters ve yaklaşık logaritmik ilişkiyi ortaya koymakta; ayrıca kabul edilebilir sonuç yüzdesi üzerinden pratik bir güven ölçütü tanımlanmaktadır. Analiz, özellikle $\varepsilon < 1$ aralığında küçük artışların faydayı hızlı biçimde yükselttiğini, $\varepsilon > 3$ sonrasında ise marjinal kazanımların sınırlı kaldığını göstermektedir. Bölüm, bu bulgulara dayanarak uygulayıcılar için sayma sorguları bağlamında somut ε seçim rehberleri önermekte ve diferansiyel mahremiyetli sistemlerin

[1] Dr. Öğr. Üyesi, Aydın Adnan Menderes Üniversitesi, Söke Sağlık Hizmetleri Meslek Yüksekokulu, Tıbbi Hizmetler ve Teknikler Bölümü, Tıbbi Görüntüleme Teknikleri Pr., ORCID: 0000-0001-5901-3699.

tasarımında gizlilik ile analitik doğruluk arasında yapılacak uzlaşmanın nasıl nicel olarak değerlendirilebileceğini göstermektedir

1.1. Diferansiyel Mahremiyetin Ortaya Çıkışı ve Uygulama Örnekleri

Dijital ekosistemde veri toplamanın neredeyse "varsayılan" hâle gelmesi, sağlık, finans ve kamu politikaları gibi yüksek etkili alanlarda güçlü analitik imkânlar sunarken, bireysel mahremiyet risklerini de belirgin biçimde artırmaktadır. Geleneksel anonimleştirme teknikleri, özellikle de k-anonimlik gibi çerçeveler, kişisel verilerin tekrar-özdeşleştirilmesini önlemede sınırlı kalmakta hem kuramsal hem de pratik saldırı senaryoları karşısında kırılganlık sergilemektedir (Sweeney, 2002).

Netflix Prize veri kümesi üzerinde gerçekleştirilen yeniden kimliklendirme çalışması, dış kaynaklarla ilişkilendirme (linkage) yoluyla "anonim" olduğu iddia edilen büyük ölçekli veri setlerinin dahi birey düzeyinde açığa çıkabileceğini çarpıcı biçimde ortaya koymuştur (Narayanan & Shmatikov, 2008). Bu tür sonuçlar, anonimleştirme tabanlı yaklaşımların, özellikle Büyük Veri bağlamında, mahremiyeti korumak için tek başına yeterli olmadığını göstermektedir. Bu boşluğu doldurmak üzere ortaya çıkan Diferansiyel Mahremiyet (Differential Privacy, DP), bir bireyin verisinin veri kümesinde yer almasının ya da almamasının, analizin çıktısını yalnızca sınırlı ve matematiksel olarak kontrol edilen bir ölçüde değiştirmesine izin veren bir güvence çerçevesi sunar (Dwork & Roth, 2014). Böylece, veri yayımlayıcıları ve analistler, belirli bir gizliliği ε altında, yaptıkları hesaplamaların bireyler hakkında ne kadar bilgi açığa çıkarabileceğini nicel olarak ifade edebilmektedir. Bu güçlü kuramsal altyapı, DP'yi modern veri analizi ve makine öğrenimi uygulamaları için "referans standart" haline getirmiştir. Nitekim

Google'ın son kullanıcı yazılımlarından istatistik toplamak üzere geliştirdiği RAPPOR sistemi (yerel DP) ve ABD Nüfus Sayım Bürosu'nun 2020 sayımında benimsediği merkezi DP tabanlı koruma mekanizması, bu yaklaşımın büyük ölçekli gerçek dünya sistemlerine başarıyla uygulanabileceğini göstermektedir (Abowd, 2018; Erlingsson, Pihur, & Korolova, 2014).

1.2. Modern Gelişmeler: DP-SGD, LLM'ler ve Fair-DP

Son yıllarda, diferansiyel mahremiyet alanı makine öğrenimi ve özellikle derin öğrenme ile birleşerek yeni bir ivme kazanmıştır. DP-SGD (Differentially Private Stochastic Gradient Descent) algoritması, derin sinir ağlarının, eğitim verisindeki bireyleri "ezberlemeden" öğrenmesini mümkün kılan temel araçlardan biri olarak öne çıkmaktadır (Abadi et al., 2016). Aynı dönemde, büyük dil modelleri (LLM'ler) ve diğer genel modeller için diferansiyel mahremiyetli ince ayar (fine-tuning) teknikleri geliştirilmiş; bu sayede, kullanıcı etkileşimlerinden öğrenen modeller için yeni gizlilik garantileri tartışılır hâle gelmiştir. Buna paralel olarak, DP garantili sentetik veri üretimi alanında da önemli gelişmeler yaşanmış; tablo verileri için diferansiyel mahremiyetli GAN ve difüzyon tabanlı modeller, gizlilik–fayda dengesini iyileştirme potansiyeliyle öne çıkmıştır (Truda, 2023). Öte yandan, DP mekanizmalarının eklediği gürültünün, azınlık gruplar üzerindeki orantısız performans kayıplarına yol açabileceğine dair bulgular, Adil Diferansiyel Mahremiyet (Fair DP) başlığı altında yeni bir araştırma hattının doğmasına neden olmuştur (Hansen & Søgaard, 2024).

Bu zengin literatüre karşın, uygulamada karşılaşılan en temel sorulardan biri hala açık şekilde yanıtlanmamıştır. Belirli bir analiz görevi için ε nasıl seçilmelidir ve bu seçim hata metrikleri üzerinde nicel olarak ne anlama gelir? Mevcut çalışmaların önemli bir kısmı ya karmaşık öğrenme

algoritmalarına (örn. DP-SGD ile derin öğrenme) ya da gelişmiş genel modellere odaklanmakta; buna karşın, pratikte çok sık kullanılan basit sayma sorguları için bile, farklı ε değerlerinin hataya ve belirsizliğe etkisini doğrudan gösteren, erişilebilir ve öğretici analizler sınırlı kalmaktadır. Özellikle veri koruma birimlerinde çalışan uygulayıcılar için, "$\varepsilon = 0.1\ ile\ \varepsilon = 1$ arasındaki fark, ortalama mutlak hata veya kabul edilebilir sonuç yüzdesi açısından ne ifade ediyor?" sorusuna sayısal ve görsel olarak yanıt veren araçlara ihtiyaç vardır.

Bu kitap bölümün temel amacı, diferansiyel mahremiyetin teorik çekirdeğini oluşturan gizlilik–fayda dengesi kavramını, merkezi DP modelinde kullanılan Laplace Mekanizması özelinde analitik ve sayısal bir çerçeveyle incelemektir. Çalışmada, sayma sorguları için:

- Laplace mekanizmasının varyans ve Ortalama Mutlak Hata (Mean Absolute Error, MAE) açısından teorik davranışı türetilmekte,
- Geniş bir ε aralığında (yaklaşık 0.03–10) 5000 tekrarlı simülasyonlarla bu teorik sonuçlar doğrulanmakta ve sonuçlar, kabul edilebilir sonuç yüzdesi gibi pratik fayda göstergeleri üzerinden görselleştirilerek, uygulayıcılar için somut ε seçim rehberleri önerilmektedir.

2. DİFERANSİYEL MAHREMİYETİN KURAMSAL TEMELİ

Bu bölümde, merkezi diferansiyel mahremiyet (Central Differential Privacy, CDP) modelinde kullanılan Laplace Mekanizması temel alınmaktadır. CDP modelinde veriler önce güvenilir bir merkezi sunucuya toplanır; daha sonra

yayımlanacak istatistiksel sorguların çıktısına rastgele gürültü eklenerek mahremiyet sağlanır (Dwork & Roth, 2014).

2.1. Diferansiyel Mahremiyet Tanımı

Merkezi modelde diferansiyel mahremiyet şu şekilde tanımlanır. D ve D' yalnızca tek bir bireyin kaydı bakımından farklı olan iki komşu veri kümesi olsun, M rastgele bir mekanizma olmak üzere, her ölçülebilir çıktı kümesi S için

$$P(M(D) \in S) \leq e^{\varepsilon} \cdot P(M(D') \in S)$$

eşitsizliği sağlanıyorsa, M mekanizması ε-diferansiyel mahremiyetli (veya saf diferansiyel mahremiyetli) olarak adlandırılır (Dwork & Roth, 2014). Bu tanım, herhangi bir bireyin verisinin veri kümesine eklenmesinin veya çıkarılmasının, mekanizmanın çıktısını en fazla e^{ε} çarpanı kadar değiştirebileceğini garanti eder, dolayısıyla gözlemci, tek bir bireyin katılımı hakkında yalnızca sınırlı bilgi elde edebilir.

2.2. Global Hassasiyet ve Gizlilik

Diferansiyel mahremiyetli mekanizmaların tasarımında temel kavramlardan biri de global hassasiyettir (global sensitivity). Tek değer döndüren bir sorgu fonksiyonu $f: D^n \rightarrow R$ için global hassasiyet

$$S(f) = max_{D,D'} |f(D) - f(D')|$$

şeklinde tanımlanır, burada maksimum, tüm komşu veri kümesi çiftleri D, D' üzerinde alınır (Dwork, McSherry, Nissim, & Smith, 2006). Sayma sorguları için tek bir bireyin eklenmesi veya çıkarılması sonucu en fazla 1 birimlik değişim olacağından $S(f) = 1$ elde edilir; bu çalışma boyunca sayma sorguları için kullanılan temel varsayım budur. Küçük ε değerleri, komşu veri kümeleri için çıktılar arasında çok küçük farklara izin vererek güçlü bir gizlilik garantisi sağlar. Buna karşılık gürültü miktarı artar ve analitik fayda azalır. Daha büyük ε değerleri ise daha zayıf bir gizlilik garantisi karşılığında daha yüksek fayda sunar.

Dolayısıyla, diferansiyel mahremiyetli mekanizmaların tasarımında ε parametresi, gizlilik-fayda dengesini belirleyen temel "ayar düğmesi" dir.

2.3. Laplace Mekanizması

Laplace Mekanizması, sayısal çıktılar üreten sorgular için en temel ve yaygın kullanılan diferansiyel mahremiyet mekanizmalarından biridir (Dwork et al., 2006). Mekanizmanın tek boyutlu hali aşağıdaki gibidir:

$$M(D) = f(D) + Y$$

burada $f(D)$: veri kümesi D üzerindeki sorgunun gerçek (gürültüsüz) sonucudur ve Y, Laplace dağılımına sahip rastgele gürültü terimidir. Gürültü terimi $Y \sim Laplace(0, b),\ b = S(f)/\varepsilon$, yani Laplace dağılımının konum parametresi 0, ölçek parametresi $b = \frac{\mathrm{S(f)}}{\varepsilon}$ dir. Sayma sorguları için $S(f) = 1$ varsayımı altında ölçek $b = \frac{1}{\varepsilon}$ olur. Laplace dağılımının yoğunluk fonksiyonu

$$p_Y(y) = \frac{1}{2b} e^{(-|y|/b)}, \qquad y \in R$$

şeklindedir. Laplace mekanizması'nın istatistiksel özellikleri, bu çalışmada incelenen gizlilik–fayda dengesi açısından doğrudan belirleyicidir. Bu durumda diferansiyel mahremiyetli çıktı $M(D)$ için aşağıdaki temel moment ilişkileri geçerlidir. Eğer $Y \sim Laplace(0, b)$ ise beklenen değer $E[Y] = 0$ olur. Dolayısıyla mekanizma yansızdır:

$$E[M(D)] = E[f(D) + Y] = f(D).$$

Varyans:

$$Var(Y) = 2b^2 = 2 \cdot (S(f)/\varepsilon)^2$$

bu ifade, ε azaldıkça (daha güçlü gizlilik) eklenen gürültünün varyansının karesel biçimde büyüdüğünü gösterir. Ortalama mutlak sapma (MAE açısından):

$$E[|Y|] = b = S(f)/\varepsilon$$

Buna göre, diferansiyel mahremiyetli çıkışın gerçek değerden ortalama mutlak sapması

$$E[|M(D) - f(D)|] = E[|Y|] = S(f)/\varepsilon$$

olur, yani teorik olarak beklenen MAE, $1 / \varepsilon$ ile ters orantılıdır.

Sayma sorguları için $S(f) = 1$ alındığında, teorik olarak beklenen $MAE \approx 1 / \varepsilon$ şeklinde elde edilir. Bu analitik ilişki, çalışmanın dördüncü bölümünde rapor edilen simülasyon bulgularının yorumlanmasında temel rol oynamaktadır. Ayrıca Laplace Mekanizması'nın, yüksek gizlilik rejiminde (ε küçükken) belirli optimalite özelliklerine sahip olduğu, yakın tarihli çalışmalarda ayrıntılı biçimde incelenmiştir (Geng & Viswanath, 2016).

3. LAPLACE MEKANİZMASI İÇİN GİZLİLİK–FAYDA ANALİZİ

Laplace Mekanizması'nın gizlilik–fayda dengesini nicel olarak incelemek için simülasyon tabanlı bir analiz tasarımı benimsenmiştir. Amaç, farklı gizliliği ε değerleri altında diferansiyel mahremiyetli sayma sorgularının istatistiksel davranışını sistematik biçimde gözlemlemektir. Tasarım, diferansiyel mahremiyet literatüründe mekanizma düzeyinde yapılan teorik ve sayısal incelemelerle uyumludur (Dwork et al., 2006; Dwork & Roth, 2014; Geng & Viswanath, 2016).

Analiz, kurgusal bir "Şehir Sağlık Anketi" senaryosu üzerinden gerçekleştirilmiştir. Bu senaryoda toplam nüfus büyüklüğü $N = 20{,}000$ olarak alınmış, ilgilenilen çıktı ise "X Hastalığına sahip kişi sayısı" biçimindeki bir sayma sorgusu olarak modellenmiştir. Çalışma boyunca, gerçek (gürültüsüz) sorgu sonucu sabit bir değer $f(D) = 750$ olarak kabul edilmektedir.

Böylece simülasyon, veri üretim sürecine dair ek rastgelelik içermeksizin, Laplace Mekanizması'nın gürültü davranışını izole etmeye odaklanmaktadır. Sayma sorguları için global hassasiyet $S(f) = 1$ olarak alınmıştır (Dwork et al., 2006). Bu varsayım altında, her bir $\varepsilon > 0$ için Laplace gürültü terimi

$$Y^{(\varepsilon)} \sim \text{Laplace}\left(0, b^{(\varepsilon)}\right), b^{(\varepsilon)} = \frac{S(f)}{\varepsilon} = \frac{1}{\varepsilon},$$

dağılımına sahip olacak şekilde üretilmektedir. Diferansiyel mahremiyetli sayma sorgusu çıktısı ise her bir simülasyon için

$$M_i^{(\varepsilon)} = f(D) + Y_i^{(\varepsilon)}, \qquad i = 1,2, \dots, N_{\text{sim}}$$

şeklinde tanımlanır, burada $N_{\text{sim}} = 5000$ tekrar sayısını, $Y^{(\varepsilon)}$ ise dağılımından bağımsız çekilen gürültü örneklerini ifade etmektedir. Başlangıçta, mekanizmanın sezgisel davranışını göstermek üzere üç temsilci gizlilik değeri seçilmiştir. Bu üç senaryo, sırasıyla "yüksek gizlilik", "dengeli yaklaşım" ve "yüksek fayda" durumlarını temsil etmekte ve Tablo 1'de gösterilmiştir.

Tablo 1. Deney Senaryoları ve Parametreleri

Deney Senaryosu	**ε Değeri**	**Laplace Ölçek Parametresi ($b = S/\varepsilon$)**	**Gizlilik / Fayda Dengesi**
Yüksek Gizlilik	0.1	10.0	Yüksek Gizlilik (Çok Gürültü)
Dengeli Yaklaşım	0.8	1.25	Dengeli Yaklaşım (Orta Gürültü)
Yüksek Fayda	3.0	0.33	Yüksek Fayda (Az Gürültü)

Her bir ε değeri için N_{sim} adet gürültülü çıktı üzerinden örnek ortalama, örnek standart sapma, Ortalama Mutlak Hata (MAE) ve "kabul edilebilir sonuç yüzdesi" gibi nicel göstergeler hesaplanmıştır.

Ardından, ε parametresinin fayda metrikleri üzerindeki etkisini daha geniş bir aralıkta incelemek üzere logaritmik ölçekli bir tarama yapılmıştır. Bu amaçla, $\varepsilon_k \in [0.03,10]$, $k = 1,2,\ldots,K$, şeklinde yaklaşık logaritmik olarak artan bir ε ızgarası tanımlanmış, her bir ε_k için aynı prosedür yeniden uygulanarak N_{sim} adet gürültülü çıktı üretilmiştir. Her ε_k için, MAE (ε_k), standart sapma ($\sigma\varepsilon_k$) ve gerçek değerin belirli bir hata payı (örneğin ±50) içinde kalan sonuçların göreli sıklığına dayalı "kabul edilebilir sonuç yüzdesi" ($U_{\text{acc}}(\varepsilon)$) değerleri hesaplanmıştır.

3.1. Simülasyonlarda Kullanılan Fayda Metrikleri

Laplace mekanizmasının ürettiği gürültülü sayma sorgusu çıktılarının kalitesini değerlendirmek için üç temel istatistiksel fayda metriği kullanılmıştır:

- Örnek standart sapma,
- Ortalama Mutlak Hata ,
- Kabul edilebilir sonuç yüzdesi.

Bu metrikler, diferansiyel mahremiyetli mekanizmaların hata davranışını inceleyen literatürde yaygın biçimde kullanılmaktadır. Sabit bir $\varepsilon > 0$ için diferansiyel mahremiyetli sayma sorgusu çıktıları

$$M_i^{(\varepsilon)} = f(D) + Y_i^{(\varepsilon)}, i = 1,2,\ldots,N_{\text{sim}}, \quad ,$$

şeklinde elde edilir. Burada $f(D)$ gerçek (gürültüsüz) sayma sorgusu sonucunu, $Y_i^{(\varepsilon)}$ ise Laplace dağılımından çekilen gürültü terimlerini ifade eder.

Örnek Standart Sapma: Önce örnek ortalama

$$\overline{M}^{(\varepsilon)} = \frac{1}{N_{\text{sim}}} \sum_{i=1}^{N_{\text{sim}}} M_i^{(\varepsilon)}$$

hesaplanmakta, ardından buna karşılık gelen örnek varyans

$$\widehat{\sigma^2}(\varepsilon) = \frac{1}{N_{\text{sim}} - 1} \sum_{i=1}^{N_{\text{sim}}} \left(M_i^{(\varepsilon)} - \overline{M}^{(\varepsilon)} \right)^2$$

ve örnek standart sapma

$$\hat{\sigma}(\varepsilon) = \sqrt{\widehat{\sigma^2}(\varepsilon)}$$

denklemleri ile elde edilmektedir.

Ortalama Mutlak Hata (MAE): Diferansiyel mahremiyetli çıktının gerçek değerden ortalama sapmasını ölçmek için her bir ε değeri altında MAE metriği kullanılmıştır. MAE,

$$\widehat{\text{MAE}}(\varepsilon) = \frac{1}{N_{\text{sim}}} \sum_{i=1}^{N_{\text{sim}}} \left| M_i^{(\varepsilon)} - f(D) \right|$$

şeklinde tanımlanır. Laplace mekanizması için teorik olarak denklem~\eqref{eq:mae-theoretical} geçerlidir; buna göre beklenen MAE yaklaşık $1/\varepsilon$ ile ters orantılıdır. Bu çalışmada elde edilen $\widehat{\text{MAE}}(\varepsilon)$ değerleri, söz konusu teorik ilişkinin geniş bir ε aralığında sayısal olarak gözlemlenmesi ve görselleştirilmesi amacıyla kullanılmıştır.

Kabul Edilebilir Sonuç Yüzdesi: Pratik uygulamalarda analistler çoğu zaman belirli bir hata eşiği içinde kalan sonuçları ``kabul edilebilir'' olarak değerlendirir. Bu sezgiyi yakalamak için her bir ε değeri altında kabul edilebilir sonuç yüzdesi tanımlanmıştır. Önceden belirlenen bir tolerans $\tau > 0$ (bu çalışmada $\tau = 50$) için, i'inci simülasyon sonucunun kabul edilebilir olup olmadığını gösteren gösterge fonksiyonu

$$1_i^{(\varepsilon)} = \begin{cases} 1, \text{eğer } \left| M_i^{(\varepsilon)} - f(D) \right| \leq \tau \\ 0, \quad aksi\ takdirde \end{cases}$$

bu durumda kabul edilebilir sonuç oranı

$$U_{\text{acc}}(\varepsilon) = \frac{1}{N_{\text{sim}}} \sum_{i=1}^{N_{\text{sim}}} \mathbf{1}_i^{(\varepsilon)}$$

olarak hesaplanmakta; yüzde cinsinden ifade edildiğinde

$$\text{Kabul edilebilir sonuç yüzdesi}(\varepsilon) = 100 \times U_{\text{acc}}(\varepsilon)$$

şeklinde raporlanmaktadır.

Bu metrik, farklı ε değerleri için ``gerçek değerin $\pm\tau$ aralığında kalan sonuçların oranı"nı doğrudan gösterdiğinden, veri koruma uzmanlarının ve analistlerin çeşitli gizlilik seviyelerinde ne ölçüde analitik doğruluk elde edebileceklerini pratik olarak yorumlamalarına imkân vermektedir.

4. BULGULAR

Laplace mekanizmasının davranışını sezgisel olarak ortaya koymak amacıyla seçilen üç temsilci gizliliği olan $\varepsilon \in \{0.1, 0.8, 3.0\}$ için $N_{\text{sim}} = 5\,000$ adet gürültülü sorgu sonucu üretilmiş, bu sonuçlar üzerinden örnek ortalama, örnek standart sapma ve ölçek parametresi hesaplanmıştır. Elde edilen özet istatistikler Tablo 2'de sunulmaktadır.

Tablo 2. Farklı ε Değerleri İçin Simülasyon Sonuçlarının Özeti

Epsilon (ε)	**Ortalama Sonuç**	**Standart Sapma (σ)**	**Laplace Ölçek Parametresi ($b = S/\varepsilon$)**	**Gizlilik/Fayda Dengesi**
0.1	749.94	13.72	10.00	Yüksek Gizlilik
0.8	749.97	1.78	1.25	Dengeli Yaklaşım
3.0	750.02	0.50	0.33	Yüksek Fayda

Tablo 2'deki bulgular, ε ile σ arasında güçlü bir ters orantı olduğunu göstermektedir. $\varepsilon = 0.1$ senaryosunda $\sigma = 13.72$ iken, $\varepsilon = 3.0$ senaryosunda σ değeri 0.50'ye düşmüştür.

Ortalama sonuçların ise tüm senaryolarda gerçek değere (750) çok yakın olduğu gözlemlenmiştir, bu da Laplace Mekanizması'nın yansızlığına ilişkin teorik sonucun sayısal olarak doğrulandığını göstermektedir.

Örnek standart sapma değerleri, beklenen teorik davranışla uyumludur. Küçük ε değerinde (yüksek gizlilik), gürültünün varyansı belirgin biçimde büyümekte; büyük ε değerinde (yüksek fayda) ise varyans hızla azalmaktadır. Bu azalma hızı, Laplace dağılımı için teorik olarak elde edilen

$$Var\left(M^{(\varepsilon)}(D)\right) = 2\left(b^{(\varepsilon)}\right)^2, \qquad b^{(\varepsilon)} = \frac{1}{\varepsilon},$$

ilişkisiyle tutarlı olacak şekilde, yaklaşık $1/\varepsilon^2$ ölçeğinde gözlenmektedir.

MAE değerleri, ε arttıkça beklenildiği gibi azalmaktadır. Özellikle yüksek gizlilikte $(\varepsilon = 0.1)$ MAE, orta ve yüksek fayda senaryolarına kıyasla birkaç kat daha büyük iken, $\varepsilon = 3.0$ için MAE, gerçek sayma değeri ölçeğine göre oldukça küçük bir seviyeye inmektedir. Bu bulgu, teorik olarak beklenen $E\left|M^{(\varepsilon)}(D) - f(D)\right| = 1/\varepsilon$
davranışının pratik bir doğrulaması niteliğindedir.

Kabul edilebilir sonuç yüzdesi (örneğin, $\left|M_i^{(\varepsilon)} - 750\right| \leq 50$ koşulunu sağlayan sonuçların oranı), ε büyüdükçe hızla artmaktadır. Yüksek gizlilikte bu oran belirgin şekilde daha düşük iken, dengeli yaklaşım ve yüksek fayda senaryolarında sonuçların büyük bir kısmı istenen hata payı içerisinde kalmaktadır.

Bu temel senaryolar, Laplace Mekanizması için ε parametresinin doğrudan "ayar düğmesi" olarak işlev gördüğünü, gizlilik lehine yapılan seçimlerin (küçük ε) varyans ve hata maliyetini önemli ölçüde artırdığını, buna karşın daha büyük ε değerlerinin analitik faydayı hızlı biçimde iyileştirdiğini nicel olarak göstermektedir.

Tablo 3. Farklı ε değerleri için gürültülü sayma sorgusu sonuçları

ε	b	MAE	σ	$U_{\text{acc}}(\varepsilon)$
0.031623	31.623	31.303	44.3	80.56
0.057362	17.433	17.014	23.88	95
0.10405	9.6108	9.7444	13.711	99.58
3.0392	0.32903	0.2298	0.50302	100
10	0.1	0.005	0.070715	100

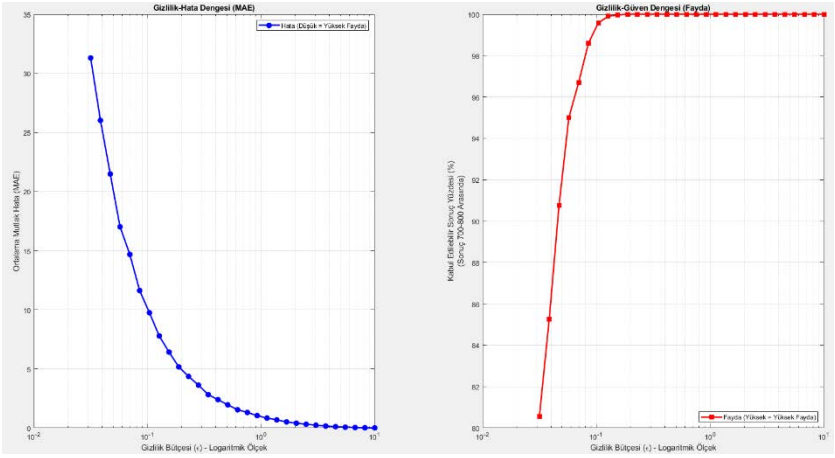

Şekil 1. (Solda) ε'ye karşı MAE eğrisi (logaritmik eksen); (sağda) ε'ye karşı kabul edilebilir sonuç yüzdesi

Şekil 1 ve Tablo 3, MAE'nin ε arttıkça hızla azaldığını göstermektedir. Özellikle $\varepsilon < 1$ aralığında ε'deki küçük artışların MAE'yi çok belirgin ölçüde düşürdüğü gözlenmiştir. Bu hızlı azalma, teorik olarak beklenen MAE $\approx 1/\varepsilon$ ilişkisiyle uyumludur ve logaritmik ölçekte neredeyse doğrusal bir yapı sergilemektedir. Buna karşılık, ε belirli bir eşik değerini (örneğin $\varepsilon \approx 3$) aştıktan sonra MAE'deki marjinal iyileşmeler giderek küçülmekte; eğri, yüksek fayda bölgesinde doyuma yaklaşan bir profil çizmektedir.

Kabul edilebilir sonuç yüzdesi açısından bakıldığında, ε ile birlikte monoton ve hızlı bir artış gözlenmektedir. Düşük ε aralığında $U_{\text{acc}}(\varepsilon)$ görece sınırlı kalırken, ε'nin orta değerlere

(yaklaşık $0.5 - 1.0$ aralığı) yükselmesiyle bu oranlarda keskin bir artış gerçekleşmektedir. Daha yüksek ε değerlerinde ise kabul edilebilir sonuç yüzdesi neredeyse $\%100$ seviyesine yaklaşmakta ve ilave gizlilikten feragat etmenin fayda artışı açısından anlamlı bir katkı sağlamadığı görülmektedir.

Şekil 2'de sırasıyla $\varepsilon = 0.1,\ \varepsilon = 0.8$ ve $\varepsilon = 3.0$ için elde edilen $M_i^{(\varepsilon)}$ değerlerinin dağılımı, histogramlar aracılığıyla görselleştirilmiştir. 750 merkezi etrafında oluşan gürültülü sorgu sonuçlarının dağılımları yan yana gösterilmektedir.

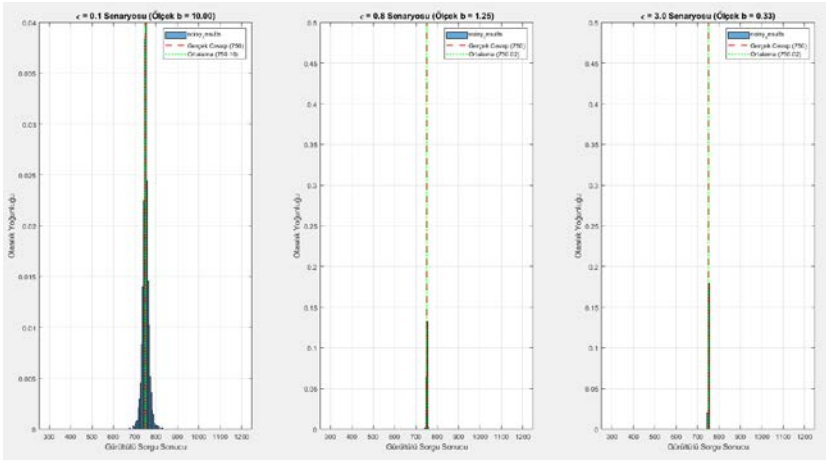

Şekil 2. Farklı gizlilik için diferansiyel mahremiyetli sayma sorgusu sonuçlarının histogramları

Şekil 2 'de şu özellikler açık biçimde görülmektedir: Yüksek gizlilikte ($\varepsilon = 0.1$), dağılım geniş ve görece düz bir yapıya sahiptir. Bu durumda, gürültü terimi $Y^{(\varepsilon)}$ büyük bir ölçek parametresiyle üretildiğinden, sayma sonuçları 750 etrafında oldukça yaygın bir aralıkta dağılmakta, hatta belirli bir oranda uç değerler (örneğin 700'ün altı veya 800'ün üstü) ortaya çıkmaktadır. Dengeli yaklaşım olarak seçilen $\varepsilon = 0.8$ senaryosunda dağılım, yüksek gizlilik senaryosuna kıyasla daha dar bir bantta yoğunlaşmakta ve gerçek değer etrafındaki oynaklık belirgin biçimde azalmaktadır. Yüksek faydada ise ($\varepsilon =$

3.0), histogram keskin bir zirve şeklini almakta; sonuçlar büyük ölçüde 750'nin hemen çevresinde toplanmakta ve geniş kuyruklar neredeyse tamamen ortadan kalkmaktadır.

5. SONUÇ

Bu çalışmada, merkezi diferansiyel mahremiyet modelinde kullanılan Laplace Mekanizması için gizlilik-fayda dengesini nicel olarak inceleyen basit fakat açıklayıcı bir analiz çerçevesi sunulmuştur. Çerçeve, bir yandan mekanizmanın temel teorik özelliklerini (yansızlık, varyans ve ortalama mutlak hata davranışı) açıkça ortaya koymakta, diğer yandan da geniş bir ε aralığında gerçekleştirilen simülasyonlar aracılığıyla bu teorik sonuçların pratik yansımalarını görünür kılmaktadır.

Bu çalışma, sayma sorguları için Laplace Mekanizması bağlamında şu tür bir pratik mesaj sunmaktadır: Çok küçük ε değerleri, güçlü gizlilik garantileri sağlamakla birlikte analitik açıdan yüksek belirsizlik maliyetine sahiptir. Orta büyüklükte ε değerleri hem MAE hem de kabul edilebilir sonuç yüzdesi açısından çoğu uygulama için makul bir denge sağlamaktadır. Çok büyük ε değerlerinde ise ek fayda artışı sınırlı olup, buna karşın gizlilik seviyesi hissedilir ölçüde zayıflamaktadır. Dolayısıyla, ε seçiminin yalnızca normatif veya politik bir karar değil, aynı zamanda nicel olarak analiz edilebilir bir mühendislik problemi olduğu vurgulanmaktadır.

Sonuç olarak, teorik sonuçlar ile simülasyon bulgularını birleştiren bu çerçeve, hem eğitim/öğretim amaçlı bir araç olarak hem de gerçek sistemlerde ε seçimine ilişkin ilk değerlendirmelerin yapılabileceği basit bir başlangıç noktası olarak kullanılabilir. Daha karmaşık mekanizmalar, öğrenme algoritmaları ve adalet odaklı senaryolar için geliştirilecek genişletmeler, diferansiyel mahremiyetin pratik tasarım

kararlarını daha şeffaf ve hesap verebilir hale getirme potansiyeli taşımaktadır.

KAYNAKÇA

Abadi, M., Chu, A., Goodfellow, I., McMahan, H. B., Mironov, I., Talwar, K., & Zhang, L. (2016). Deep learning with differential privacy. In *Proceedings of the 2016 ACM SIGSAC Conference on Computer and Communications Security (CCS '16)* (pp. 308–318). ACM. https://doi.org/10.1145/2976749.2978318

Abowd, J. M. (2018). The U.S. Census Bureau adopts differential privacy. In *Proceedings of the 24th ACM SIGKDD International Conference on Knowledge Discovery & Data Mining (KDD '18)* (p. 2867). ACM. https://doi.org/10.1145/3219819.3226070 SciSpace

Dwork, C., & Roth, A. (2014). The algorithmic foundations of differential privacy. *Foundations and Trends in Theoretical Computer Science*, *9*(3–4), 211–407. https://doi.org/10.1561/0400000042

Dwork, C., McSherry, F., Nissim, K., & Smith, A. (2006). Calibrating noise to sensitivity in private data analysis. In S. Halevi & T. Rabin (Eds.), *Theory of Cryptography Conference (TCC 2006)* (pp. 265–284). Springer. https://doi.org/10.1007/11681878_14

Dwork, C., & Roth, A. (2014). *The algorithmic foundations of differential privacy*. Foundations and Trends in Theoretical Computer Science, 9(3–4), 211–407. https://doi.org/10.1561/0400000042

Erlingsson, Ú., Pihur, V., & Korolova, A. (2014). RAPPOR: Randomized aggregatable privacy-preserving ordinal response. In *Proceedings of the 2014 ACM SIGSAC Conference on Computer and Communications Security (CCS '14)* (pp. 1054–1067). ACM. https://doi.org/10.1145/2660267.2660348

Hansen, V. P. B., Neerkaje, A., Sawhney, R., Flek, L., & Søgaard, A. (2024). The impact of differential privacy on group disparity mitigation. In *Findings of the Association for Computational Linguistics: NAACL 2024* (pp. 3952–3965). Association for Computational Linguistics. https://doi.org/10.18653/v1/2024.findings-naacl.249 aclanthology.org

Geng, Q., & Viswanath, P. (2016). The optimal noise-adding mechanism in differential privacy. *IEEE Transactions on Information Theory, 62*(2), 925–951. https://doi.org/10.1109/TIT.2015.2504967

Narayanan, A., & Shmatikov, V. (2008). Robust de-anonymization of large sparse datasets. In *Proceedings of the 2008 IEEE Symposium on Security and Privacy (SP '08)* (pp. 111–125). IEEE. https://doi.org/10.1109/SP.2008.33 collaborate.princeton.edu+1

Sweeney, L. (2002). k-anonymity: A model for protecting privacy. *International Journal of Uncertainty, Fuzziness and Knowledge-Based Systems, 10*(5), 557–570. https://doi.org/10.1142/S0218488502001648

Truda, G. (2023). Generating tabular datasets under differential privacy. *arXiv preprint* arXiv:2308.14784.

A MATHEMATICS-DRIVEN HYBRID NEURO-FUZZY APPROACH FOR PREDICTING BREAST CANCER RECURRENCE[1]

Seda GÖKTEPE KÖRPEOĞLU[2]

Şeydanur ÇELİK[3]

1. INTRODUCTION

Breast cancer remains one of the leading causes of cancer mortality worldwide (World Health Organization [WHO], 2023). With overall cancer incidence reaching nearly 20 million cases in 2022, breast cancer constitutes a substantial share of the total, and projections indicate continued growth by 2050 in the absence of targeted prevention, effective screening, and equitable access to treatment ([IARC], 2024). Clinically, accurate early diagnosis and recurrence risk stratification are crucial for guiding therapy—such as adjuvant chemotherapy and radiotherapy—while balancing the risks of overtreatment against undertreatment (Asselain et al.,2018). However, decision-making is complicated by heterogeneous, noisy, and sometimes incomplete clinical data. Prognostic factors such as tumor size, nodal status, degree of malignancy, and irradiation history often interact in nonlinear ways, and recurrence datasets typically suffer from class imbalance (Wishart et al., 2012). Classical statistical approaches are frequently insufficient to capture such nonlinearities and

[1] Some of this study's results were obtained with the support of TUBITAK 2209-A—University Students Research Projects Support Programme.

[2] Assoc. Prof. Dr., Yildiz Techical University, Chemical and Metalurgical Engineering, Mathematical Engineering, ORCID: 0000-0001-7146-0846.

[3] Student, Yildiz Techical University, Chemical and Metalurgical Engineering, Mathematical Engineering, ORCID: 0009-0008-0865-219X.

uncertain boundaries among predictors (Alizadehsani et al., 2020).

Breast cancer prediction has become a prominent research area in medical data science, aiming to improve early diagnosis and recurrence risk assessment. Traditional statistical approaches often struggle to handle high-dimensional, imbalanced, and uncertain medical data (Rashed & Popescu, 2024; Görgel et al., 2013).

From a mathematical and computational perspective, modeling complex and uncertain data structures is a fundamental challenge. Medical datasets, particularly those involving class imbalance and noise, exemplify this problem. In this context, Adaptive Neuro-Fuzzy Inference Systems (ANFIS)—which combine fuzzy logic with artificial neural networks—stand out for their capacity to represent nonlinear relationships through an interpretable rule base. Yet ANFIS is not without limitations; its most significant drawback is the rule explosion problem. As the number of input variables and membership functions increases, the rule base grows exponentially, leading to excessive computational cost and reduced generalizability. Thus, controlling model complexity is essential for the practical adoption of ANFIS in healthcare applications (Huang et al., 2012).

Among neuro-fuzzy techniques, ANFIS, introduced by Jang (1993), integrates the learning capability of neural networks with the transparency of fuzzy inference. ANFIS learns membership function parameters and rule consequents from data while retaining interpretable rule-based reasoning, a desirable property in clinical contexts where explainability complements accuracy (Huang et al., 2012; Jain & Abraham, 2004). A growing body of evidence supports neuro-fuzzy and hybrid approaches for cancer-related classification tasks, including breast cancer

diagnosis and recurrence prediction. Recent studies report that ANFIS and its hybrids can achieve competitive performance when paired with effective feature selection and membership-function tuning, and can complement tree-based or deep models by providing interpretable decision rules (Haznedar et al., 2021). However, the predictive performance of ANFIS is highly sensitive to the choice and parameterization of membership functions (e.g., triangular, Gaussian, differential sigmoidal) and the resulting rule base.

2. METHODOLOGY

2.1. Dataset

The Breast Cancer dataset obtained from the UCI Machine Learning Repository forms the foundation of this study. It includes 286 instances described by 10 clinical and demographic attributes (Zwitter & Soklic, 1988). These variables consist of both categorical (e.g., age groups, menopausal status, tumor location) and binary features (e.g., node-caps, irradiate). The diversity of variable types underscores the need for systematic preprocessing before applying hybrid neuro-fuzzy modeling techniques. Table 1 summarizes the dataset variables.

Table 1. Variables of Breast Cancer Dataset.

Variable	Role	Type	Description / Range
Class	Target	Binary	Class label: no-recurrence, recurrence
Age	Feature	Categorical	Age groups: 10-19, 20-29, …, 90-99
Inv-nodes	Feature	Categorical	
Tumor-size	Feature	Categorical	0-4, 5-9, 10-14, …, 55-59
Menopause	Feature	Categorical	lt40, ge40, premeno
Node-caps	Feature	Binary	yes, no
Deg-malig	Feature	Integer	Degree of malignancy: 1, 2, 3
Breast	Feature	Binary	left, right
Breast-quad	Feature	Categorical	left-up, left-low, right-up, right-low, central
Irradiate	Feature	Binary	yes, no

2.2. Dataset Preprocessing

Preprocessing constitutes a vital stage to transform heterogeneous raw data into an analyzable structure. The steps conducted include handling missing data, transforming categorical variables into numerical representations, scaling features to a common range, and performing feature selection. These procedures mitigate the risks of bias, overfitting, and computational inefficiency.

2.2.1. Missing Data Analysis

The dataset contained only nine missing entries, distributed across two features ('node-caps' and 'breast-quad'). Considering the low proportion of missing values, mode imputation was applied. This choice preserved the integrity of categorical variables without introducing additional complexity. After imputation, the dataset was complete and ready for further analysis.

There are missing values in a total of 2 columns in the dataset. Below are the columns with missing data: Node-caps: 8 missing values, Breast-quad: 1 missing value.

2.2.2. Data Transformation

Since most machine learning models, including ANFIS, operate exclusively on numerical input, categorical variables were transformed accordingly. Label encoding was applied to variables with ordinal characteristics, while one-hot encoding was employed for nominal categories such as 'breast-quad'. Ordered variables, such as age ranges and tumor size intervals, were converted into continuous numeric representations by calculating their mean values. This ensured that medical information embedded in categorical formats was preserved in a computationally tractable manner.

The data in the dataset were analyzed and the following strategies were applied for numerical transformation:

- Columns with label encoding applied: Menopause, Node-caps, Breast, Irradiate.
- Column with one-hot encoding applied: Breast-quad.
- Columns converted to numeric format by calculating the range mean of each categorical value: Age, Tumor-size, Inv-nodes.

2.2.3. Feature Scaling

Feature scaling was conducted to ensure that attributes with different ranges contributed equally to the learning process. Min-max normalization mapped all numeric features into the [0,1] interval, thereby standardizing the input space. This procedure prevented the dominance of variables with larger ranges, which could otherwise bias the training process.

In a dataset, some features may have a wide range of values while others may have a narrower range. For example, “tumor-size” has 12 categories in the range 0-60, while “deg-malig” in the range 1-3. In this case, the model cannot give equal weight to the features. This causes the model to learn unbalanced. It either overfit these features or ignores them. Normalization brings all features into the same range. It prevents this imbalance by equally weighting features. All numerical features are normalized to the interval [0, 1] with min-max normalization. This means that 0 is the lowest value and 1 is the highest value.

2.2.4. Feature Selection

Feature selection is defined as selecting the features that best represent the dataset. The aim is to reduce the number of inputs by determining the most useful and most important features for the problem. By evaluating the features, the best k features are selected from the n features in the dataset according

to the algorithms used. In this way, the training time of the model is decreased, and the generalization ability is increased (Guyon & Elisseeff, 2003).

In this study, the main reason for feature selection is to control the number of input variables used in the ANFIS model. ANFIS creates rules for each input variable and membership value. The number of rules changes depending on the number of input variables and membership values. In the data set, the number of input variables is 12:

- If the membership value is 3: $3^{12} = 531.441$, rules are generated.
- If the membership value is 5: $5^{12} = 244.140.625$, rules are generated.

Through feature selection, only meaningful and effective features are identified, and the model runs more efficiently. In this study, different feature selection methods were used:

Correlation Analysis: Pearson correlation coefficient was used to measure the linear relationship between features. The correlation matrix is given in Figure 1.

SelectKBest (Chi-Square Test): Chi-square test was applied to measure the effect of each feature on the target variable.

Random Forest Importance Score: It ranked the importance of features based on the voting of decision trees.

RFE (Recursive Feature Elimination): The Recursive feature elimination method was applied with Decision Tree. This method identifies the optimal sub-features by removing the least effective feature at each step.

Comparative results of the methods are given in Table 2.

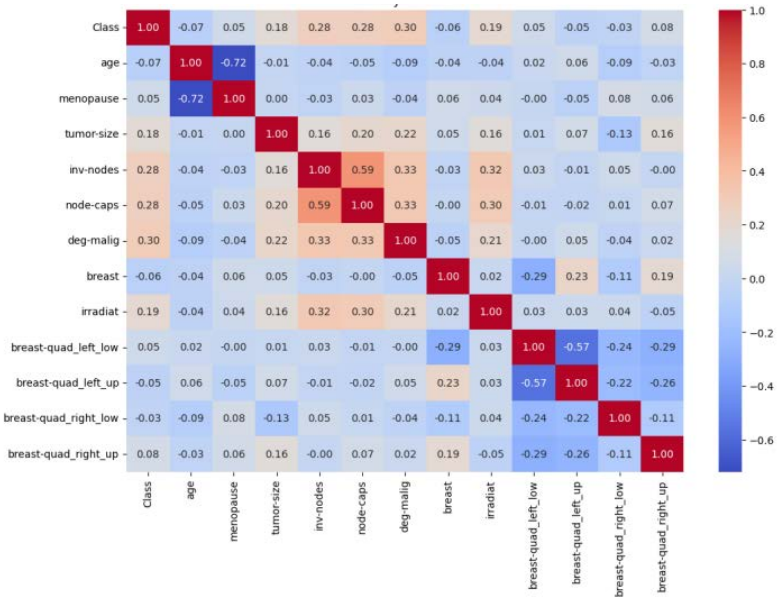

Figure 1. Correlation matrix.

Table 2. Feature selection.

Correlation	SelectKBest	Random Forest	RFE
deg-malig	✗	✓	✓
node-caps	✓	✓	✗
inv-nodes	✓	✓	✗
tumor-size	✗	✓	✓
irradiat	✓	✓	✗
age	✗	✓	✓
breast	✗	✓	✗
menopause	✗	✓	✗
breast-quad_right_up	✗	✗	✗
breast-quad_left_low	✗	✗	✗
breast-quad_left_up	✗	✗	✗
breast-quad_right_low	✗	✗	✗

According to the results of these methods, the features that have a meaningful relationship with the target variable were selected by majority voting: deg-malig (degree of malignancy),

node-caps, inv-nodes (number of involved lymph nodes), tumor-size, and irradiate.

These attributes formed the input space for all ANFIS configurations evaluated in this study.

3. PROPOSED MODEL DEVELOPMENTS AND TECHNIQUES

3.1. Fuzzy Logic

Fuzzy logic is a modeling approach that seeks to replicate two core human faculties—reasoning and the capacity to perform various cognitive tasks—by mechanizing them (Zadeh, 1965). In this framework, rather than strictly relying on numerical values, linguistic terms are employed for modeling. Essentially, fuzzy modeling functions as a rule-based methodology, often referred to as a fuzzy inference system (FIS). As illustrated in Figure 1, a typical fuzzy logic system is composed of four main components. When constructing a fuzzy rule-based model, several key steps are involved:

Identification of Variables: Determine the input and output variables.

Definition of Fuzzy Sets: Specify the fuzzy sets for each variable.

Creation of Membership Functions: Develop membership functions for all fuzzy inputs and outputs.

Formulation of Fuzzy IF-THEN Rules: Establish the rules that relate input variables to output variables.

Specification of the Inference Process: Choose between common FIS types—primarily Sugeno or Mamdani (Takagi & Sugeno, 1985). These differ in certain respects: Sugeno produces linear or constant outputs and typically relies on training with a

data set, whereas Mamdani generates outputs expressed as membership functions (e.g., triangular or trapezoidal) and draws on expert knowledge. In this study, a Mamdani-type fuzzy inference system is selected to benefit from domain expertise. Under the Mamdani framework, input variables are first fuzzified according to relevant membership functions. Subsequently, fuzzy operators such as “AND” or “OR” combine these inputs to form a single value, and the weight of each rule is determined before applying the rule’s implication. All rules are then aggregated—methods for this include max (maximum), probor (probabilistic OR), or sum. The aggregated fuzzy output ultimately requires defuzzification (Mamdani & Assilian, 1975).

Defuzzification: Convert the aggregated fuzzy result into a crisp output.

By following these steps, a robust fuzzy logic system can be developed that mimics human-like reasoning processes and handles linguistic information effectively.

3.2. Adaptive neuro-fuzzy inference systems (ANFIS)

The term "neuro-fuzzy" introduces the hybrid methodology that combines artificial neural networks (ANN) and fuzzy logic (FL). It was first presented by Jang in the beginning of the 1990s (Jang, 1993). It demonstrates ANN learning capabilities with FL decision-making skills and adjusts its parameters according on inputs. Mamdani and Takagi-Sugeno are the two types of fuzzy inference systems (FIS) (Mamdani & Assilian, 1975; Takagi & Sugeno, 1985). Similar to the structure of an ANN, the ANFIS architecture is made up of nodes grouped in layers with specific functions. Additionally, the membership functions MF use IF-THEN fuzzy rules to determine the connections between the premise and consequences, which are the primary components of ANFIS. Figure 2 illustrates the five layers that make up the ANFIS structure.

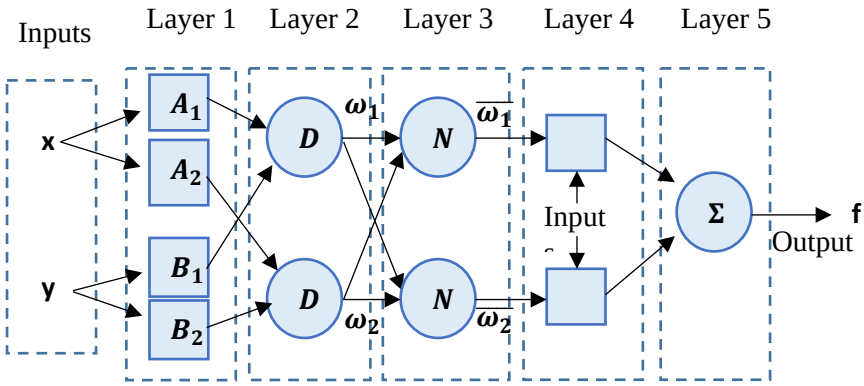

Figure 2. ANFIS Structure (Jang, 1993).

We assume the following two fuzzy if-then rules to explain the rules of each layer:

Rule 1: if x is A_1 and y is B_1 then $f_1 = p_1x + q_1y + r_1$, (1)

Rule 2: if x is A_2 and y is B_2 then $f_2 = p_2x + q_2y + r_2$, (2)

where f is the output (linguistic variables), x and y are the input variables, and A_i and B_i are fuzzy sets. The following parameters should be measured during the ANFIS training process: $\{p_i, q_i, r_i\}$. Each layer's function can be quantified as follows (Jang, 1993):

Layer 1 (Fuzzification): A membership function defines each node, i, in this layer. Membership functions are used in fuzzy logic to make the variables fuzzy. These membership functions are curves that specify the mapping from a point in the input space to a membership value in the [0,1] interval.

$$O_{1,i} = \sigma_{A_i(x)}, \text{ for } i = 1,2, \dots, n \quad (3)$$

$$O_{1,i} = \sigma_{B_{i-2}(y)}, \text{ for } i = 3,4, \dots, n \quad (4)$$

$$O_{3,i} = \overline{\omega_i} = \frac{\omega_i}{\omega_1+\omega_2}, \text{ for } i = 1,2. \quad (6)$$

where n is the number of fuzzy sets for each input variable, and $\sigma_{A_i(x)}$ and $\sigma_{B_{i-2}(y)}$ are membership functions.

Layer 2 (Product Layer): This layer, also referred to as the firing strength of a rule, receives input values from the first layer and outputs the following:

$$O_{2,i} = \omega_i = \sigma_{A_i(x)}\sigma_{B_i(y)}, \text{ for } i = 1,2. \quad (5)$$

Layer 3 (Normalized Layer): Layer 3's output is calculated as follows:

$\overline{\omega_i}$ is a rule's normalized firing strength.

Layer 4 (Defuzzification): The following formula is used to determine Layer 4's output:

$$O_{4,i} = \overline{\omega_i} f_i = \overline{\omega_i}(p_i x + q_i y + r_i), \text{ for } i = 1,2. \quad (7)$$

Layer 5 (Output Layer): The arrival signals are added up to form the output model.

$$O_{5,i} = \text{overall output} = \sum_i \overline{\omega_i} f_i = \frac{\sum_i \omega_i f_i}{\sum_i \omega_i}, \text{ for } i = 1,2. \quad (8)$$

The parameters of the adaptive neural fuzzy inference system are trained to minimize the error term between the predicted and actual output. The process is as follows: the least square estimator updates the consequent parameters (r_i, q_i and p_i) during the forward pass, while gradient descent and neural network trains update the premise parameters (in the membership functions) during the backward phase.

4. MODELING RESULTS

The input data must be normalized before being used in the models because the independent variables were collected in various units. In order to improve learning speed and model stability, data normalization results in dimensionless input data that stays between 0 and +1.

4.1. ANFIS Configuration

In this study, ANFIS model is applied using deg-malig, node-caps, inv-nodes, tumor-size, and irradiate features. ANFIS is a hybrid model that combines both the flexibility of fuzzy logic and the learning ability of artificial neural networks. Using a given input/output dataset, the ANFIS toolbox creates a fuzzy inference system (FIS) that is tuned by combining the membership function parameters with a back-propagation algorithm or a method such as least squares. This regularization makes it possible for fuzzy systems to learn from the data they are modeling.

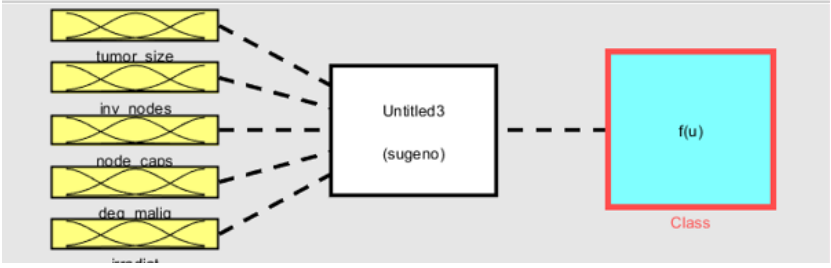

Figure 3. Structure of the fuzzy rule-based model.

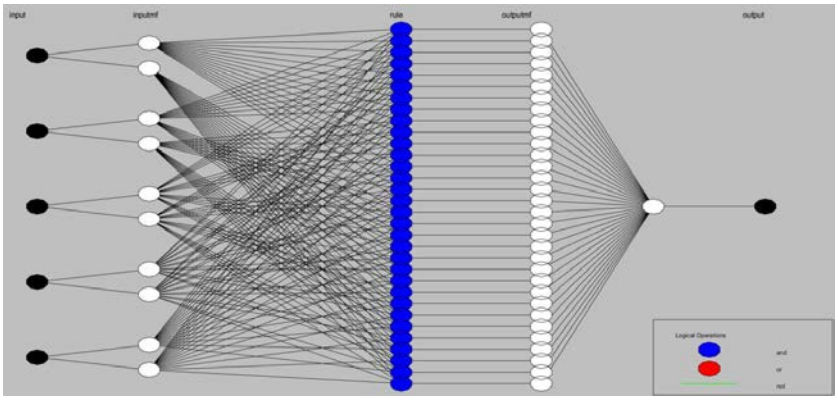

Figure 4. ANFIS structure with five inputs and two membership rules.

ANFIS is formed by the combination of points in layers as shown in Fig. 3 and Fig. 4. The first layer contains the inputs, and the last layer contains the output.

In order to use the Fuzzy and ANFIS model, the number and type of MFs as well as the number of iterations (epoch number) must be set. The first step in modeling is the creation of pattern vectors; the second step is pattern development using an input condition vector and matching target vector. It is impossible to overlook the input and output data range when adjusting different operating range settings. The ANFIS may be effectively taught by scaling or normalizing without degrading the outcomes. One of the major difficulties in modeling nonlinear systems is choosing the input parameter for learning, which is crucial for ANFIS. As a result, the processed data needs to be divided into train and test datasets. The dataset is split into 70% training and 30% testing. This ratio is a standard approach to evaluate the generalization performance of the model. In the initial stage of the training, as shown in Figure 3, the Sugeno type fuzzy model was used, and the input variables were determined. For the training process, the epoch value was set to 1000 and the error

value to 0. The error value of the model was monitored and stopped manually after it stopped decreasing for a while.

There are no precise techniques or procedures to forecast the required MFs number, as the literature states (Wang & Mendel, 1992). The ANFIS model uses commonly used membership functions to transform the input data into fuzzy logic. These are dsigmf (differential sigmoid membership function) and trimf (triangular membership function) with configurations 22222 and 33333, and gausmf (Gaussian membership function) with configurations 33333. The meaning of 33333 is that 3 membership functions are used for each input. Likewise, 22222 means 2 membership functions are used for each input.

4.2. Findings

Two ANFIS structures were systematically compared to explore the trade-off between complexity and performance:

22222 Configuration – each of the five inputs represented by two membership functions (MFs), yielding

$$R(x) = 2^5 = 32\, rules$$

This structure represents a lightweight system with reduced computational burden and enhanced interpretability.

33333 Configuration – each input represented by three MFs, yielding

$$R(x) = 3^5 = 243\, rules$$

This structure provides higher modeling flexibility but introduces substantial rule growth.

Three MF types—Gaussian (gausmf), triangular (trimf), and difference of sigmoids (dsigmf)—were examined for both configurations. The number of premise parameters p_t is defined

by each MF type. For instance, for $p_t = 2$ Gaussian, which has an immediate impact on the overall number of parameters:

$$P(x) = \sum_{i=1}^{d} m_i . p_t + (d+1).R(x) \quad (9)$$

Configurations 33333 and 22222 are compared in terms of the metrics mentioned. For a better understanding of the performance differences, both configurations are analyzed separately.

In this study, the ANFIS model is tested with different membership functions and configurations, focusing on classification performance. The performance of the model was evaluated with accuracy, precision, recall, *F1* score and Area Under the ROC Curve (AUC) values.

The results produced by ANFIS are categorized with a cut-off value of *0.5*. Those below this value are categorized as "0" and those above this value are categorized as "1". In this way, the success rate of the system could be calculated.

The model was tested on the "No Recurrence" and "Recurrence" classes. Table 3 presents the results of the different membership functions and configurations:

Table 3. Classification metrics for recurrence class.

Number of MF	Type of MF	Accuracy	Precision	Recall	F1 Score	AUC
33333	dsignmf	81	0.83	0.46	0.59	0.7095
22222	dsignmf	80	0.85	0.4	0.54	0.6851
33333	trimf	81	0.83	0.46	0.59	0.7095
22222	trimf	80	0.81	0.41	0.55	0.6860
33333	gausmf	81	0.83	0.46	0.59	0.7095

Accuracy rates for all models were similar. Accuracy rates between 80% and 81% were obtained with both dsigmf, trimf and gausmf membership functions. Although the 33333-

configuration increased complexity by generating more rules, it did not provide a significant advantage in terms of accuracy. This shows that similar accuracy rates can be obtained with fewer membership functions (22222).

AUC is an important metric that shows the overall discriminative capacity of the models. With both membership functions, the highest AUC value of 0.7095 was obtained in configuration 33333. However, with the 22222-configuration, the AUC value decreased to around 0.685. This shows that when fewer membership functions are used, the discriminative ability of the model decreases.

The 33333-configuration performed slightly better than the other configuration with an F1 score of 0.59. This is due to the balanced values of both precision and recall. The trimf 22222-configuration provides a slightly greater value (0.41) for recall but performs lower in terms of precision and F1 score. In general, configuration 33333 with more membership functions was more effective in increasing the correct prediction rate. The low recall rates (in the range of 40-46%) suggest that the model needs further optimization to increase its capacity to make accurate predictions in this class. This could be improved with a more balanced data set or different modeling techniques.

The membership functions dsigmf and trimf gave similar accuracy and AUC results with different configurations. From this situation, it can be concluded that the choice of the membership function does not have a major impact on the overall performance of the model. The gausmf membership function was only tested with the 33333 configuration and provided the same results as dsigmf. This suggests that more complex membership functions do not always give better performance.

5. DISCUSSION

In this study, using the UCI Breast Cancer dataset, the ANFIS model was developed, and its performance was evaluated in detail. The dataset was applied to data preprocessing to be suitable for the model. Since the model gives memory error when it is tried to be evaluated with more inputs, the number of inputs was decreased. For this purpose, various feature selection methods were used and inputs were selected by majority voting.

The performance of the ANFIS model was evaluated with different membership functions (dsigmf, trimf, gausmf) and different configurations (33333 and 22222). The model is analyzed with classification metrics. The dsigmf 33333 model stood out with an accuracy of 81% and an AUC value. However, it was shown that the sensitivity (recall) was low in the "Recurrence" class. It brought a new perspective to the literature by analyzing the effects of different membership functions and configurations on model performance. The imbalance of the dataset was a factor affecting the performance of the "Recurrence" class in specific. Only specific membership functions and configurations were tested in the study.

More comprehensive testing could be applied. Different results can be obtained by applying methods to improve the balance of the dataset. Different fuzzy logic methods or hybrid approaches (e.g. a combination of ANFIS and optimization algorithms) could be tested. The generalizability of the model can be studied with larger and different data sets. The ANFIS model has important potential in breast cancer prediction. The results show that model performance is directly affected by the choice and configuration of the membership function. The results of this study have both helped in the development of breast cancer prediction models and showed the applicability of the ANFIS method in the health field.

REFERENCES

Alizadehsani, R., Roshanzamir, M., Hussain, S., Khosravi, A., Koohestani, A., Zangooei, M. H., Abdar, M., Beykikhoshk, A., Shoeibi, A., Zare, A., Panahiazar, M., Nahavandi, S., Srinivasan, D., Atiya, A. F., & Acharya, U. R. (2021). Handling of uncertainty in medical data using machine learning and probability theory techniques: a review of 30 years (1991-2020). *Annals of operations research*, 1–42. Advance online publication. https://doi.org/10.1007/s10479-021-04006-2.

Asselain, B., Barlow, W., Bartlett, J., Bergh, J., Bergsten-Nordström, E., Bliss, J., ... & Zujewski, J. A. (2018). Long-term outcomes for neoadjuvant versus adjuvant chemotherapy in early breast cancer: meta-analysis of individual patient data from ten randomised trials. *The Lancet Oncology*, *19*(1), 27-39.

Görgel, P., Sertbaş, A., & Turusbekova, A. (2013). Classification of breast masses using ANFIS-based fuzzy algorithms: A comparative study. *Electrica, 13*(1), 1–10.

Guyon, I., & Elisseeff, A. (2003). An introduction to variable and feature selection. Journal of Machine Learning Research, 3, 1157–1182.

Haznedar, B., Arslan, M. T., & Kalınlı, A. (2021). Optimizing ANFIS using simulated annealing algorithm for classification of microarray gene-expression cancer data. *Medical & Biological Engineering & Computing, 59*(3), 497–509. https://doi.org/10.1007/s11517-021-02331-z.

Huang, M. L., Hung, Y. H., Lee, W. M., Li, R. K., & Wang, T. H. (2012). Usage of case-based reasoning, neural network and adaptive neuro-fuzzy inference system classification techniques in breast cancer dataset classification

diagnosis. *Journal of Medical Systems, 36*(2), 407–414. https://doi.org/10.1007/s10916-010-9485-0.

International Agency for Research on Cancer. (2024). *Breast cancer cases and deaths are projected to rise globally by 2050*. https://www.iarc.who.int.

Jain, A., & Abraham, A. (2004). A comparative study of fuzzy classification methods on breast cancer data. *arXiv preprint arXiv:cs/0405008*. https://arxiv.org/abs/cs/0405008

Jang, J. S. R. (1993). ANFIS: Adaptive-network-based fuzzy inference system. *IEEE Transactions on Systems, Man, and Cybernetics, 23*(3), 665–685. https://doi.org/10.1109/21.256541.

Mamdani, E. H., & Assilian, S. (1975). An experiment in linguistic synthesis with a fuzzy logic controller. *International Journal of Man-Machine Studies, 7*(1), 1–13. https://doi.org/10.1016/S0020-7373(75)80002-2.

Rashed, B. M., & Popescu, N. (2024). Medical image-based diagnosis using a hybrid adaptive neuro-fuzzy inference system (ANFIS) optimized by a genetic algorithm with a deep network model for feature extraction. *Mathematics, 12*(5), Article 633. https://doi.org/10.3390/math12050633.

Takagi, T., & Sugeno, M. (1985). Fuzzy identification of systems and its applications to modeling and control. *IEEE Transactions on Systems, Man, and Cybernetics, 15*(1), 116–132. https://doi.org/10.1109/TSMC.1985.6313399.

Wang, L. X., & Mendel, J. M. (1992). Generating fuzzy rules by learning from examples. *IEEE Transactions on Systems, Man, and Cybernetics, 22*(6), 1414–1427. https://doi.org/10.1109/21.199466

World Health Organization. (2023). *Breast cancer: Key facts*. https://www.who.int.

Wishart, G. C., Bajdik, C. D., Dicks, E., Provenzano, E., Schmidt, M. K., Sherman, M., ... & Pharoah, P. D. P. (2012). PREDICT: A new UK prognostic model that predicts survival following breast cancer. *Breast Cancer Research, 12*(1), R1. https://doi.org/10.1186/bcr2464.

Zadeh, L. A. (1965). Fuzzy sets. *Information and Control, 8*(3), 338–353. https://doi.org/10.1016/S0019-9958(65)90241-X.

Zwitter, M., & Soklic, M. (1988). *Breast Cancer Data (Original)* [Data set]. UCI Machine Learning Repository. University of California, Irvine. Retrieved from https://archive.ics.uci.edu/ml/datasets/Breast+Cancer.

THE ENDOMOPRHISM GREEN FUNCTOR IN MACKEY FUNCTOR THEORY[1]

Mehmet UC[2]

1. INTRODUCTION

The theory of Mackey functors, originally developed to unify the phenomena of induction, restriction, and conjugation in representation theory and algebraic topology, has evolved into a powerful categorical framework for examining how group actions behave in algebraic structures (Thévenaz & Webb, 1995; Uc, 2008). While classical representation theory examines these phenomena at the level of modules on a group algebra, Mackey functors broaden the perspective, organizing information that extends to all subgroups of a finite group. In this context, transfer maps, restriction morphisms, and conjugation actions coexist within a coherent system governed by the Mackey axiom. This categorical structure allows for the establishment of decomposition theorems, analysis of some correspondences, and structural invariants that are not accessible solely through module theory.

One of the most influential ideas in classical modular representation theory is Green correspondence, introduced by J. A. Green in the 1960s (Green, 1964). Green correspondence relates indecomposable kG-modules to their counterparts on appropriate subgroups; it identifies the vertex and source

---

[1] This chapter is derived from the author's master's thesis titled *"Green Correspondence for Mackey Functors,"* completed at the Institute of Engineering and Science, İhsan Doğramacı Bilkent University, Ankara, Türkiye, in 2008.

[2] Assistant Professor, Department of Mathematics, Faculty of Science and Letters, Burdur Mehmet Akif Ersoy University, ORCID: 0000-0003-3680-9103.

structures of these modules and sheds light on the study of blocks and defect groups (Alperin, 1982; Green, 1964). The strength of this approach lies in its ability to make representation problems that seem difficult across the whole group more understandable by reducing them to manageable subgroups. Over the last few decades, significant work has been done to extend this approach to broader contexts, such as biset functors, Mackey functors, cohomological functors, and other equivariant algebraic structures.

In this respect, Sasaki's contribution is a turning point (Sasaki, 1982). Sasaki named Mackey functors with additional structural compatibility conditions G-functors and established a Green correspondence for these structures. This generalization relies on the use of the endomorphism Green functor defined for a Mackey functor. While the classical Green correspondence works with modules (Alperin, 1982; Green, 1964), Sasaki's approach uses an internal hom-functor that captures the endomorphisms of a Mackey functor across all subgroups of a finite group (Sasaki, 1982; Thévenaz & Webb, 1995; Uc, 2008). The resulting structure is not merely a collection of endomorphism rings but a Green functor, that is a ring-valued Mackey functor that satisfies a Frobenius reciprocity condition generalizing the algebraic behavior of induction and restriction. This functorial perspective shows that the vertices and correspondents of a Mackey functor can be understood through primitive idempotents of its endomorphism Green functor.

Despite its fundamental importance, the endomorphism Green functor (Sasaki, 1982; Uc, 2008) has not been discussed in sufficient detail in the literature. Most sources merely introduce this structure, leaving the verification of the axioms to the reader, or summarize the process without going into detail. Therefore, critical points such as how the interaction between transfer and restriction occurs in their internal hom-objects, or how Frobenius

reciprocity is fully validated at the functorial level, have not been clearly and systematically set forth. However, these details are of great importance: establishing Green correspondence for Mackey functors depends on proving that the endomorphism construction actually yields a Green functor and that this functorial behaves consistently under induction and restriction.

The aim of this chapter is to present a comprehensive and explicit examination of the endomorphism Green functor associated with a Mackey functor (Sasaki, 1982; Uc, 2008). Our goal is twofold. First, we verify in a complete and detailed manner that the endomorphism structure satisfies all the axioms of a Green functor, including the Frobenius axioms and the Mackey axiom expressed at the level of morphism families. Unlike previous works, we make the subtle interaction between the Mackey structure and the algebraic structure of the endomorphism rings transparent by carefully considering each step (Uc, 2008). In this respect, we believe that we offer a comprehensive and systematic verification available in the literature.

Secondly, we highlight the conceptual role of the endomorphism Green functor in the context of Green correspondence (Sasaki, 1982; Uc, 2008). Specifically, the endomorphism Green functor is a categorical replacement for the endomorphism rings seen in classical representation theory. When examining a Mackey functor M, the concept of a vertex can be reduced to the vertex of the related endomorphism, the Green functor; similarly, Green counterparts are obtained by observing the behavior of primitive idempotents under restriction. Thus, the correspondence for Mackey functors becomes a functorial counterpart to Green's classical correspondence. This perspective unifies different approaches within a single framework and reveals the structural importance of internal endomorphisms in equivariant algebra.

The importance of the endomorphism Green functor extends beyond Green correspondence. Green's functors are fundamental algebraic objects in many areas, including biset functor theory, Burnside rings, and representation theory-based Mackey categories. Therefore, the internal structure of endomorphism Green functor is an important tool in studying decomposition phenomena, projectivity, defect groups, and other structural properties. For instance, identifying a Mackey functor's vertex through its endomorphism Green functor allows the transfer of many classical tools, e.g., relative projectivity and source modules, into the domain of functor categories. Furthermore, understanding how conjugation interacts with endomorphisms is critical to determining whether a Mackey functor is irreducible or whether two functors belong to the same Green correspondence class (Sasaki, 1982; Thévenaz & Webb, 1995; Uc, 2008).

This chapter is structured to increase accessibility while maintaining full mathematical rigor. First, we give the definition of the Green functor. Next, we give the definition of the endomorphism Green functor for a Mackey functor M and explicitly specifying the restriction, transfer, and conjugation maps on each component $\mathrm{End}_H(M)$. We then demonstrate that these maps satisfy the Mackey axiom, using a careful analysis of double coset decompositions and the functorial behavior of morphisms. We also verify the Frobenius axiom highlighting how compatibility between transfer and restriction manifests at the level of internal hom-objects. Finally, we discuss the significance of these results.

The aim of this review is not only to formalize the structure of the endomorphism Green functor, but also to highlight how concepts from classical representation theory are transferred to functor categories. By offering a unified conceptual framework, this chapter positions the endomorphism Green

functor as a fundamental tool in Mackey functor theory, biset functors, and equivariant algebra.

2. THEORETICAL BACKGROUND

The study of the endomorphism Green functor (Sasaki, 1982; Uc, 2008) lies within a broader hierarchy of functorial structures designed to encode restriction, induction, and conjugation phenomena along a subgroup lattice of a finite group. To contextualize the results presented in this section, it is important to explicitly define the relationship between four fundamental concepts: Mackey functors (Thévenaz & Webb, 1995; Uc, 2008), G-functors (Sasaki, 1982), Green functors (Bouc et al., 1997; Thévenaz & Webb, 1995; Uc, 2008), and the endomorphism Green functor of a Mackey functor (Sasaki, 1982; Uc, 2008).

For a finite group G, the Mackey functor is a pair of covariant and contravariant functors that define transfer and restriction maps among the subgroups of G. These maps satisfy the Mackey axiom, which describes the linearity conditions and the interaction between induction and restriction via double coset decompositions (Thévenaz & Webb, 1995; Uc, 2008). Mackey functor generalizes many classical structures such as fixed-point functors, cohomology functors, and Burnside rings, offering a unifying framework for equivariant algebraic structures.

In Sasaki's definition (Sasaki, 1982), a G-functor is a Mackey functor equipped with an additional family of conjugation maps that satisfy the appropriate consistency conditions. This additional structure allows the functor to respond naturally to the conjugation effect of G. Every Green functor is a G-functor, but not every G-functor carries the richer algebraic properties required of a Green functor.

A Green functor is a ring-valued G-functor such that for each subgroup $H \leq G$, the value $A(H)$ is a unital associative algebra, and the restriction and conjugation maps are algebra homomorphisms. Furthermore, Green functors satisfy the Frobenius reciprocity axioms, which generalize the compatibility between induction and restriction in modular representation theory. These axioms guarantee that transfer images form two-sided ideals and that the induction is compatible with the algebraic structure (Bouc et al., 1997).

Within this hierarchy, the endomorphism Green functor occupies a special position. Given a Mackey functor M, the collection of sets $\mathrm{End}_H(M) = \mathrm{Hom}_{\mathrm{Mack}_k(H)}(\downarrow_H^G M, \downarrow_H^G M)$ across all subgroups $H \leq G$ forms a family of algebras via composition. Restriction, transfer, and conjugation maps can be defined functorially, and as Sasaki has shown, this structure forms a Green functor (Sasaki, 1982; Uc, 2008). Thus, the endomorphism Green functor emerges as a categorical analogue of the endomorphism algebras in modular representation theory.

This conceptual framework allows for the natural extension of Green classical correspondence from modules to Mackey functors. The determination of the vertex of a Mackey functor through primitive idempotents in the endomorphism Green functor exhibits a complete parallel with the classical theory of indecomposable modules. Similarly, Green correspondences are obtained by tracing the behavior of these idempotents under restriction. This categorical perspective not only unifies ideas from representation theory but also reveals structural similarities between modules and functors.

This background forms the theoretical basis for the results developed in this section and highlights the central role of the endomorphism Green functor in equivariant algebra and functor categories.

3. GREEN FUNCTOR

A Green functor for G over R is defined as a Mackey functor A such that, for every subgroup H in $S(G)$, the component $A(H)$ is equipped with a unital associative R-algebra structure. Here, $S(G)$ denotes the family of all subgroups of G. These structures are subject to the following axioms:

- All restriction maps $r_K^H: A(H) \to A(K)$ and the conjugation maps $c_H^g: A(H) \to A(K)$ are unitary homomorphisms of R-algebras.
- (Frobenius Axiom) For all $K \subseteq H$, $\alpha \in A(K), \beta \in A(H)$, then

$$t_K^H(\alpha . r_K^H(\beta)) = t_K^H(\alpha).\beta$$

$$t_K^H(r_K^H(\beta).\alpha) = \beta . t_K^H(\alpha)$$

It should be stressed that t_K^H does not, in general, define a ring homomorphism. In fact, the Frobenius axiom ensures that the image of t_K^H is a two sided ideal in $A(H)$. The expressions occurring in the Frobenius axiom are often known as the projection formulas (Bouc et al., 1997; Uc, 2008).

Since the conjugation maps are unitary homomorphisms of R-algebras, G acts on $\prod_{H \in S(G)} A(H)$ as a group of algebra automorhisms, and in particular $\bar{N}(H)$ acts on $A(H)$ as a group of algebra automorphisms. So, $A(H)$ is an $\bar{N}(H)$-algebra, and in particular $A(1)$ is equipped with an action of G by R-algebra automorphisms (Bouc et al., 1997; Uc, 2008).

Furthermore, there is a natural notion of a morphism between Green functors: a morphism ϕ from the Green functor A to the Green functor B is a morphism of Mackey functors such that, for any subgroup H of G, the morphism $\phi_H: A(H) \to B(H)$ is a morphism of rings. The morphism ϕ is said to be unitary if the

morphism ϕ_H preserves the unit for all H. It is enough that morphism ϕ_G preserves the unit, since

$$\phi_G(1_{A(H)}) = \phi_G(r_H^G)1_{A(G)} = r_H^G\phi_G(1_{A(G)}) = r_H^G 1_{B(G)} = 1_{B(H)}.$$

A module over the Green functor A, or A-module, is defined as a Mackey functor M for the group G, such that for any subgroup H of G, the module M(H) has a structure of A(H)-module with unit. Furthermore, the structure must be compatible with the Mackey structure, in the following sense:

- If $x \in G$ and $K \subseteq G$, let $m \mapsto^x m$ be the conjugation by x from M(K) to $M({}^xK)$. If $a \in A(K)$ and $M \in m(K)$, then ${}^x(a.m) = {}^x(a).{}^a(m)$.
- If $H \subseteq K$ are subgroups of G, if $a \in A(K)$ and $m \in M(K)$, then $r_H^K(a.m) = r_H^K(a).r_H^K(m)$.
- In the same conditions, if $a \in A(K)$ and $m \in M(H)$, then

  $$a.t_H^K(m) = t_H^K(r_H^K(a).m)$$

  and if $a \in A(H)$ and $m \in M(K)$, then

  $$t_H^K(a).m = t_H^K(a.r_H^K(m)).$$

A morphism ϕ from the A-module M to the A-module N is a morphism of Mackey functors from M to N such that any subgroup H of G, the morphism ϕ_H is a morphism of A(H)-modules (Bouc et al., 1997; Thévenaz & Webb, 1995; Uc, 2008):.

We now introduce another category, denoted $\mathcal{A}_k(G)$, which we define as a subcategory of $\mathrm{Mack}_k(G)$ as follows:

Definition 3.1. Let A, B be Green functors where G is a group. Then a ring homomorphism $\psi = (\theta_H)_{H\subseteq G}: A \to B$ is a morphism between Green functors such that each θ_H is an algebra of $\mathrm{Mack}_k(G)$ whose objects are all Green functors and morphisms are ring homomorphisms (Bouc et al., 1997; Uc, 2008):.

A fundamental example of a Green functor is given by $\mathrm{End}(M)$, arising from any Mackey functor M via the following procedure

$$\mathrm{End}(M)(H) = \mathrm{End}_H(M) = \mathrm{Hom}_{\mathrm{Mack}(H)}(\downarrow_H^G M, \downarrow_H^G M)$$

(Sasaki, 1982; Thévenaz & Webb, 1995; Uc, 2008). We will examine $\mathrm{End}(M)$ in the next section.

4. ENDOMORPHISM GREEN FUNCTOR

Let G be a finite group and M a Mackey functor. In this section, we investigate the Green functor defined by Sasaki (Sasaki, 1982), referred to as the endomorphism Green functor associated with a Mackey functor M (Sasaki, 1982; Thévenaz & Webb, 1995; Uc, 2008). The endomorphism Green functor plays a crucial role in the Green correspondence for Mackey functors, as the vertex of a Mackey functor M is defined to be the vertex of its associated endomorphism Green functor (Sasaki, 1982; Thévenaz & Webb, 1995; Uc, 2008).

We start by introducing the notion of the endomorphism Green functor and subsequently demonstrate that it complies with the axiomatic framework of Green functors.

Definition 4.1. Let M be a Mackey functor for G over k. Then the Green functor $\mathrm{End}_H(M) = (\mathrm{End}_H(M), T, R, C)$ is defined as follows. For each $H \subseteq G$ we define $\mathrm{End}_H(M) = \mathrm{Hom}_{\mathrm{Mack}_k(H)}(\downarrow_H^G M, \downarrow_H^G M)$, the set of morphisms from $\downarrow_H^G M$ to $\downarrow_H^G M$ in $\mathrm{Mack}_k(H)$. Let $H \subseteq K \subseteq G$ and $g \in G$. Define the transfer map; $T_H^K: \mathrm{End}_H(M) \to \mathrm{End}_K(M): \theta \mapsto T_H^K(\theta)$ as follows. Writing $(\theta_Y)_{Y \subseteq H} \mapsto ((T_H^K(\theta))_L)_{L \subseteq K}$ then, for $L \subseteq K$, the map $(T_H^K(\theta))_L: M(L) \to M(L)$ is such that, for $x \in M(L)$, we have

$$x \mapsto \sum_{HgL \subseteq K} t^{H}_{H \cap {}^{g}L}\, c^{g} \theta_{H^{g} \cap L} r^{H^{g}}_{H^{g} \cap L} c_{H}^{g^{-1}}(x).$$

Define the restriction map; $R^{K}_{H}: End_{K}(M) \to End_{H}(M): \psi \mapsto R^{K}_{H}(\psi)$ as follows. Writing $(\psi_{Y})_{Y \subseteq K} \mapsto ((R^{K}_{H}(\psi))_{D})_{D \subseteq H}$ then for $E \subseteq K$, the map $(R^{K}_{H}(\psi))_{D}: M(E) \to M(D)$ is such that, for $y \in M(D)$, we have $y \mapsto \psi_{D}(y)$. Define the conjugation map; $C^{g}_{H}: End_{H}(M) \to End_{{}^{g}H}(M): \varphi \mapsto C^{g}_{H}(\varphi)$ as follows. Writing $(\varphi_{Y})_{Y \subseteq K} \mapsto ((C^{g}_{H}(\varphi))_{E})_{E \subseteq {}^{g}H}$ then for $E \subseteq K$, the map $(C^{G}_{H}(\varphi))_{E}: M(E) \to M(E)$ is such that, for $z \in M(E)$, we have $z \mapsto C^{g^{-1}}_{{}^{g}E} \varphi_{{}^{g}E} C^{g}_{E}(z)$ (Sasaki, 1982; Uc, 2008).

We now proceed to demonstrate in detail that the endomorphism Green functor $End_{G}(M)$ satisfies the full collection of axioms required of a Green functor, thereby confirming that it fits naturally into the general framework of Green functor theory.

Theorem 4.2. If M is a Mackey functor for the group G, then $(End_{G}(M), T, R, C)$ is a Green functor (Sasaki, 1982; Uc, 2008).

Proof. Let M be a Mackey functor for G.

(1) For $L \leq K \leq H$, $R^{K}_{L} R^{H}_{K} = R^{H}_{L}$.

Indeed, if $D \subseteq K$, $m \in M(D)$, and $\varphi \in End_{H}(M)$, then $R^{H}_{K}(\varphi) \in End_{K}(M)$ satisfies

$$(R^{H}_{K}(\varphi))(m) = (\varphi_{D})_{D \subseteq K}(m).$$

For $E \subseteq L$ and $R^{H}_{K} \in End_{K}(M)$, we get

$$\begin{aligned} R^{K}_{L}(R^{H}_{K}(\varphi))(m) &= (((\varphi)_{D})_{E})_{D \subseteq K, E \subseteq L}(m) = (\varphi_{E})_{E \subseteq L}(m) \\ &= (R^{H}_{L}(\varphi))(m) \end{aligned}$$

where $\varphi \in End_{H}(M)$.

(2) For $L \leq K \leq H$, $T^{K}_{H} T^{K}_{L} = T^{L}_{H}$.

Indeed, if $S \subseteq K$, $m \in M(S)$, and $\varphi \in End_L(M)$, then $T_L^K(\varphi) \in End_K(M)$ satisfies

$$(T_L^K(\varphi)(m))_S = \sum_{SkL \subseteq K, k \in K} t^S_{S \cap {}^k L}\, c^k \varphi_{S^k \cap L} r^{S^k}_{S^k \cap L} c_S^{k^{-1}}(m).$$

If $R \subseteq K$, $n \in M(R)$ and $\psi \in End_K(M)$, then $T_K^H(\psi) \in End_H(M)$ satisfies

$$(T_K^H(\psi)(n))_R = \sum_{RhK \subseteq H, h \in H} t^R_{R \cap {}^h K}\, c^h \psi_{R^h \cap K} r^{R^h}_{R^h \cap K} c_R^{k^{-1}}(n).$$

If $R \subseteq H$, $n \in M(R)$ and $\varphi \in End_L(M)$, then

$$\begin{aligned}(T_K^H(T_L^K(\psi)(n))_L &= \sum_{RhK \subseteq H, h \in H} t^R_{R \cap {}^h K}\, c^h (t_L^K)_{R^h \cap K} r^{R^h}_{R^h \cap K} c_R^{k^{-1}}(n)\\ (T_L^K(\psi)(n))_{R^h \cap K} &= \sum_{(R^h \cap K)kL \subseteq K, h \in K} t^{R^h \cap K}_{R^h \cap K \cap {}^k L}\, c^k \psi_{R^{hk} \cap K^k \cap L} r^{R^{hk} \cap K^k}_{R^{hk} \cap K^k \cap L} c^{k^{-1}}(n)\end{aligned}$$

So,

$$\begin{aligned}(T_K^H(T_L^K(\psi)) &= \sum_{(R^h \cap K)kL \subseteq K, RhK \in H} t^R_{R \cap {}^h K}\, c^h t^{R^h \cap K}_{R^h \cap K \cap {}^k L} c^k \psi_{R^{hk} \cap K^k \cap L} r^{R^{hk} \cap K^k}_{R^{hk} \cap K^k \cap L} c^{k^{-1}} r^{R^h}_{R^h \cap K} c_R^{h^{-1}}\\ &= \sum_{(R^h \cap K)kL \subseteq K, RhK \in H} t^R_{R \cap {}^h K}\, t^{R \cap {}^h K}_{R \cap {}^x K \cap {}^x L} c^x \psi_{R^x \cap K \cap L} c^{x^{-1}} r^{R \cap {}^h K}_{R \cap {}^h K \cap {}^x L} r^R_{R \cap {}^h K}\\ &= \sum_{RxL \subseteq H} t^L_{R \cap {}^x (H \cap L)}\, c^x \psi_{R^x \cap K \cap L} c^{x^{-1}} r_{R \cap {}^x (H \cap L)}.\end{aligned}$$

where $x = hk$.

The conclusion is exactly what we asserted, because as k and h vary over double coset representatives $RkK \subseteq H$ and $(R^h \cap K)hL \subseteq H$, then $x = hk$ exhaust the set of double coset representatives $RkK \subseteq H$.

(3) For a finite group H, $R_H^H = id_{End_H(M)}$.

If $D \leq H$, $m \in M(D)$ and $\psi \in End_H(M)$, then $R_H^H(\psi) \in End_H(M)$ satisfies

$$(R_H^H(\psi))(m) = (\psi_D)_{D \subseteq H}(m).$$

Since $(\psi_D)_{D \subseteq H}$ is a family of homomorphisms over $D \subseteq H$, then

$$(\psi_D)_{D\subseteq H}(m) = \psi(m)$$

as asserted above.

(4) For a finite group H, $T_H^H = id_{End_H(M)}$.

Indeed, if $S \subseteq H$, $m \in M(S)$ and $\psi \in End_H(M)$, then $T_H^H(\psi) \in End_H(M)$ satisfies

$$\begin{aligned}
T_H^H(\psi)(m) &= \sum_{ShH\subseteq H, h\in S} t^S_{S\cap {}^hH}\, c^h \psi_{S^h\cap H} r^{S^h}_{S^h\cap H} c_S^{h^{-1}}(m).\\
&= \sum_{ShH\subseteq H, h\in S} t^S_S\, c^h_{S^h\cap H} \psi_{S^h\cap H} r^{S^h}_{S^h\cap H} c_S^{h^{-1}}(m)\\
&= \sum_{ShH\subseteq H, h\in S} t^S_S\, c^h_{S^h} \psi_{S^h} r^{S^h}_{S^h} c_S^{h^{-1}}(m)\\
&= \sum_{ShH\subseteq H, h\in S} \psi_{S^h}(m)\\
&= \sum_{ShH\subseteq H, h\in H} \psi_{S^h}(m)\\
&= \psi(m)
\end{aligned}$$

as previously claimed.

(5) For a finite group G with a subgroup H, we have

$$C_H^{gh} = C^g_{{}^hH} C_H^h \text{ where } h, g \in G.$$

Indeed, if $m \in M(E)$, $E \subseteq^{gh} H$ and $\alpha \in End_H(M)$, then $C_H^{gh}(\alpha) \in End_H(M)$ satisfies

$$\begin{aligned}
(C_H^{gh})(m) &= c_E^{gh} \alpha_{E^{gh}} c^{h^{-1}g^{-1}}_{{}^{gh}E}(m)\\
&= c^g_{{}^hE}(c_E^h \alpha_{E^{gh}} c^{h^{-1}}_{g^{-1}E}) c_E^{g^{-1}}(m)\\
&= c^g_{{}^hE}(C_H^H(\alpha)_{E^{gh}}) c_E^{g^{-1}}(m)\\
&= C^g_{{}^hH} C_H^h(m).
\end{aligned}$$

(6) For a finite group H and $h \in H$, $C^h: \mathrm{End}_H(M) \to \mathrm{End}_H(M)$ is the identity.

Indeed, if $m \in M(E)$, where $E \subseteq^h H = H$, and if $\theta \in \mathrm{End}_H(M)$, then

$$\begin{aligned}(C_H^h(\theta))(m) &= c_{h_E}^{h^{-1}}(\theta_{h_E})_{h_{E\subseteq H}} c_E^h(m)\\ &= \theta(m)\end{aligned}$$

with $(\theta_{h_E})_{h_{E\subseteq H}}$ denoting the corresponding family of homomorphisms.

(7) Let G be finite group, $K \subseteq H \subseteq G$, and $g \in G$. Then, we have

$$C_K^g R_K^H = R_{g_K}^{g_H} C_H^g.$$

Indeed, if $D \subseteq K$, $E \subseteq^g K$, $m \in M(D)$ and $\alpha \in \mathrm{End}_H(M)$, then

$$\begin{aligned}C_K^g R_K^H(\alpha)(m) &= C_K^g(\alpha_D)(m)\\ &= C_{g_E}^{g^{-1}}(\alpha_D)_{g_E} C_E^g(m)\\ &= C_{g_E}^{g^{-1}} \alpha_{g_E} C_E^g(m)\\ &= (C_{g_Y}^{g^{-1}} \alpha_{g_Y} C_Y^g)_E(m)\\ &= R_{g_K}^{g_K}(C_{g_Y}^{g^{-1}} \alpha_{g_Y} C_Y^g)(m)\\ &= R_{g_K}^{g_H} C_H^g(\alpha)(m)\end{aligned}$$

where $Y \in^g H$.

(8) (Mackey axiom) Let $\theta \in \mathrm{End}_H(M)$. If $L, K \subseteq H$, then we have

$$R_H^L T_H^K(\theta) = \sum_{LgK\subseteq H, g\in H} T_{L\cap g_k}^L R_{L\cap g_K}^{g_K} c_K^g(\theta).$$

Indeed, we must prove that for any $X \subseteq L$

$$(R_H^L T_H^K)_X(x) = \sum_{LgK\subseteq H, g\in H} (T_{L\cap g_k}^L R_{L\cap g_K}^{g_K} C_K^g(\theta))_X(x)$$

where $x \in L$. We now demonstrate that the expressions on the left-hand side (LHS) and the right-hand side (RHS) are equal. LHS is the following:

$$\begin{aligned}(R_H^L T_H^K(\theta))_X(x) &= R_H^L(T_H^K(\theta))_X(x)\\ &= (T_K^H(\theta))_X(x)\\ &= \sum_{XgK\subseteq H} t^X_{X\cap {}^gK}\, c^g \theta_{X^g\cap K} r^{X^g}_{X^g\cap K} c_X^{g^{-1}}(x)\end{aligned}$$

RHS is the following:

$$\sum_{LgK\subseteq H,g\in H}(T^L_{L\cap {}^gK} R^{{}^gK}_{L\cap {}^gK} C^g_K(\theta))_X(x) = \sum_{LgK\subseteq H,g\in H}(T^L_{L\cap {}^gK}\left(R^{{}^gK}_{L\cap {}^gK} C^g_K(\theta)\right))_X(x)$$

$$= \sum_{LgK\subseteq H}\sum_{Xu(L\cap {}^gK)\subseteq L} t^X_{X\cap {}^u(L\cap {}^gK)}\, c^u (C^g_K(\theta))_{X^u\cap (L\cap {}^gK)} r^{X^u}_{X^u\cap (L\cap {}^gK)} c_X^{u^{-1}}(x)$$

$$= \sum_{LgK\subseteq H}\sum_{Xu(L\cap {}^gK)\subseteq L} t^X_{X\cap {}^u(L\cap {}^gK)}\, c^u (C^g_K(\theta))_{X^u\cap (L\cap {}^gK)} r^{X^u}_{X^u\cap (L\cap {}^gK)} c_X^{u^{-1}}(x)$$

$$= \sum_{LgK\subseteq H}\sum_{Xu(L\cap {}^gK)\subseteq L} t^X_{X\cap {}^u(L\cap {}^gK)}\, c^u c^g(\theta)_{(X^u\cap (L\cap {}^gK))^g} c^{g^{-1}} r^{X^u}_{X^u\cap (L\cap {}^gK)} c^{u^{-1}}(x)$$

$$= \sum_{LgK\subseteq H, Xu(L\cap {}^gK)\subseteq L} t^X_{X\cap {}^u(L\cap {}^gK)}\, c^{ug}(\theta)_{(X^{ug}\cap (L\cap {}^gK))^g} r^{X^{ug}}_{X^{ug}\cap (L\cap {}^gK)^g} c^{g^{-1}u^{-1}}(x)$$

$$= \sum_{XgK\subseteq H} t^X_{X\cap {}^gK}\, c^g \theta_{X^g\cap K} r^{X^g}_{X^g\cap K} c_X^{g^{-1}}(x)$$

because u and g runs over $Xu(L\cap {}^gK)$ and LgK, respectively, then ug runs over XugK. Since $X\subseteq L$ and $u\in L$, then ug runs over XgK. It follows that the left-hand side and the right-hand side are indeed equal.

(9) (Frobenius axiom) If $K\subseteq H$, $\alpha\in End_K(M), \beta\in End_H(M)$, then the following multiplicative structures are both satisfied:

$$T_K^H(\alpha.R_K^H(\beta)) = T_K^H(\alpha).\beta$$

$$T_K^H(R_K^H(\beta).\alpha) = \beta.T_K^H(\alpha)$$

Indeed, for the first assertion of the Frobenius axiom, we verify that the left-hand side coincide with the RHS. Let $S\subseteq H$.

LHS:

$$T_K^H(\alpha.R_K^H(\beta)) = \sum_{ShK\subseteq H,h\in H} t^S_{S\cap {}^hK}\, c^h(\alpha.R_K^H(\beta))_{S^h\cap K} r^{S^h}_{S^h\cap K} c_S^{h^{-1}}$$

$$= \sum_{ShK\subseteq H,h\in H} t^S_{S\cap {}^hK}\, c^h \alpha_{S^h\cap K}(R_K^H(\beta))_{S^h\cap K} r^{S^h}_{S^h\cap K} c_S^{h^{-1}}$$

$$= \sum_{ShK\subseteq H,h\in H} t^S_{S\cap {}^hK}\, c^h \alpha_{S^h\cap K}\beta_{S^h\cap K} r^{S^h}_{S^h\cap K} c_S^{h^{-1}}$$

RHS:

$$T_K^H(\alpha).\beta = \left(\sum_{ShK\subseteq H,h\in H} t^S_{S\cap {}^hK}\, c^h \alpha_{S^h\cap K} r^{S^h}_{S^h\cap K} c_S^{h^{-1}}\right).\beta_H$$

$$= \sum_{ShK\subseteq H,h\in H} t^S_{S\cap {}^hK}\, c^h \alpha_{S^h\cap K}\beta_{S^h\cap K} r^{S^h}_{S^h\cap K} c_S^{h^{-1}}$$

by application of conjugation and restriction on β_H. Because the left-hand side agrees with the right-hand side, the first statement of the Frobenius axiom is satisfied.

In a similar manner, the endomorphism Green functor also satisfies the second assertion of the Frobenius axiom. We may therefore conclude that the endomorphism Green functor fulfils all the axioms required in the definition of a Green functor. Hence, $End_G(M)$ can be regarded as a fully valid Green functor, compatible with the underlying Mackey functor structure and the axiomatic operations of restriction, induction, and conjugation (Uc, 2008).

Example 4.3. In this example, we consider the Klein four group $V_4 = \{1, a, b, ab\}$ to illustrate the structure and operation of the endomorphism Green functor through a clear calculation. This group is abelian, and each element has order 2. The subgroup lattice $\{1\}$ consists of three 2-order subgroups, $H_1 = \langle a\rangle, H_2 = \langle b\rangle, H_3 = \langle ab\rangle$, and the whole group V_4. Since V_4 is abelian, all conjugation operations are trivial; this allows for a simplified examination of the internal algebraic structure of the endomorphism Green functor.

We consider a Mackey functor M obtained from the permutation module $k[V_4/1]$. Explicitly, $M(1) \cong k$, $M(H_i) \cong k^2$ for each subgroup of order two, and $M(V_4) \cong k^4$. The restriction maps $M(V_4) \to M(H_i)$ correspond to summing coordinates along cosets ofH_i, while transfer maps $M(H_i) \to M(V_4)$ duplicate coordinates along cosets in the opposite direction. These linear structures allow us to compute the endomorphism Green functor $\mathrm{End}_G(M)$, whose value at each subgroup H is $\mathrm{End}_G(M)(H) = \mathrm{End}_{\mathrm{Mack}_k(H)}(\downarrow_H^G M)$ the algebra of natural transformations of the restricted Mackey Functor $\downarrow_H^G M$.

For $H = 1$, we have $\mathrm{End}_G(M)(1) \cong \mathrm{End}_k(k) \cong k$, since $M(1)$ is one-dimensional. For any order-two subgroup H_i, the Mackey restriction $\downarrow_{H_i}^G M$ behaves as a two-point permutation representation, giving $\mathrm{End}_G(M)(H_i) \cong M_2(k)$, the full 2×2 matrix algebra. At the full group V_4, the functor $M(V_4) \cong k^4$ with decomposition into four orbits gives $\mathrm{End}_G(M)(V_4) \cong M_4(k)$. Each algebra $\mathrm{End}_G(M)(H)$ is thus explicitly computable, and together these algebras form the values of the endomorphism Green functor.

The restriction maps $R_K^H: \mathrm{End}_G(M)(H) \to \mathrm{End}_G(M)(K)$ arise by pre- and post-composition with the restriction maps of M. Similarly, transfer maps T_K^H correspond to conjugation of endomorphisms through the transfer structure of M. Since conjugation in V_4 is trivial, the conjugation maps $C_g: \mathrm{End}_G(M)(H) \to \mathrm{End}_G(M)(H)$ for $g \in V_4$ reduce to the identity. One may verify directly that these maps satisfy the axioms of a Green functor: compatibility of restriction with multiplication, Frobenius reciprocity expressed via the identity $T_K^H(\alpha . R_K^H(\beta)) = T_K^H(\alpha) . \beta$, and associativity of endomorphism composition.

This example clearly demonstrates how the endomorphism Green functor organizes the internal algebraic structure of a Mackey functor across all subgroups of a finite group. Even in the simple case of V_4, the functor organizes the matrix algebras and homomorphisms reflecting the transfer-restriction structure. Such calculations provide a powerful intuition for understanding the fundamental role of the endomorphism Green functor in analyzing the behavior and internal symmetries of Mackey functors.

5. CONCLUSION

The endomorphism of the Green functor plays a central role in extending Green correspondence from the classical module theory to Mackey functors, a broader and more flexible structure. This work establishes a robust algebraic foundation for the study of vertex, correspondence, and decomposition structures within functor categories by demonstrating that the endomorphism structure rigorously satisfies all the axioms of a Green functor, including the Mackey axiom, Frobenius reciprocity, and the internal compatibility of constraint, transfer, and conjugation maps.

The results show that many structural concepts associated with modular representation theory; for example, primitive idempotent decompositions and related projectivity; can be naturally generalized when the internal endomorphism structure is added to Mackey functors. In particular, the determination of the vertex of a Mackey functor through primitive idempotents in the endomorphism Green functor is identical to the classical theory of indecomposable modules. This functorial perspective clarifies the internal algebraic behavior of Mackey functors and unifies many ideas in representation theory under a single categorical framework.

This approach has given rise to numerous promising research directions. One of these is investigating how endomorphism Green functors interact with biset functors, particularly in the context of block decompositions and defect group structures. Another line of research is the development of novel structural tools such as functorial radicals or homological invariants that can be derived from the endomorphism Green functor. Extending the theory to infinite groups, derived Mackey functors may reveal deeper structural relationships. Finally, developing computational methods for calculating vertices and Green correspondents using endomorphism Green functors could contribute to clear classification results for small or complex groups.

In conclusion, the endomorphism Green functor offers a conceptually elegant and structurally powerful tool for extending Green correspondence to the level of Mackey functors. The richness of this field suggests it will continue to guide future developments in representation theory and functor categories.

REFERENCES

Alperin, J. L. (1982). Local representation theory. Cambridge: Cambridge University Press.

Bouc, S., Dold, A., & Takens, F. (1997). Green functors and G-sets (Vol. 1671). Springer.

Green, J. A. (1964). A transfer theorem for modular representations. Journal of Algebra, 1, 73–84.

Sasaki, H. (1982). Green correspondence and transfer theorems of Wielandt type for G-functors. Journal of Algebra, 79, 98–120.

Thévenaz, J., & Webb, P. (1995). The structure of Mackey functors. Transactions of the American Mathematical Society, 347, 1865–1963.

Uc, M. (2008). Green correspondence for Mackey functors (Master's thesis). The Institute of Engineering and Science, İhsan Doğramacı Bilkent University, Ankara, Türkiye.

ON COMPLEX FIBONACCI AND LUCAS HYBRID NUMBERS

Ali Imad Mohammed QARAH BASH[1]

Anıl ALTINKAYA[2*]

1. INTRODUCTION

W. R. Hamilton introduced quaternions in order to extend complex numbers to a three-dimensional space. The quaternion set constitutes a real algebra in which multiplication is not commutative. In this algebra, a quaternion is expressed in the form [2]:

$$\mathbb{H} = \{q = a + bi + cj + dk : a, b, c, d \in \mathbb{R}\}, \quad (1.1)$$

where $i^2 = j^2 = k^2 = -1$. One of the most striking properties is that multiplication is not commutative, meaning that in general, $ij \neq ji$. This structure allows transformations to be represented more compactly compared to matrices. Therefore, quaternions are widely used in computer graphics, robotics, aeronautics, and all fields where 3D rotations are computed. The $n-th$ Fibonacci and Lucas quaternions were described by the following definitions [3]:

$$\mathbb{HF}_n = F_n + F_{n+1}i + F_{n+2}j + F_{n+3}k, \quad (1.2)$$

$$\mathbb{HL}_n = L_n + L_{n+1}i + L_{n+2}j + L_{n+3}k, \quad (1.3)$$

[1] Student, Gazi University, Graduate School of Natural and Applied Sciences, ORCID: 0009-0001-3232-6967.

[2] Asst. Prof., Gazi University, Faculty of Science, Department of Mathematics, ORCID: 0000-0003-2382-6596.

* Corresponding Author

where $F_n = F_{n-1} + F_{n-2}$, $F_0 = 0, F_1 = 1$ and $L_n = L_{n-1} + L_{n-2}, L_0 = 2, L_1 = 1$.

The literature includes several studies related to Fibonacci and Lucas quaternions [4-9]. According to [4], Halici focused on the quaternionic extensions of the Fibonacci and Lucas sequences and derived their generating functions as well as Binet-type formulas, enriching the existing literature on number sequences in non-commutative algebraic structures. In [8], the authors gave some characterizations for the Pell quaternions and *k*-Fibonacci quaternions.

Complex Fibonacci numbers were introduced by Horadam, these numbers are simply pairs expressed as [3]:

$$\widetilde{F_n} = F_n + iF_{n+1}, \qquad (1.4)$$

where $i^2 = 1$. The discovery of complex Fibonacci numbers led to many studies in the field of complex analysis and number theory. Complex Fibonacci numbers form interesting spiral-like geometric shapes in the complex plane and produce visually and analytically rich results in areas such as dynamical systems, fractal structures, and chaos theory. After the discovery of complex numbers, many authors have studied on complex Fibonacci quaternions. Some of these are [11–14]. In [11], Halici specified the complex Fibonacci and Lucas quaternions and discovered the relations between these quaternions. In [14], Aydin denoted the bicomplex Fibonacci quaternions and studied some algebraic properties of these numbers.

In [1], M. Özdemir introduced hybrid numbers as an algebraic structure that unifies complex, dual, and hyperbolic numbers, given by:

$$\mathbb{K} = \{a + bi + c\varepsilon + dh : i^2 = -1, \varepsilon^2 = 0, h^2 = 1\}, \qquad (1.5)$$

$$FH_n = F_n + F_{n+1}\, i + F_{n+2}\varepsilon + F_{n+3}h (1.6)$$

$$LH_n = L_n + L_{n+1}\, i + L_{n+2}\varepsilon + L_{n+3}h. (1.7)$$

In [15], Liana gave some properties of Horadam-type hybrid sequences, including their Binet representation and generating function.

This study first defines complex Fibonacci-type and complex Lucas-type hybrid numbers, and presents a detailed account of their fundamental algebraic properties. Following these definitions, the Binet formula for complex Fibonacci-type hybrid sequences is derived, and the Cassini identity, one of the classical Fibonacci identities, is proven in the context of this new number system. Finally, the generating function for complex Fibonacci-type hybrid sequences is derived, offering an alternative approach for analytically expressing them. Thus, the study expands the range of applications of hybrid numbers in the literature and reveals new and original results for complex Fibonacci-type and Lucas-type hybrid sequences, which have not been previously studied.

2. PRELIMINARIRES

The complex numbers are defined by the set $\mathbb{C} = \{z = z_1 + iz_2 : z_1, z_2 \in \mathbb{R},\ i^2 = -1\}$. The addition and multiplication on this set are given as follows [16]:

$$(z_1 + iz_2) + (w_1 + iw_2) = (z_1 + w_1) + i(z_2 + w_2),$$
$$(z_1 + iz_2).(w_1 + iw_2) = (z_1w_1 - z_2w_2) + i(z_1w_2 + z_2w_1).$$

For any complex number $z = z_1 + iz_2$, $z_1 =$

·	1	i	ε	h
1	1	i	ε	h
i	i	-1	1-h	ε+i
ε	ε	h+1	0	-ε
h	h	-ε-i	ε	1

$\big(Re(z)\big), z_2 = (Im(z))$. The hybrid number set is defined by [1]:

For any hybrid number $a = a_0 + a_1 i + a_2 \varepsilon + a_3 h$,

the scalar component of a is represented as

$$S_a = a_0,$$

and the vector component is represented as

$$V_a = a_1 i + a_2 \varepsilon + a_3 h.$$

Given two hybrid numbers $a = a_0 + a_1 i + a_2 \varepsilon + a_3 h$, $b = b_0 + b_1 i + b_2 \varepsilon + b_3 h$, their addition is written as

$$a + b = S_{(a+b)} + V_{(a+b)}.$$

Product of two hybrid numbers is defined by

$$ab = (a_0 + a_1 i + a_2 \varepsilon + a_3 h)(b_0 + b_1 i + b_2 \varepsilon + b_3 h), \quad (2.2)$$

which is obtained by performing the algebraic expansion in the standard way [1]. The product of scalar is defined as [1]:

$$\bar{a} = S_a - V_a.$$

In [10], the authors introduced the Binet's formula for the Fibonacci-type and Lucas-type hybrid numbers as:

$$FH_n = \frac{\widetilde{r_1} r_1^n - \widetilde{r_2} r_2^n}{r_1 - r_2}, \quad (2.3)$$

$$LH_n = \widetilde{r_1} + r_1^n + \widetilde{r_2} r_2^n, \quad (2.4)$$

where $\widetilde{r_1} = 1 + r_1 i + r_1^2 \varepsilon + r_1^3 h$, $r_1 = \frac{1+\sqrt{5}}{2}, r_2 = \frac{1-\sqrt{5}}{2}$.

3. COMPLEX FIBONACCI AND LUCAS HYBRID NUMBERS

Definition 3.1. The n^{th} complex Fibonacci-type and Lucas-type hybrid sequences are defined by

$$\widetilde{FH_n} = FH_n + iFH_{n+1}, \tag{3.1}$$

$$\widetilde{LH_n} = LH_n + iLH_{n+1}, \tag{3.2}$$

respectively.Here $FH_n = F_n + F_{n+1}\,i + F_{n+2}\varepsilon + F_{n+3}h$ and $LH_n = L_n + L_{n+1}\,i + L_{n+2}\varepsilon + L_{n+3}h$ are n^{th} Fibonacci-type and Lucas-type hybrid sequences. i denotes the imaginary unit ($i^2 = -1$), ε denotes the complex unit ($\varepsilon^2 = 0$) and h denotes the hyperbolic unit ($h^2 = 1$).

If the complex Fibonacci hybrid number is arranged according to the previous definition, we get

$$\widetilde{FH_n} = (F_n + F_{n+1}\,i + F_{n+2}\varepsilon + F_{n+3}h) + i(F_{n+1} + F_{n+2}\,i + F_{n+3}\varepsilon + F_{n+4}h)$$

$$=(F_n + iF_{n+1}) + (F_{n+1} + iF_{n+2})i + (F_{n+2} + iF_{n+3})\varepsilon + (F_{n+3} + iF_{n+4})h$$

$$=\widetilde{F_n} + \widetilde{F_{n+1}}i + \widetilde{F_{n+2}}\varepsilon + \widetilde{F_{n+3}}h.$$

Similarly, we can write

$$\widetilde{LH_n} = \widetilde{L_n} + \widetilde{L_{n+1}}i + \widetilde{L_{n+2}}\varepsilon + \widetilde{L_{n+3}}h.$$

Theorem 3.1. Let $\widetilde{FH_n}$ be any complex Fibonacci hybrid number and $\widetilde{LH_n}$ be any complex Lucas hybrid number. Then, we have the following equations:

i) $\widetilde{FH_{n+1}} + \widetilde{FH_n} = \widetilde{FH_{n+2}}$

ii) $\widetilde{LH_{n+1}} + \widetilde{LH_n} = \widetilde{LH_{n+2}}$

iii) $\widetilde{FH_{n-1}} + \widetilde{FH_{n+1}} = \widetilde{LH_n}$

iv) $F\widetilde{H_{n+2}} - F\widetilde{H_{n-2}} = L\widetilde{H_n}$

Proof. i) By applying the addition rule for complex Fibonacci-type hybrid sequences, we get

$$F\widetilde{H_{n+1}} + F\widetilde{H_n} = (FH_{n+1} + iFH_{n+2}) + (FH_n + iFH_{n+1})$$

$$= (FH_{n+1} + FH_n) + i(FH_{n+2} + FH_{n+1})$$

$$= ((F_{n+1} + F_{n+2}\,i + F_{n+3}\varepsilon + F_{n+4}h) + (F_n + F_{n+1}\,i + F_{n+2}\varepsilon + F_{n+3}h) + i((F_{n+2} + F_{n+3}\,i + F_{n+4}\varepsilon + F_{n+5}h) + (F_{n+1} + F_{n+2}\,i + F_{n+3}\varepsilon + F_{n+4}h))$$

$$= (F_{n+1} + F_n) + i(F_{n+2} + F_{n+1})i + (F_{n+3} + F_{n+2})\varepsilon + (F_{n+4} + F_{n+3})h + i((F_{n+2} + F_{n+1}) + (F_{n+3} + F_{n+2})i + (F_{n+4} + F_{n+3})\varepsilon + (F_{n+5} + F_{n+4})h)$$

$$= (F_{n+2} + F_{n+3}i + F_{n+4}\varepsilon + F_{n+5}h) + i(F_{n+3} + F_{n+4}i + F_{n+5}\varepsilon + F_{n+6}h)$$

$$= FH_{n+2} + iFH_{n+3}$$

$$= F\widetilde{H_{n+2}}.$$

ii) Similarly, if we use the addition property of the complex Lucas hybrid number, we get

$$L\widetilde{H_{n+1}} + L\widetilde{H_n} = (LH_{n+1} + iLH_{n+2}) + (LH_n + iLH_{n+1})$$

$$= (LH_{n+1} + LH_n) + i(LH_{n+2} + LH_{n+1})$$

$$= LH_{n+2} + iLH_{n+3}$$

$$= L\widetilde{H_{n+2}}.$$

iii) Considering the identity $F_{n-1} + F_{n+1} = L_n$, we can write

$$F\widetilde{H_{n-1}} + F\widetilde{H_{n+1}} = (FH_{n-1} + iFH_n) + (FH_{n+1} + iFH_{n+2})$$

$$= (FH_{n-1} + FH_{n+1}) + i(FH_n + FH_{n+2})$$

$$= LH_n + iLH_{n+1}$$

$$= \widetilde{LH_n}.$$

iv) Similarly, from the identity $F_{n+2} - F_{n-2} = L_n$, we have

$$\begin{aligned}\widetilde{FH_{n+2}} - \widetilde{FH_{n-2}} &= (FH_{n+2} + iFH_{n+3}) - (FH_{n-2} + iFH_{n-1}) \\ &= (FH_{n+2} - FH_{n-2}) + i(FH_{n+3} - FH_{n-1}) \\ &= LH_n + iLH_{n+1} \\ &= \widetilde{LH_n}.\end{aligned}$$

Theorem 3.2. Let $\widetilde{FH_n}$ be any complex Fibonacci hybrid number and $\widetilde{LH_n}$ be any complex Lucas hybrid number. For each integer $n \geq 0$, the Binet type formulas of $\widetilde{FH_n}$ and $\widetilde{LH_n}$ take the following form:

$$\widetilde{FH_n} = \frac{r_1^* r_1^n - (r_2)^* r_2^n}{r_1 - r_2}, \tag{3.3}$$

$$\widetilde{LH_n} = r_1^* r_1^n + (r_2)^* r_2^n, \tag{3.4}$$

where $r_1^* = \tilde{r}_1(1 + ir_1)$, $\tilde{r}_1 = 1 + r_1 i + r_1^2 \varepsilon + r_1^3 h$ and $(r_2)^* = \tilde{r}_2(1 + ir_2)$, $\tilde{r}_2 = 1 + r_2 i + r_2^2 \varepsilon + r_2^3 h$.

Proof. Using (3.1) and the Binet representation of the Fibonacci-type hybrid sequences, we have

$$\begin{aligned}\widetilde{FH_n} &= FH_n + iFH_{n+1} \\ &= \frac{\tilde{r}_1 r_1^n - \tilde{r}_2 r_2^n}{r_1 - r_2} + i\frac{\tilde{r}_1 r_1^{n+1} - \tilde{r}_2 r_2^{n+1}}{r_1 - r_2} \\ &= \frac{\tilde{r}_1 r_1^n (1 + ir_1) - \tilde{r}_2 r_2^n (1 + ir_2)}{r_1 - r_2} \\ &= \frac{r_1^* r_1^n - (r_2)^* r_2^n}{r_1 - r_2}.\end{aligned}$$

From the equations (3.2) and the Binet representation of the Lucas-type hybrid sequences, we obtain

$$\begin{aligned}\widetilde{LH_n} &= LH_n + iLH_{n+1}\\ &= (\widetilde{r_1} + r_1^n + \widetilde{r_2}r_2^n) + i(\widetilde{r_1}r_1^{n+1} + \widetilde{r_2}r_2^{n+1})\\ &= \widetilde{r_1}r_1^n(1 + ir_1) + \widetilde{r_2}r_2^n(1 + ir_2)\\ &= r_1^* r_1^n + (r_2)^* r_2^n.\end{aligned}$$

Theorem 3.3. Let $\widetilde{FH_n}$ and $\widetilde{LH_n}$ denote the n-th complex Fibonacci-type hybrid sequence and the n-th complex Lucas-type hybrid sequence. When, $n \geq 1$, the Cassini identities of $\widetilde{FH_n}$ and $\widetilde{LH_n}$ are given by:

$$\widetilde{FH_{n-1}}\widetilde{FH_{n+1}} - \widetilde{FH_n}^2 = \frac{(-1)^{n-1}}{\sqrt{5}}(r_1^* r_2^* r_2 - r_2^* r_1^* r_1),$$

$$\widetilde{LH_{n-1}}\widetilde{LH_{n+1}} - \widetilde{LH_n}^2 = (-1)^{n-1}\sqrt{5}\left(\frac{r_1^* r_2^*}{r_2} + \frac{r_2^* r_1^*}{r_1}\right).$$

Proof. By using (3.3) and (3.4), we can calculate the following equations:

$$\begin{aligned}&\widetilde{FH_{n-1}}\widetilde{FH_{n+1}} - \widetilde{FH_n}^2\\ &= \left(\frac{r_1^* r_1^{n-1} - (r_2)^* r_2^{n-1}}{r_1 - r_2}\right)\left(\frac{r_1^* r_1^{n+1} - (r_2)^* r_2^{n+1}}{r_1 - r_2}\right)\\ &\quad - \left(\frac{r_1^* r_1^n - (r_2)^* r_2^n}{r_1 - r_2}\right)^2\\ &= \frac{(r_1^*)^2 r_1^{2n} - r_1^* r_2^* r_1^{n-1} r_2^{n+1} - (r_2)^* r_2 r_2^{n-1} r_1^{n+1} + (r_2^*)^2 (r_2^n)^2}{(r_1 - r_2)^2}\\ &\quad - \frac{(r_1^*)^2 r_1^{2n} - r_1^* r_2^* r_1^n r_2^n - (r_2)^* (r_1)^* r_2^n r_1^n + (r_2^*)^2 (r_2^n)^2}{(r_1 - r_2)^2}\\ &= \frac{r_1^* r_2^* r_1^{n-1} r_2^n (r_1 - r_2) - r_2^* r_1^* r_2^{n-1} r_1^n (r_1 - r_2)}{(r_1 - r_2)^2}\\ &= \frac{r_1^* r_2^* r_1^{n-1} r_2^n - r_2^* r_1^* r_2^{n-1} r_1^n}{r_1 - r_2}\end{aligned}$$

$$= \frac{(-1)^{n-1}}{\sqrt{5}}(r_1^* r_2^* r_2 - r_2^* r_1^* r_1).$$

$$\begin{aligned}\widetilde{LH_{n-1}}\widetilde{LH_{n+1}} - \widetilde{LH_n}^2 &= (r_1^* r_1^{n-1} + r_2^* r_2^{n-1})(r_1^* r_1^{n+1} + r_2^* r_2^{n+1}) \\ &\quad - (r_1^* r_1^n + r_2^* r_2^n)^2 \\ &= (r_1^*)^2 r_1^{2n} + r_1^* r_2^* r_1^{n-1} r_2^{n+1} + \\ &\quad r_2^* r_1^* r_2^{n-1} r_1^{n+1} + (r_2^*)^2 r_2^{2n} - (r_1^*)^2 r_1^{2n} - \\ &\quad r_1^* r_2^* r_1^n r_2^n + r_2^* r_1^* r_2^n r_1^n \\ &= r_1^* r_2^* (-1)^{n-1} \frac{\sqrt{5}}{r_2}\left(\frac{r_1^* r_2^*}{r_2} + \frac{r_2^* r_1^*}{r_1}\right).\end{aligned}$$

Theorem 3.4. Let $\widetilde{FH_n}$ be any complex Fibonacci hybrid number. Then the generating function of $\widetilde{FH_n}$ is given as follows:

$$\begin{aligned}G(x) &= \frac{\widetilde{FH_0} + \mathrm{x}(\widetilde{FH_1} - \widetilde{FH_0})}{1 - x - x^2} \\ &= \frac{(3 - 2\varepsilon + 3h) + x(2 - 2\varepsilon + 2h)}{1 - x - x^2}.\end{aligned}$$

Proof. Suppose that $G(x)$ is a generating function of complex Fibonacci hybrid number $\widetilde{FH_n}$. Then we get,

$$G(x) = \sum_{n=0}^{\infty} \widetilde{FH_n}\, x^n.$$

If we organize this equality, we have

$$\begin{aligned}G(x) &= \widetilde{FH_0} + x\widetilde{FH_1} + x^2\widetilde{FH_2} + \cdots \\ xG(x) &= x\widetilde{FH_0} + x^2\widetilde{FH_1} + x^3\widetilde{FH_2} + \cdots \\ x^2G(x) &= x^2\widetilde{FH_0} + x^3\widetilde{FH_1} + x^4\widetilde{FH_2} + \cdots \\ G(x) - xG(x) - x^2G(x) &= \widetilde{FH_0} + x\left(\widetilde{FH_1} - \widetilde{FH_0}\right) + \\ x^2&\left(\widetilde{FH_2} - \widetilde{FH_1} - \widetilde{FH_0}\right) + \cdots.\end{aligned}$$

So, we can write,

$$G(x) = \frac{\widetilde{FH_0} + \mathrm{x}(\widetilde{FH_1} - \widetilde{FH_0})}{1 - x - x^2} = \frac{(3 - 2\varepsilon + 3h) + x(2 - 2\varepsilon + 2h)}{1 - x - x^2}.$$

4. CONCLUSION

Hybrid number system combines these three different algebraic structures into a single structure, creating a new algebraic structure. While various studies on hybrid numbers have been conducted in the literature, no research exists on complex Fibonacci and complex Lucas hybrid numbers. In the third part of this article, we first define the n-th complex Fibonacci-type hybrid sequence and the n-th complex Lucas-type hybrid sequence. Through these definitions, we clearly demonstrate the relationship of hybrid numbers to complex Fibonacci and Lucas sequences. Then, we derive some fundamental relations for complex Fibonacci-type and complex Lucas-type hybrid numbers and demonstrate the role of these relations within the hybrid number structure. Finally, we prove Binet's formulas for these hybrid numbers and use these formulas to derive the Cassini identities. Showing that the Cassini identities hold in the context of hybrid numbers reveals the similarities and differences between the algebraic properties of hybrid numbers and those of classical Fibonacci-type and Lucas-type sequences. Finally, we find the generating function for complex Fibonacci and complex Lucas hybrid numbers and explain how this function can be used to investigate the analytic properties of hybrid numbers.

REFERENCES

Akyigit, M., Kosal, H. H., Tosun, M. (2013). Split Fibonacci Quaternions., Advances in Applied Clifford Algebras. 23, 535–545.

Brown, J. W. and Churchill, R. V. (2014). Complex Variables and Applications. McGraw-Hill Education, 2 Penn Plaza, New York.

Gungor, M. A., Azak, A. Z. (2017). Investigation of Dual-Complex Fibonacci, Dual-Complex Lucas Numbers and Their Properties. Advances in Applied Clifford Algebras. 27, 3083–3096.

Halici, S. (2012). On Fibonacci Quaternions., Advances in Applied Clifford Algebras, 22, 321–32.

Halici, S. (2013). On Complex Fibonacci Quaternions. Advances in Applied Clifford Algebras. 23, 105–112.

Halici, S., Karata¸s, A. (2017). On a generalization for Fibonacci quaternions. Chaos, Solitons and Fractals. 98, 178–182.

Hamilton, W. R. (1844). On quaternions or on a new system of imagniaries in algebra. Lond. Edinb. Dublin Philos. Mag. J. Sci., 25, 489–495.

Horadam, A. F. (1963). Complex Fibonacci Numbers and Fibonacci Quaternions. The American Mathematical Monthly, 70, 289–291.

Kaya Nurkan, S., Arslan Guven, I. (2015). Dual Fibonacci Quaternions. Advances in Applied Clifford Algebras. 25, 403–414.

Ozdemir, M. (2018). Introduction to hybrid numbers. Adv. Appl. Clifford Algebras. 28(11), 1–32.

Sentürk, G. Y. (2022). Construction of dual-generalized complex Fibonacci and Lucas quaternions. Carpathian Mathematical Publications. 14(2), 406–418.

Szynal-Liana, A. (2018). The Horadam Hybrid Numbers. Discussiones Mathematicae General Algebra and Applications. 38, 91–98.

Szynal-Liana, A., Wloch, I.:Introduction to Fibonacci and Lucas hybrinomials. Complex Variables and Elliptic Equations. 65, 1736–1747 (2019).

Tan, E., Yilmaz, S., Sahin, M. (2016).On a new generalization of Fibonacci quaternions. Chaos, Solitons and Fractals. 82, 1–4.

Torunbalci Aydin, F. (2018). Bicomplex Fibonacci quaternions. Chaos, Solitons and Fractals. 106, 147–153.

Yuce, S, Torunbalci Aydin, F.. (2016). A New Aspect of Dual Fibonacci Quaternions. Advances in Applied Clifford Algebras. 26, 873–884.

THE CONCEPT OF INEQUALITY IN MATHEMATICS: MATHEMATICAL MEANING, HISTORICAL DEVELOPMENT, THEORETICAL POWER, AND DIDACTIC–PHILOSOPHICAL DIMENSIONS

Alaattin AKYAR[1]

1. INTRODUCTION

Mathematics is often seen as the "science of equality." In students' early encounters with mathematics, the main focus is solving equations and ensuring that both sides are equal. This approach presents mathematics mostly as a task of finding the right answer and leads to the idea that mathematical knowledge is about reaching correct results.

However, when we look deeper into mathematical thinking, we see that inequalities play an equally important, often even more fundamental role. Mathematics is not only about determining what is equal but also about understanding what is greater or smaller, what stays within certain limits, and how we can measure being "close enough" in a precise way (Apostol, 1974; Rudin, 1976). In this sense, mathematics deals not only with results but also with behaviors and their boundaries.

In modern analysis, core concepts such as limit, continuity, derivative, and integral are defined using inequality-based structures (Apostol, 1974; Cauchy, 1821/2009; Weierstrass, 1874/1986). Whether a function approaches a value, is continuous, or is integrable depends on satisfying specific

[1] Düzce University, Düzce Vocational School, ORCID: 0000-0003-4759-8313.

inequalities. Concepts like convergence, compactness, and continuity are built upon the idea of "reducing the margin of error as much as desired," and the language used to express this idea is the language of inequalities (Rudin, 1976).

Therefore, inequality is not just a tool using symbols like $<$, $>$, $\leq$, $\geq$ to compare values; it is a theoretical language that organizes mathematical objects, limits behaviors, and makes mathematical precision possible. Yet, this role of inequality is often underestimated. In textbooks and teaching practices, inequalities are usually presented only as technical steps or tools, without highlighting their foundational role in mathematical thought.

However, many modern mathematical definitions cannot be clearly expressed or logically secured without inequalities. In this context, inequality is not just a tool used in mathematics, it is a fundamental way of thinking that makes mathematical knowledge possible.

This chapter aims to explore the mathematical meaning and foundational role of inequality through conceptual, historical, and philosophical lenses. It will examine the historical development of inequality and key turning points that shaped the foundations of analysis. It will also show in detail why key mathematical concepts must be defined using the language of inequalities. Furthermore, it will discuss the theoretical insights provided by classic inequalities such as Cauchy–Schwarz, Hölder, Minkowski, and Jensen, and critically analyze why inequality often fails to gain its deserved central place in math education. Finally, it will explore the difference between the value-neutral use of inequality in mathematics and the moral or ethical meanings attached to the term "inequality" in every day and philosophical contexts highlighting why this distinction is important for mathematical thinking and teaching (Lakatos, 1976;

Tall, 2013; Tall & Vinner, 1981; Ubuz, 1999; Baki, 2018; Altun, 2014; Doruk & Kaplan, 2013; İnam, 1995; Çüçen, 2012).

2. LIMIT: NOT "REACHING" BUT "APPROACHING"

In everyday thinking, a limit is often seen as a quantity "reaching" a certain value. In daily language and early math education, this is expressed as a function or sequence getting closer to a specific point over time. However, this kind of explanation is mathematically vague, it does not tell us how close we get or how that closeness is measured. In modern mathematics, the concept of a limit becomes precise and controllable through inequalities. This precision is given by the classical ε–δ definition of a limit:

$$\forall \varepsilon > 0, \exists \delta > 0 \text{ such that } 0 < |x - a| < \delta \Rightarrow |f(x) - L| < \varepsilon$$

In this definition, the important part is not saying "f(x) becomes L," but showing that the difference between f(x) and L can be made smaller than any ε (Apostol, 1974). Thus, a limit is not about achieving equality but about controlling the difference.

Historically, this idea becomes even clearer. In ancient mathematics, especially in Archimedes' method of exhaustion, values like area and volume were not calculated directly. Instead, they were bounded from above and below, and the gap between them was gradually reduced. Archimedes' method can be seen as an early version of the modern idea of a limit. Here too, the goal was not to "reach" a value but to trap it between two inequalities in a narrowing interval.

The modern form of the limit was formalized in the 19th century during the foundation of analysis by Cauchy and Weierstrass. Weierstrass's ε–δ approach replaced vague ideas like "it looks like it's getting closer" with inequalities that could

be quantitatively controlled (Cauchy, 1821/2009; Weierstrass, 1874/1986).

Philosophically, the concept of a limit clearly shows how mathematics connects precision and approximation. A limit does not aim for absolute equality. Instead, it provides assurance that one can stay within an arbitrarily small error margin. Inequalities are the mathematical language of this "small enough." In this sense, a limit is not just a technical term in analysis, it is a fundamental example of how mathematical thinking works.

2.1. Continuity: A Quantitative Guarantee of Local Behavior

In mathematical intuition, continuity is often associated with the idea that a graph can be "drawn without lifting the pen." While this visual idea is useful in geometric contexts, it is mathematically vague it doesn't specify what a "small" change means or how this smallness is measured. In modern mathematics, continuity is formalized through a precise, inequality-based definition that removes this vagueness. Formal definition: For all $\varepsilon > 0$, there exists $\delta > 0$ such that if $|x - a| < \delta$, then $|f(x) - f(a)| < \varepsilon$.

Here, continuity is not expressed as a visual "smoothness" but as the ability to control how a small change in the input affects the output (Rudin, 1976). In other words, continuity guarantees that the function's local behavior can be controlled within a certain margin of error.

Historically, this approach became important during the 19th-century formalization of analysis. As more pathological examples were discovered, the modern approachwhich separates continuity from visual intuition and reduces it to a system of inequality-based error control—became dominant.

Philosophically, continuity represents the technical side of the idea of "local reliability" in mathematics: the reliability of behavior depends not on exact equalities but on tolerances.

From a teaching perspective, studies in Turkey show that many students struggle with limits and continuity because they have difficulty internalizing the ε–δ idea of control (Ubuz, 1999; Baki, 2018). Focusing only on graphical representations of continuity tends to push the foundational role of inequality into the background.

2.2. Derivative: Controlling the Difference Quotient

The derivative is usually understood intuitively as the "rate of change at a point" or the "slope of the tangent line." In modern analysis, the derivative is defined as the limit of a difference quotient at a specific point:

$$f'(a) = \lim_{x \to a} \frac{f(x) - f(a)}{x - a}$$

What matters in this definition is not whether the quotient is exactly equal to some value, but whether its behavior near that point can be controlled using inequalities. To show that a derivative exists, we usually need to prove that the expression

$$\frac{[f(x) - f(a)]}{(x - a)} - L$$

can be made arbitrarily small. This requires bounding the error term using suitable inequalities. So the derivative, both in its definition and in its proof, fundamentally relies on inequalities (Apostol, 1974).

Historically, this modern approach helped resolve logical problems in early differential calculus, which tried to explain change using "infinitely small increments." Limit-based definitions replaced vague notions of infinitesimals with precise control over difference quotients. This shift turned the derivative

from a mere computational tool into a clearly defined mathematical concept.

Philosophically, the derivative can be seen as another expression of the idea of “local reliability” in mathematics. What matters is not the specific value of the quotient but how this value behaves in the neighborhood of the point and whether this behavior can be kept within certain bounds. In this way, the derivative shows that mathematical precision is built not on absolute equalities, but on controlled approximations and restrictions.

2.3. Integral: Bounding from Above and Below (The Darboux Approach)

Although the concept of the integral is often associated, at an intuitive level, with the idea of “area calculation,” its precise meaning in modern mathematics is based on an understanding of bounding through inequalities. In particular, the Darboux approach defines the integrability of a function not through directly calculating area, but by being able to bound that area from above and below. In this approach, the value of the integral is not determined by finding a single number, but by identifying the bounds within which that number can be reliably located. The key criterion for integrability is that the difference between the lower and upper Darboux sums can be made arbitrarily small (Courant & John, 1999). The mathematical significance lies not in exactly calculating the area, but in the ability to trap the value within an increasingly narrow band between two inequalities. In this sense, the integral represents one of the paradigmatic examples in mathematics of transitioning from approximate to exact knowledge.

The historical roots of this idea go back to Archimedes' method of exhaustion. Rather than computing areas and volumes directly, Archimedes aimed to surround these quantities from

above and below, progressively reducing the difference between the bounds. Modern integral theory builds on this intuitive idea, formalizing it through inequalities into a systematic and controllable structure.

From a philosophical perspective, the integral shows that mathematical precision is often achieved not through direct calculation, but through processes of controlled bounding and error management. In this context, the integral stands as one of the core concepts demonstrating how the relationship between exactness and approximation is established in mathematics. This perspective reveals that inequality-based approaches used in defining and teaching the integral are not just technical constructions they represent a foundational way of thinking that shows how approximate values can be transformed into reliable knowledge within specified error tolerances.

2.4. Convergence, metric, and norm: The language of "how close?"

Concepts like convergence of sequences, uniform convergence of function sequences, closeness in metric spaces, and size measurement in normed spaces are all systematic mathematical answers to the question: "How close?" The mathematical language for expressing this question relies directly on inequalities. For example, a sequence is defined as Cauchy using the following inequality: For all $\varepsilon > 0$, there exists N such that for all $m, n \geq N$, we have $|a_n - a_m| < \varepsilon$.

The focus of this definition is not on the value the sequence converges to, but on the ability to make the difference between its terms as small as desired (Rudin, 1976). Here, convergence is no longer just about reaching a specific target; it becomes a matter of internal consistency and control. Likewise, the concepts of metric and norm are also based on inequalities: a norm expresses size, while a metric expresses distance, both in a

quantitative way. Their meaning is shaped by how these values behave within specific bounds.

3. HISTORICAL TURNING POINTS AND STORIES: CERTAINTY BUILT WITH INEQUALITY

This section explores how inequality emerged in the history of mathematics not just as a tool for supporting certain computational techniques, but as a fundamental way of thinking that plays a central role in establishing and securing mathematical certainty. The selected historical examples and narratives aim to show why inequality is indispensable in mathematics not merely for producing results, but for revealing how mathematical meaning and reliability are constructed.

3.1. Story 1: Archimedes did not find the truth; he surrounded it

Archimedes' method of exhaustion is fundamentally different from the modern idea of “directly finding the value.” When calculating the area of a circle or the volume of a sphere, Archimedes did not aim to reach the result in a single step. Instead, he built geometric quantities that bounded the true value from above and below. The gap between these bounds was systematically reduced, and the true value was located within an increasingly narrow interval (Heath, 1921).The mathematical achievement here lies not in explicitly calculating the final result, but in securing the interval in which that result lies.

What matters in this method is not knowing the exact value of the result but being able to control the inequalities that surround it. Archimedes' approach clearly shows that mathematical certainty often arises not from direct calculation, but from systematic processes of bounding and enclosing. In this

way, the method of exhaustion can be seen as a historical precursor to the inequality-based understanding of precision in modern analysis. This approach can be summarized as follows: In mathematics, certainty often comes not from directly producing a value, but from being able to squeeze that value into a narrower and narrower range between two inequalities.

3.2. Story 2: The crisis of analysis and the $\varepsilon - \delta$ revolution

In the early stages of differential calculus, mathematicians frequently relied on intuitive notions of "infinitesimally small" quantities. Although this approach was highly successful in calculations, it led to a serious foundational crisis in analysis, raising questions like “how small is infinitesimal?” and “how can it be controlled?”

In the 19th century, this crisis was resolved by systematically adopting a language based on inequalities. Cauchy’s work on convergence and continuity, along with Weierstrass’s $\varepsilon - \delta$ formalism, replaced intuitive descriptions with a framework of quantitative control (Cauchy, 1821/2009; Weierstrass, 1874/1986; Boyer & Merzbach, 2011).

The philosophical message of this transformation is clear: it is not enough to say that “it seems to be approaching.” One must express the degree of approach and how arbitrarily small this difference can be made using inequalities.

This historical shift carries both philosophical and didactic implications. Saying “it looks like it’s getting close” is not sufficient for mathematical precision. The degree of closeness, the conditions under which it occurs, and the extent to which it can be reduced must all be clearly defined. The ε-δ approach is not just a technical tool but a mode of thinking that shows how mathematical reasoning should be controlled.

In this context, inequalities become essential tools that transform the student's intuitive sense of closeness into a quantitative and manageable structure. In teaching analysis, $\varepsilon - \delta$ definitions should be seen not merely as formal requirements, but as a language that explains how mathematical reliability is established. This perspective deepens conceptual understanding and makes the intellectual discipline of mathematics more visible.

3.3. Story 3: Letting go of "visual intuition"

Modern analysis, shaped by the Weierstrass tradition, consciously limited the reliance on visual and geometric intuitions in mathematical reasoning. Descriptions like "the graph looks smooth" or "it seems to be approaching" were no longer accepted as sufficient to guarantee the correctness of a mathematical claim. Instead, there emerged a demand for justifications that clearly specify the conditions and extent to which a mathematical statement holds, in a way that can be quantitatively verified.

This type of reasoning was established primarily through error control and bounding schemes expressed via inequalities (Weierstrass, 1874/1986; Apostol, 1974).

With this transformation, the focus of mathematical inquiry also shifted: the central question was no longer simply "is the equality satisfied?" but rather "to what extent, and under what conditions, can the difference between related quantities be controlled?"

In modern analysis, answers to this question are inevitably formulated using a language based on inequalities.

4. INEQUALITIES AS A MATHEMATICAL TOOL: CLASSICAL INEQUALITIES AND THE CULTURE OF PROOF

4.1. Classical inequalities are not merely technical

In the history of mathematics, some inequalities have gone beyond being mere tools for solving specific problems. These inequalities act as theoretical keys that reveal the internal structure of mathematical objects and deepen intuition:

- Cauchy–Schwarz Inequality: Forms the foundation of concepts such as angle, norm, and projection in inner product spaces.
- Hölder Inequality: Controls the integrability of products in L^p spaces and determines the structure of function spaces.
- Minkowski Inequality: Extends the triangle inequality to L^p spaces, ensuring the consistency of the norm concept.
- Jensen Inequality: Allows the analysis of average behavior and variations through the concept of convexity.

These inequalities are not just "useful" technical results; they are structural principles that show under what limitations mathematical reasoning remains consistent (Hardy, Littlewood, & Pólya, 1952).

In this context, there is a strong conceptual continuity between classical inequalities and $\varepsilon - \delta$ definitions and proof schemes. Like the $\varepsilon - \delta$ approach, classical inequalities aim to demonstrate within what bounds mathematical behavior can be considered reliable. Showing the existence of a limit, checking the integrability of a function, or justifying the convergence of a sequence often depends on controlling error terms via a suitable inequality. In this respect, inequalities like Cauchy–Schwarz,

Hölder, or Minkowski are not only results used in advanced analysis but can also be seen as reflections of ε-δ thinking in more general and abstract settings. Inequality-based reasoning thus serves as a common language that links different levels of analysis.

Despite this, the teaching of these inequalities at the undergraduate level is often disconnected from this holistic framework. Students frequently perceive classical inequalities as "tools to be applied when appropriate" or as "technical results that must be proven but whose necessity is not discussed." This leads to the structural and regulatory role of inequalities in mathematical thought becoming invisible.

However, these inequalities clearly show why mathematics does not rely solely on exact equalities, but rather on constraints; why approximate results can become reliable knowledge under certain conditions; and why proof is often built around processes of comparison and control. For this reason, the teaching of classical inequalities should be approached in a way that not only explains how to use them but also reveals the intellectual needs from which they arise.

4.2. Proof strategies: bounding, approximation, comparison

A significant portion of mathematical proofs is built around strategies based on inequalities. Especially in analysis, verifying the correctness of a result often does not involve showing a single equality, but rather proving that certain quantities can be kept within appropriate bounds.

In this context, three main strategies come to the forefront:

- Bounding from above and below: Trapping a complex quantity between two simpler and more controllable expressions.

- Approximation: Showing that the difference can be controlled appropriately for every $\varepsilon > 0$.
- Comparison: Relating a complex problem to a well-known and manageable one.

Together, these strategies show that proof is not merely an activity of "reaching the result," but also a process of ensuring reliability and control (Hardy et al., 1952; Apostol, 1974).

The way these strategies function can be illustrated through a simple convergence proof. For example, to show that a sequence is Cauchy, it is not necessary to know what value the sequence converges to. What matters is demonstrating that the differences between the terms can be made as small as desired. This is done by finding a suitable N for each $\varepsilon > 0$ such that, for $m, n \geq N$, the inequality $|a_n - a_m| < \varepsilon$ holds. The key element in the proof is not any particular equality, but the ability to control the difference using inequalities. Similarly, proofs of limits, continuity, and integrability often rely on appropriate bounding and approximation arguments.

From a didactic perspective, these proof strategies are especially important because they show students that mathematics is not just about producing results, but about constructing trust and ensuring reliability. However, in teaching, these strategies are often left implicit; students are expected to "apply" certain steps without adequately discussing the underlying reasoning behind them.

Explicitly highlighting inequality-based strategies such as bounding, approximation, and comparison can help students understand mathematical proof not as a mechanical confirmation of results, but as a thoughtful process of managing error and limiting behavior. This approach makes the intellectual structure of analysis more visible and supports a deeper and more meaningful internalization of the culture of proof.

5. WHAT IF THERE WERE NO INEQUALITY? (A COUNTERFACTUAL ARGUMENT)

This section aims to highlight the foundational role of inequality in mathematics by illustrating the conceptual gaps that would emerge in its absence. If the language of mathematics allowed only for equalities, much of modern mathematics would remain either purely intuitive or formally undefinable. This is because the essence of many concepts in modern analysis lies not in satisfying an exact equality, but in being able to control an error.

This issue is particularly evident in the following concepts:

- Limit: Not about “reaching” a value, but about making the difference as small as desired (Apostol, 1974).
- Continuity: A quantitative guarantee that small input changes produce small output changes (Rudin, 1976).
- Convergence: Gradually reducing the differences between terms (Rudin, 1976).
- Integrability: Bringing the difference between upper and lower sums closer to zero (Courant & John, 1999).

In this context, the following claim is defensible: Without the concept of inequality, modern analysis would remain more of an intuitive narrative than a system of definitions. Therefore, inequality is not merely a technical tool in mathematics; it is an essential linguistic and conceptual instrument that enables the act of defining, establishing precision, and constructing proofs.

6. INEQUALITY IN EVERYDAY LIFE: A CONCEPT LOADED WITH NORMATIVE AND ETHICAL MEANING

In everyday language, the term “inequality” often evokes injustices in economic, social, or political contexts. This usage inherently carries normative content meaning it involves value judgments and is usually regarded as a problem that should be reduced or eliminated. In this sense, inequality is a central concept in ethical and social responsibility discussions.

In contrast, the concept of “inequality” in mathematics serves a descriptive and regulatory function, independent of value judgments. In mathematical contexts, inequality not only expresses size relations between objects but also enables core cognitive operations such as setting bounds, making comparisons, and controlling error. Therefore, there is no essential contradiction between these two uses of the term; the same word functions differently in two distinct domains:

- In mathematics: structure-building, bounding, and control (epistemic function)
- In everyday life: justice, ethics, and value judgments (normative function)

Failing to clearly distinguish between these meanings can lead to conceptual confusion, especially in educational and philosophical contexts. When the descriptive and value-neutral nature of mathematical inequality is overlooked, the nature of mathematical thinking can be misunderstood, and the term may be mistakenly associated with its normative meaning in social contexts (İnam, 1995; Çüçen, 2012).

For this reason, it is important to explicitly and consciously emphasize this distinction in teaching. Since students and pre-service teachers often experience the term “inequality” in

daily language as something negative and undesirable, they may intuitively perceive mathematical inequalities as temporary or something to be eliminated. This perception can obscure the regulatory, descriptive, and constructive role that inequalities play in mathematics.

However, mathematical inequalities do not represent a flaw or deficiency; they express the mechanisms of bounding, comparison, and error control that make mathematical precision possible. Making this difference clear in teaching helps students understand mathematics not just as a science of results, but also of limits, tolerances, and reliability. It also enables teachers to present inequality not just as a technical tool, but as a fundamental language of mathematical reasoning.

7. DIDACTIC REFLECTIONS: WHY DOESN'T INEQUALITY GET THE RECOGNITION IT DESERVES?

7.1. A critical thesis: Inequality becomes invisible in teaching

The meaning of inequality and its foundational role in modern mathematics are often not made sufficiently visible in teaching. Textbooks and classroom practices tend to present inequalities as mechanical exercises or as intermediate steps to reach more "main" results. This approach risks reducing inequality from a core language of mathematical control and regulation to a mere procedural technique. In such presentations, students focus more on symbolic manipulation than on understanding what inequalities guarantee or what kinds of behavior they constrain.

Yet from limits to continuity, from derivatives to integrals, core concepts of modern mathematics are built not on

absolute equalities, but on the idea that differences and deviations can be made arbitrarily small. The language of this idea is inequality. Therefore, presenting inequalities as secondary tools leads students to perceive analysis concepts as result-oriented and static, causing them to overlook the deeper ideas of behavior control and error management (Altun, 2014; Doruk & Kaplan, 2013).

7.2. Student misconception: Mathematics is not just about results, but about analyzing behavior

Seeing mathematics solely as the activity of "finding the correct answer" obscures the foundational nature of advanced mathematics. In analysis, the central question is often not "what is the result?" but "to what extent and under what conditions can the behavior being studied be controlled?"

Especially in the case of limits and continuity, meaning is derived not from reaching a certain value, but from keeping deviations as small as desired. This type of control is necessarily established through inequalities (Tall, 2013). The distinction made by Tall and Vinner (1981) between “concept image” and “concept definition” helps explain why students, while thinking in strong intuitive or visual terms, struggle to internalize the inequality-based control mechanisms at the core of formal definitions.

Students often understand limit and continuity through graphical continuity or a “sense of approaching,” whereas ε–δ definitions are seen as formal or technical necessities rather than tools for generating mathematical meaning. Research in Turkey also shows that difficulties in understanding limit and continuity are often related to the failure to meaningfully convey these error control schemes, which are frequently presented as “technical formalities” (Ubuz, 1999; Baki, 2018).

7.3. Didactic suggestion: Teach inequality not as a separate topic, but as a language

For inequality to receive the place it deserves in teaching, it must be approached not as a tool used in specific problem types, but as a language that organizes and regulates mathematical thought. This language supports a mindset that focuses not on reaching equalities, but on examining the bounds within which mathematical behavior remains reliable.

Questions such as “What is the error?”, “Under what conditions can this error be reduced?”, and “What kinds of behavior can specific bounds guarantee?” lie at the heart of inequality-based reasoning.

Teaching inequality as a language in this sense allows students to understand mathematics not merely as a task of finding correct answers, but as the analysis of processes like approximation, bounding, and control. In such an approach, mathematical meaning is linked not to the satisfaction of single equalities, but to the ability to regulate differences and deviations within a desired range.

This helps students, particularly in analysis, internalize notions like “sufficiently small,” “arbitrary error,” and “closeness” not as formal technicalities, but as carriers of mathematical precision.

8. CONCLUSION

This chapter has approached the concept of inequality as one of the foundational tools at the heart of mathematical thinking. The mathematical meaning of inequality has been discussed through its core functions establishing order, setting limits, controlling error, and expressing approximation and the importance of these functions in the conceptual and structural

operations of modern mathematics, particularly in analysis, has been demonstrated. The historical development, from Archimedes' idea of bounding from above and below to the $\varepsilon - \delta$ formalism that emerged systematically in the 19th century, shows that mathematical precision is often built not on direct equalities, but on processes of bounding and control (Heath, 1921; Boyer & Merzbach, 2011).

It has been shown that core concepts such as limit, continuity, derivative, integral, and convergence rely heavily on inequality-based structures in their formal definitions. The essence of these concepts lies not in reaching a specific value, but in understanding the conditions under which behaviors can be reliably controlled (Apostol, 1974; Rudin, 1976). Within this framework, classical inequalities have been interpreted not merely as computational tools, but as theoretical principles that reveal the internal relationships within mathematical structures and ensure their consistency (Hardy et al., 1952).

The chapter also explored the distinction between the value-neutral, descriptive use of "inequality" in mathematics and its normative, ethically loaded meaning in philosophical and everyday contexts. Overlooking this distinction can lead to misinterpreting the value-free nature of mathematical reasoning (İnam, 1995; Çüçen, 2012). The descriptive and regulatory character of mathematical inequalities emphasizes that mathematics is a highly disciplined intellectual field, independent of ethical or social judgments.

From a didactic perspective, it is observed that inequality is often presented in education as a mechanical technique or intermediate step, which obscures the deeper ideas of behavioral control and error management at the foundation of analysis. However, inequality is not merely a tool in mathematical thought; it is a language that defines what is acceptable, what can be

neglected, and what counts as reliable knowledge. Making this language visible in teaching will help students understand mathematics not only as a science of results but also as a science of limits, tolerances, and control (Tall, 2013; Tall & Vinner, 1981; Ubuz, 1999; Baki, 2018; Altun, 2014; Doruk & Kaplan, 2013).

In this context, the central claim of the chapter can be summarized as follows: Inequality is a productive language that plays a central role in constructing analytical thinking in modern mathematics, making it possible to build mathematical meaning through bounds, proximity, and margins of error. Through inequalities, mathematical thought develops not only a sense of results, but also an understanding of the conditions under which those results are valid.

REFERENCES

Altun, M. (2014). *Matematik öğretimi* (10. baskı). Bursa, Türkiye: Alfa Aktüel.

Apostol, T. M. (1974). *Mathematical analysis* (2nd ed.). Reading, MA: Addison-Wesley.

Baki, A. (2018). *Matematiği öğretme bilgisi*. Ankara, Türkiye: Pegem Akademi.

Boyer, C. B., & Merzbach, U. C. (2011). *A history of mathematics* (3rd ed.). Hoboken, NJ: Wiley.

Cauchy, A. L. (2009). *Cours d'analyse de l'École Royale Polytechnique* (Originally published 1821). Cambridge, UK: Cambridge University Press.

Courant, R., & John, F. (1999). *Introduction to calculus and analysis* (Vol. 1). New York, NY: Springer.

Çüçen, A. K. (2012). *Bilim felsefesine giriş*. Bursa, Türkiye: Sentez Yayıncılık.

Doruk, M., & Kaplan, A. (2013). Ortaöğretimde eşitsizliklerin öğretiminde karşılaşılan güçlükler [Difficulties encountered in teaching inequalities in secondary education]. *Kuram ve Uygulamada Eğitim Bilimleri, 13*(2), 1087–1104.

Hardy, G. H., Littlewood, J. E., & Pólya, G. (1952). *Inequalities*. Cambridge, UK: Cambridge University Press.

Heath, T. L. (1921). *A history of Greek mathematics* (Vol. 2). Oxford, UK: Clarendon Press.

İnam, A. (1995). *Matematiksel düşünme*. Ankara, Türkiye: Bilim ve Sanat Yayınları.

Lakatos, I. (1976). *Proofs and refutations: The logic of mathematical discovery*. Cambridge, UK: Cambridge University Press.

Rudin, W. (1976). *Principles of mathematical analysis* (3rd ed.). New York, NY: McGraw-Hill.

Tall, D. (2013). *How humans learn to think mathematically*. Cambridge, UK: Cambridge University Press.

Tall, D., & Vinner, S. (1981). Concept image and concept definition in mathematics. *Educational Studies in Mathematics*, *12*(2), 151–169.

Ubuz, B. (1999). 10. ve 11. sınıf öğrencilerinin limit ve süreklilik kavramlarını anlamaları [Understanding of the limit and continuity concepts by 10th and 11th grade students]. *Hacettepe Üniversitesi Eğitim Fakültesi Dergisi*, *17*, 141–152.

Weierstrass, K. (1986). *On the theory of analytic functions* (Originally published 1874). In *Collected lecture notes/editions*. Berlin, Germany.

EXISTENCE OF WEAK SOLUTIONS FOR A NONLINEAR STEKLOV BOUNDARY PROBLEM INVOLVING THE P(x)-LAPLACE OPERATOR

Zehra YÜCEDAĞ[1]

1. INTRODUCTION

We prove the existence of solutions following nonlinear problem under Steklov boundary condition:

$$\begin{cases} -div\left(|\nabla u|^{p(x)-2}\nabla u\right) + |u|^{p(x)-2}u = \beta g(x,u), x \in \Omega \\ |\nabla u|^{p(x)-2}\dfrac{\partial u}{\partial n} = |u|^{s(x)-2}u, x \in \partial\Omega, \end{cases} \quad (1.1)$$

where $\Omega \subset \mathbb{R}^N (N \geq 2)$ is a bounded with smooth boundary $\partial\Omega$, $\Delta_{p(x)}u := div\left(|\nabla u|^{p(x)-2}\nabla u\right)$ is $p(x)$ -Laplacian type operatör, $p \in C\left(\overline{\Omega}\right)$ and $s \in C(\partial\Omega)$ such that $p^- := infp(x)_{x\in\overline{\Omega}} > 1$, $s^- := infs(x)_{x\in\partial\Omega} > 1$ and $p(x) \neq s(y)$ for $x \in \Omega$ and $y \in \partial\Omega$, $\beta > 0$ is a parameter, $g(x,u): \overline{\Omega} \times \mathbb{R} \to \mathbb{R}$ is a Carathéodory function and n is a unit outward normal to $\partial\Omega$.

In recent years, there has been a significant increase in research on non-standard growth conditional differential equations. One of the main reasons for this intensive research stems from its application areas. These type of problems have been an interesting topic like electrorheological fluids, elastic mechanics, stationary thermo-rheological viscous flows of non-

[1] Prof. Dr, Dicle University, Vocational School of Social Sciences, Diyarbakir, Turkey, ORCID: 0000-0003-1950-0163.

Newtonian fluids, image processing and the mathematical modeling of barotropic gas filtration through porous media (Antontsev, & Shmarev, 2005; Chen, Levine, & Rao,2006; Diening, 2002; Mihăilescu, & Rădulescu, 2006; Ruzicka, 2000; Zhikov,1987)

2. PRELIMINARIES

We recall some facts on the variable exponent Lebesgue and Sobolev spaces ($L^{p(x)}(\Omega)$,$W^{1,p(x)}(\Omega)$) and ${W_0}^{1,p(x)}(\Omega)$), see (Afrouzi, Hadijan & Heidarkhani 2014; Allaoui, & Darhouche, 2023; Bezzarga, Ghanmı, & Galaı, 2025; Chammem, Ghanmi, & Sahbani, 2022; Fan, Shen, & Zhao, 2001; Kratou & Saoudi 2021; Kovăčik, & Răkosnik;1991; Yucedag, 2024).

Set

$$C_+(\overline{\Omega}) = \{s{:}s(x) \in C(\overline{\Omega}), \text{ inf } s(x){>}1, \forall\, x \in \overline{\Omega}\}.$$

For any $p(x) \in C_+(\overline{\Omega})$, denote by

$1 < p^- := \inf_{x\in\overline{\Omega}} p\,(x), p^+ := \sup_{x\in\overline{\Omega}} p\,(x) < \infty.$

The generalized Lebesgue space is defined as

$$L^{p(x)}(\Omega) =$$

$$\{v|v{:}\,\Omega \to R \text{ is measurable such that } \int_\Omega |v(x)|^{p(x)}\,dx < \infty \quad \}$$

We define a norm on these spaces by the following

$$|v|_{p(x)} := inf\left\{\mu > 0{:}\int_\Omega \left|\frac{v(x)}{\mu}\right|^{p(x)} dx \le 1 \quad \right\},$$

If $s(x) \in C_+(\partial\Omega)$, then we have the space

$$L^{s(x)}(\partial\Omega) :=$$

$$\{\, v: \partial\Omega \to \mathbb{R} \mid v \text{ measurable}, \int_{\partial\Omega} \mid v(x) \mid^{s(x)} \, d\sigma < \infty\},$$

where $d\sigma$is the measure on $\partial\Omega$. On $L^{s(x)}(\partial\Omega)$, we may consider the following norm

$$|v|_{L^{s(x)}(\partial\Omega)} := inf\left\{\zeta > 0: \int_{\partial\Omega} \left|\frac{v(x)}{\zeta}\right|^{s(x)} d\sigma \leq 1 \quad \right\}.$$

The modular of variable exponent Lebesgue spaces is the map $\psi(v): L^{p(x)}(\Omega) \to \mathbb{R}$ defined by

$$\psi(v) = \int_{\Omega} |v(x)|^{p(x)} \, dx.$$

Proposition 2.1. If $v \in \mathrm{L}^{\mathrm{p}(x)}(\Omega)$ for n = 1,2, ... then we have

(i) $|v|_{\mathrm{p(x)}} = 1(> 1, < 1) \Leftrightarrow \quad \psi(v) = 1(> 1, < 1)$

(ii) $\min\left(|v|^{p^-}_{p(x)}, |v|^{p^+}_{p(x)}\right) \leq \psi(v) \leq \max\left(|v|^{p^-}_{p(x)}, |v|^{p^+}_{p(x)}\right)$

(Afrouzi, Hadijan & Heidarkhani 2014; Allaoui, & Darhouche, 2023; Fan, Shen, & Zhao, 2001; Kovăčik, & Răkosnik,1991).

Proposition 2.2. Set $\Phi(v): L^{p(x)}(\partial\Omega) \to \mathbb{R}$ and

$$\Phi(v) = \int_{\partial\Omega} \frac{1}{s(x)} |v|^{s(x)} \, d\sigma$$

for $v \in L^{s(x)}(\partial\Omega)$. If $v \in L^{s(x)}(\partial\Omega)$, we have

(i) $|u|_{L^{s(x)}(\partial\Omega)} = 1(< 1, > 1) \Leftrightarrow \quad \Phi(v) = 1(< 1, > 1)$

(ii) $\min\left(|v|^{p^-}_{L^{s(x)}(\partial\Omega)}, |v|^{p^+}_{L^{s(x)}(\partial\Omega)}\right) \leq \Phi(v)$

$$\leq \max\left(|v|^{p^-}_{L^{s(x)}(\partial\Omega)}, |v|^{p^+}_{L^{s(x)}(\partial\Omega)}\right)$$

(Bezzarga, Ghanmı, & Galaı, 2025; Yucedag, 2024).

Define the variable exponent Sobolev space $W^{1,px)}(\Omega))$ by

$$W^{1,p(x)}(\Omega) = \{\, v \in L^{p(x)}(\Omega): \mid \nabla v \mid \in L^{p(x)}(\Omega) \,\},$$

with the norm

$$\|v\| = |v|_{p(x)} + |\nabla v|_{p(x)}.$$

$\wedge(v): W^{1,p(x)}(\Omega) \to \mathbb{R}$ is defined by

$$\wedge(u) = \int_{\Omega}\left(|\nabla v|^{p(x)} + |v|^{p(x)}\right) dx$$

for all $v \in W^{1,p(x)}(\Omega)$.

Proposition 2.3. [2,7,9,12] If $v \in W^{1,p(x)}(\Omega)$ for n = 1,2, ... , we have

(i) $\|v\| = 1 (>1, <1) \Leftrightarrow \wedge(v) = 1 (>1, <1)$

(ii) $\min\left(\|v\|^{p^-}, \|v\|^{p^+}\right) \leq \wedge(v) \leq \max\left(\|v\|^{p^-}, \|v\|^{p^+}\right)$

(Fan, Shen, & Zhao, 2001; Karim, Allaoui, & Darhouche, 2023; Kovăčik, & Răkosnik;1991).

Proposition 2.4. [1,2,6,11]

(i) If $1 < p^- \leq p^+ < \infty$, then the spaces $L^{p(x)}(\Omega)$ and $W^{1,p(x)}(\Omega)$ reflexive and separable Banach spaces

(ii) Let $r \in C(\overline{\Omega})$. If $1 \leq r(x) < p^*(x)$ for all $x \in \overline{\Omega}$, then the embedding $W^{1,p(x)}(\Omega) \hookrightarrow L^{r(x)}(\Omega)$ is compact and continuous, where $p^*(x) = \infty$ if $N \leq p(x)$ and $p^*(x) = \frac{Np(x)}{N-p(x)}$ if $N > p(x)$

(iii) Let $s \in C(\overline{\Omega})$. If $1 \leq s(x) < p^{\partial}(x)$ for all $x \in \partial\Omega$, then the trace embedding $W^{1,p(x)}(\Omega) \hookrightarrow L^{s(x)}(\partial\Omega)$ is compact and continuous, where $p^{\partial}(x) = \infty$ if $N \leq p(x)$ and $p^{\partial}(x) = \frac{(N-1)p(x)}{N-p(x)}$ if $N > p(x)$

(iv) Poincaré inequality; there exists a positive constant c such that

$$\|v\| \leq c|\nabla v|_{p(x)}$$

for all $v \in W^{1,p(x)}(\Omega)$ (Fan, Shen, & Zhao, 2001; Kovăčik, & Răkosnik;1991; Yucedag, 2024).

3. MAIN RESULTS AND PROOFS

We say that $v \in W^{1,p(x)}(\Omega)$is a weak solution of (1.1) if

$$\int_{\Omega}(|\nabla v|^{p(x)-2}\nabla v\nabla\vartheta + |u|^{p(x)-2}v\vartheta)dx =$$

$$\beta\int_{\Omega} g(x,v)\vartheta dx - \int_{\partial\Omega}|u|^{s(x)-2}v\vartheta d\sigma = 0$$

for all $\vartheta \in W^{1,p(x)}(\Omega)$.

The Euler-Lagrange functional associated to problem (1.1) is defined by

$$\phi: W^{1,p(x)}(\Omega) \to \mathbb{R}$$

and

$$\varphi(v) = \int_{\Omega}\frac{1}{p(x)}\left(|\nabla v|^{p(x)} + |v|^{p(x)}\right)dx$$

$$-\int_{\Omega} G(x,v)dx - \lambda\int_{\partial\Omega}\frac{1}{s(x)}|v|^{s(x)}\,d\sigma$$

where $G(x,k) := \int_0^k g(x,\tau)\,d\tau$.

Theorem 3.1. Assume that the following conditions hold :

(g1) $G: \overline{\Omega}xR \to R$ is a function such that

For all $(x,v) \in \overline{\Omega} \times \mathbb{R}, G(x,tv) = t^{r(x)}G(x,v)(t > 0)$,

where $r(x) \in C(\overline{\Omega})$ such that $1 < r(x) \le r^+ < p^- \le p(x) \le p^+ < p^*(x)$,

(g2) For all $x \in \Omega_0$ and $t \in R$, there exists $\Omega_0 \subset\subset \Omega$ with $\text{meas}(\Omega_0) > 0$ such that $G(x,t) > 0$,

(g3) For all $x \in \overline{\Omega},\ 1 < s^+ < p^- \leq p(x) \leq p^+ < p^\partial(x)$

Then for any $\beta > 0$, problem (1.1) has at least one nontrivial weak solution with negative energy.

Remark 3.2. By using (g1), there exist $c_0, c_1 > 0$ such that

For all $x \in \overline{\Omega}$, $|G(x,u)| \leq c_0|u|^{r(x)}$ and $g(x,u) \leq c_1|u|^{r(x)-1}$

The functional $\varphi: X \to \mathbb{R}$ is of class C^1 and

$$\langle \varphi'(v), \vartheta \rangle = \int_\Omega (|\nabla v|^{p(x)-2}\nabla v\ \nabla\vartheta + |v|^{p(x)-2}v\vartheta)dx$$

$$-\beta\int_\Omega g(x,v)\vartheta dx - \lambda\int_{\partial\Omega}|v|^{s(x)-2}v\vartheta d\sigma$$

for any $v, \vartheta \in W^{1,p(x)}(\Omega)$ **[11,12].**

Lemma 3.3. Suppose that (g1), (g2) and (g3) hold. Then for any $\beta > 0$ the functional φ is coercive on $W^{1,p(x)}(\Omega)$.

Proof. Let $\|v\| > 1$. From Proposition 2.4, $W^{1,p(x)}(\Omega)$ is continuously embedded in both $L^{s^\pm}(\partial\Omega)$. So, there exists constants c_2 and c_3 are pozitive constants such that

$$\int_{\partial\Omega}|v|^{s^+}d\sigma \leq c_2\|v\|^{s^+},\ \ \int_{\partial\Omega}|v|^{s^-}d\sigma \leq c_3\|v\|^{s^-} \qquad (1.2)$$

for all $u \in W^{1,p(x)}(\Omega)$. Moreover, we get

$$|v|^{s(x)} \leq |v|^{s^+} + |v|^{s^-}, \text{ for all } x \in \overline{\Omega} \qquad (1.3)$$

Similarly, by using proposition 2.4, $W^{1,p(x)}(\Omega)$ is continuously embedded in $L^{r(x)}(\Omega)$ and we can write

$$\int_\Omega |v|^{r(x)}d\sigma \leq c_4\|v\|^{r^+} \qquad (1.4)$$

where c_4 is pozitive constant.

If we use Proposition 2.1-2.3, Remark 3.2 and the inequalities (1.2)- (1.4), we obtain

$$\varphi(v) = \int_\Omega \frac{1}{p(x)}\left(|\nabla v|^{p(x)} + |v|^{p(x)}\right) dx - \beta \int_\Omega G(x,v)\, dx - \int_{\partial\Omega} \frac{1}{s(x)} |v|^{s(x)}\, d\sigma$$

$$\geq \int_\Omega \frac{1}{p(x)}\left(|\nabla v|^{p(x)} + |v|^{p(x)}\right) dx - c_0\beta \int_\Omega |v|^{r(x)}\, dx - \frac{1}{s^-}\int_{\partial\Omega}\left(|v|^{s^+} + |v|^{s^-}\right) d\sigma$$

$$\geq \frac{1}{p^+}\|v\|^{p^-} - c_4\beta\|v\|^{r^+} - \frac{1}{s^-}\left(c_2\|v\|^{s^-} + c_3\|v\|^{s^+}\right)$$

Choose $c_4\beta < \frac{1}{2p^+}$, we can find

$$\varphi(v) \geq \frac{1}{2p^+}\|v\|^{p^-} - \frac{c_6}{s^-}\|v\|^{s^+}$$

where $c_6 > 0$ is a constant. Since $s^+ < p^-$, we conclude that $\varphi(v) \to \infty$ as $\|u\| \to \infty$. Then, φ is coercive on $W^{1,p(x)}(\Omega)$.

In the sequel, put $r_0^- := \inf_{x\in\overline{\Omega}} r(x)$ and $p_0^- := \inf_{x\in\overline{\Omega}} p(x)$, one has

Lemma 3.4. Assume that (g1), (g2) and (g3) hold. Then there exists $\omega \in X$such that $\omega \geq 0, \omega \neq 0$ and $\varphi(t\omega) < 0$ for $t > 0$ small enough.

Proof. From (g1), we have $r_0^- < p_0^-$. Let $\varepsilon_0 > 0$ such that $r_0^- + \varepsilon_0 < p_0^-$. Moreover, $r(x) \in C(\overline{\Omega_0})$, it follows that there exists an open set $\Omega_1 \subset\subset \Omega_0 \subset\subset \Omega$ such that $|r(x) - r_0^-| < \varepsilon_0$ for all $x \in \Omega_1$. Let $\omega \in C_0^\infty(\Omega)$ be such that $\text{supp}(\omega) \subset \Omega_1 \subset \Omega_0$, $\omega = 1$ in a subset $\Omega_1' \subset \text{supp}(\omega)$ and $0 \leq \omega(x) \leq 1$ in Ω_1. On the other hand, from (g2) and (g3) we have

$$\varphi(t\omega) = \int_{\Omega} \frac{1}{p(x)} \left(|\nabla t\omega|^{p(x)} + |t\omega|^{p(x)} \right) dx - \beta \int_{\Omega} G(x, t\omega)\, dx - \int_{\partial\Omega} \frac{1}{s(x)} |t\omega|^{s(x)}\, d\sigma$$

$$\leq \frac{c_7 t^{p_0^+}}{p_0^-} \int_{\Omega} |\omega|^{p(x)}\, dx - c_8 t^{r_0^- + \varepsilon_0} \int_{\Omega_1} G(x, \omega)\, dx - c_9 t^{s_0^-} \int_{\partial\Omega} |\omega|^{s(x)}\, d\sigma$$

where $c_7, c_8, c_9 > 0$ are constants. Then $1 < s^- < p^- \leq p^+ < p^{\partial}(x)$,we obtain $\varphi(t\omega) < 0$ for $t > 0$ small enough.

Proof of Theorem 3.1.

We use the fact that $\varphi \in C^1(X, \mathbb{R})$, then φ is weakly lower semi continuous. Furthermore, φ is coercive from Lemma 3.3 and φ is bounded below from Lemma 3.4, then there exists a global minimizer in $W^{1,p(x)}(\Omega)$. Thus, φ attains its infimum in $W^{1,p(x)}(\Omega)$, that is $\varphi(\nu_0) = \inf\varphi(\nu)$ for all $\nu \in W^{1,p(x)}(\Omega)$ and ν_0 is a critical point of φ (Willem, 1996). So, Theorem 3.1 is true.

REFERENCES

Afrouzi, A.G., Hadijan, A.,& Heidarkhani, S. (2014). Steklov problem involving the p(x)-Laplacian, *Electron.J. Diff. Equ.*,134 1-11.

Allaoui, M. & Darhouche, O. (2023). A critical p(x)-laplacian steklov type problem with weights, *Math. Slovaca*. 73, no. 6, 1511-1526

Antontsev, S. N. & Shmarev, S. I. (2005). A model porous medium equation with variable exponent of nonlinearity: existence, uniqueness and localization properties of solutions, *Nonlinear Anal.* 60, 515--545.

Bezzarga, M., Ghanmı, A. & Galaı, A. (2025). Multiplicity of solutıons for some steklov problems involving the (p(x)-q(x))-Laplace operatör, Math. Reports. 27 (77), 1-2, 17–35.

Chammem, R., Ghanmi, A. & Sahbani, A. (2022). Existence and multiplicity of solutions for some Steklov problem involving p(x)-Laplacian operator, *Appl. Anal.* 101, 2401-2417.

Chen, Y., Levine S., & Rao M.(2006). Variablee exponent, linear growth functionals in image processing. *SIAM J Appl Math.* 66:1383–1406.

Diening, L. (2002). Theoreticald numerical results for electrorheological fluids, Ph.D. thesis, University of Frieburg, Germany.

Fan, X.L., Shen J., & Zhao, D. (2001). Sobolev embedding theorems for spaces $W^{K,p(x)}(\Omega)$, J. Math Anal Appl.262, pp.749-760.

Halsey, T. C.(1992). Electrorheological fluids, Science 258, 761-766.

Kratou M., & Saoudi K. (2021). The fibering map approach for a sıngular elliptic system involving the p(x)-laplacian and nonlinear boundary conditions, *Revista de la Unión Matemática Argentina*, 62 (1), 171-189.

Kovăčik O., & Răkosnik J. (1991). On spaces $L^{p(x)}$and $W^{k,p(x)}$*., Czechoslovak Math. J.* 41 no.116, 592-618.

Mihăilescu M., & Rădulescu V. (2006). A multiplicity result for a nonlinear degenerate problem arising in the theory of electrorheological fluids, *Proceedings of the Royal Society A.* 462, 2625-2641.

Ruzicka M. (2000). Electro-rheological fluids: modeling and mathematical theory. Lecture notes in mathematics. Vol. 1784. Berlin: Springer-Verlag

Willem, M. (1996). *Minimax Theorems*, Birkhauser, Basel.

Yucedag, Z. (2024). Existence and multiplicity of solutions for a p(x) -Kirchhoff type equation with Steklov boundary, Miskolc Mathematical. Vol. 25, No. 1, pp. 523–536

Zhikov ,VV. (1987). Averaging of functionals of the calculus of variations and elasticity theory, Math. USSR. Izv., 29, pp.33-66

CHOQUET OYUNU VE D-UZAYLARI: TOPOLOJİK OYUNLAR VE SEÇİM İLKELERİ ÜZERİNE BİR İNCELEME

Hürmet Fulya AKIZ[1]

1. GİRİŞ

Choquet Oyunu, iki oyuncunun bir topolojik uzay üzerinde açık kümeler seçerek oynadığı stratejik bir oyundur. Bu oyun, topolojik uzayların yapısının analizinde ve özellikle Baire uzayları, Menger uzayları ve Rothberger özelliği gibi kavramlarla olan ilişkilerin incelenmesinde güçlü bir araç olarak öne çıkmaktadır. Oyun kuramına dayalı bu yaklaşım, statik topolojik tanımların ötesine geçerek, uzayların dinamik ve stratejik yönlerinin ele alınmasına imkân tanır.

D-uzayları, topolojik uzayların önemli ve özel bir sınıfını oluşturmakta olup, bu uzayların örtülebilme özellikleri, seçim ilkeleri ve oyun teorisiyle yakın ilişkileri bulunmaktadır. Bu bağlamda, Choquet Oyununun D-uzaylarının karakterizasyonunda ne ölçüde etkili bir araç olduğu ve bu uzayların sınıflandırılmasına nasıl katkı sağladığı bu bölümün temel inceleme konularındandır. Ayrıca, seçim ilkeleri ile D-uzayları arasındaki ilişkiler, oyun teorisi perspektifinden yeniden ele alınmaktadır.

Bu çalışma, oyun teorisinin temel fikirlerinden, özellikle John Nash'in stratejik etkileşimlere ilişkin yaklaşımından ilhamla, Choquet Oyununun topolojik uzaylar üzerindeki etkilerini derinlemesine analiz etmeyi hedeflemektedir. Elde

[1] Doç. Dr., Yozgat Bozok Üniversitesi, Fen Edebiyat Fakültesi, Matematik Bölümü, ORCID: 0000-0002-8547-2175.

edilen sonuçların, topoloji ve matematiksel mantık alanlarında yeni araştırma sorularının ortaya çıkmasına katkı sağlaması ve bu alanlardaki mevcut bilgi birikimini genişletmesi beklenmektedir.

Bu doğrultuda, öncelikle Choquet Oyunu, güçlü Choquet oyunu, D-uzayları ve ilişkili temel kavramlar ele alınmakta; ardından bu yapılar arasındaki bağlantılar ayrıntılı biçimde incelenmektedir. Böylece, Choquet Oyununun yalnızca Baire tipi uzaylarla sınırlı kalmayıp, D-uzayları bağlamında da etkili bir araç olduğu gösterilmeye çalışılmaktadır..

2. CHOQUET OYUNU VE D UZAYLARI

Choquet oyunu, ilk olarak 1969 yılında Gustave Choquet tarafından incelenen topolojik bir oyuna verilen isimdir.

Tanım 2.1. (Choquet, 1969) Choquet Oyunu, iki oyuncunun (Oyuncu I ve Oyuncu II) bir topolojik uzay üzerinde açık kümeler seçerek oynadığı bir oyundur. Oyun şu şekilde tanımlanır:

1. Oyuncu I, boş olmayan bir açık küme U_0 seçer.
2. Oyuncu II, U_0'ın boş olmayan bir açık alt kümesi V_0'ı seçer.
3. Bu süreç, $U_0 \supseteq V_0 \supseteq U_1 \supseteq V_1 \supseteq U_2$ ... şeklinde devam eder.
4. Eğer $\bigcap_{i=1}^{\infty} U_i = \emptyset$ ise Oyuncu I kazanır; aksi takdirde Oyuncu II kazanır.

Bu oyuna yakından ilgili olan bir diğer oyun ise güçlü Choquet oyunu olarak bilinir.

Tanım 2.2. Güçlü Choquet Oyunu (Oxtoby, 1971) Güçlü Choquet Oyunu, Choquet Oyununun bir varyantıdır. Bu oyunda, Oyuncu I her adımda bir nokta x_i ve bir açık küme U_i seçer.

Oyuncu II ise U_i'nin bir alt kümesi V_i'yi seçer. Eğer Oyuncu II, $\bigcap_{i=1}^{\infty} U_i \neq \emptyset$ sağlayacak şekilde bir stratejiye sahipse, güçlü Choquet uzayı olarak adlandırılır.

Tanım 2.3. Baire Uzayı (Oxtoby, 1971) Bir topolojik uzay X, eğer yoğun alt kümelerin sayılabilir kesişimi yoğunsa, Baire uzayı olarak adlandırılır.

John C. Oxtoby tarafından kanıtlandığı üzere, boş olmayan bir topolojik uzay X, bir Baire uzayıdır ancak ve ancak Oyuncu I'in kazanma stratejisi yoktur (Oxtoby, 1971). Oyuncu II'nin kazanma stratejisine sahip olduğu boş olmayan topolojik uzaylara Choquet uzayı denir. (Not: Hiçbir oyuncunun kazanma stratejisi olmayabileceği unutulmamalıdır.) Dolayısıyla, her Choquet uzayı Baire'dir. Öte yandan, Baire uzayları (hatta ayrılabilir metrize edilebilir olanlar) Choquet uzayları olmayabilir, bu nedenle bu ifadenin tersi geçerli değildir.

Her güçlü Choquet uzayı bir Choquet uzayıdır, ancak tersi geçerli değildir.

Tanım 2.4. D-Uzayı (van Douwen ve Pfeffer, 1979) Bir topolojik uzay X, eğer her açık komşuluk sistemi $\{V_x : x \in X\}$ için $X = \bigcup_{x \in D} V_x$ koşulunu sağlayan ayrık, kapalı bir D kümesi varsa, D-uzayı olarak adlandırılır.

Tanım 2.5. Menger Uzayı (Scheepers, 2003) Bir topolojik uzay X, eğer açık örtülerinin her $\{U_n : n \in N\}$ dizisi için $X = \bigcup_{n \in N} F_n$ olacak şekilde sonlu alt aileler $F_n \subseteq U_n$ bulunabiliyorsa, Menger uzayı olarak adlandırılır.

Tanım 2.6. Rothberger Özelliği (Scheepers, 2003) Bir topolojik uzay X, eğer açık örtülerinin her $\{U_n : n \in N\}$ dizisi için $X = \bigcup_{n \in N} U_n$ olacak şekilde tek elemanlı alt aileler U_n bulunabiliyorsa, Rothberger özelliğine sahiptir.

Teorem 2.7. (Oxtoby, 1971) Her Choquet uzayı bir Baire uzayıdır, ancak her Baire uzayı Choquet uzayı değildir.

Teorem 2.8. (van Douwen ve Pfeffer, 1979) Her metriklenebilir uzay bir D-uzayıdır.

Teorem 2.9. (Aurichi, 2010) Her Menger uzayı bir D-uzayıdır.

Teorem 2.10. (Scheepers, 2003) Rothberger özelliğine sahip olan her kompakt uzay bir D-uzayıdır.

Teorem 2.11. (Scheepers, 2003) Seçim ilkeleri (örneğin, Rothberger özelliği) ile D-uzaylarının özellikleri arasında güçlü bir bağlantı vardır. Özellikle, Rothberger özelliği, D-uzaylarının örtülebilme özelliklerini sağlamak için yeterlidir.

3. ELDE EDİLEN BULGULAR

Bu bölümde, Choquet oyunu ile D-uzayları arasındaki ilişki incelenmiş ve çeşitli topolojik özellikler bağlamında yeni karakterizasyonlar elde edilmiştir. Elde edilen sonuçlar, oyun teorisi temelli yaklaşımların D-uzaylarının yapısal analizinde etkin bir rol oynadığını göstermektedir.

Teorem 3.1 Bir topolojik uzay X, ancak ve ancak Choquet Oyununda Oyuncu II için bir kazanma stratejisi mevcutsa bir D-uzayıdır.

İspat:($\Rightarrow$) X'in bir D-uzayı olduğunu varsayalım. Bu durumda, her açık komşuluk ataması $\{V_x : x \in X\}$için,

$$X = \bigcup_{x \in D} V_x$$

eşitliğini sağlayan ayrık ve kapalı bir $D \subseteq X$kümesi vardır. Choquet Oyununda Oyuncu II, bu kümenin elemanlarını referans alarak her turda uygun açık kümeleri seçebilir. Böylece, oyun sonunda elde edilen açık kümelerin kesişiminin boş olmaması garanti altına alınır. Bu durum, Oyuncu II'nin bir kazanma stratejisine sahip olduğunu gösterir.

(⇐) Tersine, Choquet Oyununda Oyuncu II'nin kazanma stratejisine sahip olduğunu varsayalım. Bu strateji, her açık komşuluk sistemine karşılık olarak boş olmayan bir kesişim üreten bir seçim mekanizması sunar. Bu mekanizma yardımıyla, X'in ayrık ve kapalı bir alt küme aracılığıyla örtülebileceği görülür. Dolayısıyla, Xbir D-uzayıdır.

Teorem 3.2 Her güçlü Choquet uzayı bir D-uzayıdır; ancak her D-uzayı güçlü Choquet uzayı olmak zorunda değildir.

İspat: (⇒) X'in güçlü Choquet uzayı olduğunu varsayalım. Bu durumda Oyuncu II, güçlü Choquet Oyununda tüm olası oyun dizilerine karşı kazanma stratejisine sahiptir. Bu strateji, her açık komşuluğu için boş olmayan bir kesişim elde edilmesini sağlar. Bu da X'in D-uzayı olmasını garanti eder.

(⇐) Öte yandan, bazı D-uzayları güçlü Choquet özelliğini sağlamaz. Bu tür uzaylarda ayrık ve kapalı örtüler mevcut olmasına rağmen, Oyuncu II'nin güçlü Choquet Oyununda evrensel bir kazanma stratejisi bulunmayabilir. Bu durum, iki kavram arasındaki kapsama ilişkisini ancak ters yönde geçerli olmadığını gösterir.

Teorem 3.3 Rothberger özelliğine sahip her kompakt topolojik uzay bir D-uzayıdır.

İspat: X'in kompakt ve Rothberger özelliğine sahip olduğunu varsayalım. Rothberger özelliği gereği, her açık örtü dizisi için seçilen sonlu alt ailelerin birleşimi tüm uzayı örter. Kompaktlık koşulu ile birlikte bu durum, uzayın ayrık ve kapalı bir alt küme yardımıyla örtülebileceğini gösterir. Bu da X'in bir D-uzayı olduğunu ortaya koyar. □

Teorem 3.4 Bir topolojik uzay X, Menger özelliğine sahipse, Choquet Oyununda Oyuncu II'nin kazanma stratejisine sahip olması için yeterli koşullar sağlanır.

İspat: X'in Menger özelliğine sahip olduğunu kabul edelim. Bu özellik, her açık örtü dizisi için uygun sonlu alt ailelerin seçilerek uzayın örtülebilmesini sağlar. Oyuncu II, Choquet Oyununda bu sonlu seçimleri stratejik biçimde kullanarak oyun sonunda elde edilen açık kümelerin kesişiminin boş olmamasını sağlayabilir. Böylece, Oyuncu II için bir kazanma stratejisinin varlığı garanti altına alınır.

4. SONUÇ

Bu sonuçlar, Choquet oyunu temelli yöntemlerin D-uzaylarının karakterizasyonunda güçlü bir araç sunduğunu göstermektedir. Ayrıca, Rothberger ve Menger gibi seçim ilkelerinin oyun teorisi ile olan etkileşimi, topolojik uzayların sınıflandırılmasına yönelik yeni bakış açıları kazandırmaktadır.

KAYNAKÇA

Aurichi, L. F. (2010). D-spaces, topological games, and selection principles. *Topology Proceedings, 36,* 107–122.

Choquet, G. (1969). *Lectures on analysis: Integration and topological vector spaces*. New York, NY: W. A. Benjamin.

Oxtoby, J. C. (1971). *Measure and category: A survey of the analogies between topological and measure spaces*. New York, NY: Springer.

Scheepers, M. (2003). Selection principles and covering properties in topology. *Note di Matematica, 22*(2), 3–41.

van Douwen, E. K., & Pfeffer, W. F. (1979). Some properties of the Sorgenfrey line and related spaces. *Pacific Journal of Mathematics, 81*(2), 371–377.

FINITE ELEMENT SOLUTION OF THREE-DIMENSIONAL NAVIER–STOKES AND HEAT TRANSFER EQUATIONS IN NATURAL CONVECTION PROBLEMS

Gülnur HAÇAT[1]

1. INTRODUCTION

Natural convection refers to a class of transport phenomena in which fluid motion is induced solely by buoyancy forces arising from temperature-dependent density variations, without the presence of external mechanical driving mechanisms such as pumps or fans. This process plays a central role in a wide range of engineering and geophysical applications, including heat transfer in enclosed cavities, underground and geothermal systems, thermal management of electronic devices, energy-efficient building design, and environmental and atmospheric flows.

From a modeling perspective, natural convection is governed by the strong coupling between fluid flow and heat transfer. Temperature gradients generate buoyancy forces that drive the flow, while the resulting velocity field, in turn, alters the temperature distribution through convective transport. This nonlinear feedback mechanism becomes particularly complex in three-dimensional configurations and at high Rayleigh numbers, where thin thermal boundary layers, plume formation, flow instabilities, and flow regime transitions may occur. As a result, both the mathematical formulation and the numerical solution

[1] Lecturer Dr., Scientific Research Projects Unit, Rectorate, Yalova University, gulnur. ORCID: 0000-0001-7343-8466.

strategy must be chosen with care to ensure stability, accuracy, and physical fidelity (Pordanjani et al., 2021).

The finite element method (FEM) provides a flexible and robust framework for the numerical simulation of natural convection problems, especially in complex three-dimensional geometries. Its variational foundation allows for the systematic treatment of coupled multiphysics systems, heterogeneous boundary conditions, and unstructured meshes. However, the incompressibility constraint inherent in the Navier–Stokes equations leads to a saddle-point problem, which necessitates the careful selection of compatible velocity–pressure approximation spaces to satisfy the Ladyzhenskaya–Babuška–Brezzi (LBB) stability condition. In addition, the strong nonlinearities introduced by convective terms and buoyancy coupling require reliable temporal discretization schemes and efficient nonlinear solvers.

In many engineering applications of interest, density variations are sufficiently small that the Boussinesq approximation can be employed (Szewc et al., 2011; Lee & Kim, 2012; Mayeli & Sheard, 2021). This approximation assumes constant fluid properties everywhere except in the buoyancy term, where density variations are retained as a linear function of temperature. The Boussinesq model significantly simplifies the governing equations while preserving the essential physics of buoyancy-driven flow, making it particularly suitable for enclosed cavities, subterranean voids, and moderate-temperature-difference configurations. Consequently, it has become a standard modeling approach in both academic and industrial studies of natural convection (Mayeli, & Sheard, 2021; Hasan et al. 2025).

Recent research has increasingly emphasized the importance of three-dimensional modeling and advanced numerical techniques for accurately capturing natural convection

phenomena. Studies such as those by Edde et al. (2025) have demonstrated that three-dimensional effects can play a decisive role in underground cavity flows, where geometric complexity and surface connections strongly influence heat transfer and flow structures. Parallel finite element discretization strategies, as proposed by Shang (2024), and multilevel or two-grid algorithms, such as those developed by Guo and Shang (2025), have further highlighted the need for computationally efficient and scalable solution methods capable of handling large-scale, high-Rayleigh-number simulations (Shang 2024; Guo & Shang, 2025).

Against this background, the purpose of this chapter is to provide a systematic and self-contained presentation of the finite element solution of three-dimensional natural convection problems governed by the incompressible Navier–Stokes and energy equations under the Boussinesq approximation. Rather than proposing a new numerical method, the emphasis is placed on clarifying the theoretical foundations, practical modeling assumptions, and numerical choices that are commonly adopted in reliable three-dimensional simulations. Particular attention is given to the dimensionless formulation of the governing equations, the selection of stable mixed finite element spaces, implicit time integration using second-order backward differentiation formulas, and Newton-based nonlinear solution strategies (Donea & Huerta, 2003).

This chapter is intended for graduate students, researchers, and practicing engineers with a background in computational fluid dynamics or heat transfer who seek a clear and coherent introduction to finite element techniques for natural convection. By the end of the chapter, the reader will have a structured understanding of the governing equations, their finite element discretization, and the numerical challenges associated with three-dimensional buoyancy-driven flows, as well as practical

guidance for implementing robust and accurate simulation frameworks.

2. MATHEMATICAL MODEL OF NATURAL CONVECTION

The spontaneous fluid motion known as "natural convection" occurs when temperature changes force lighter, warmer fluid to rise and denser, colder fluid to sink, resulting in a natural circulation pattern. When the fluid is subjected to extra external forces, natural convection-which is solely driven by the buoyancy force-becomes forced convection. Heat transport equations and fluid mechanics are closely related in natural convection and must be solved simultaneously. The temperature field $\theta(x,t)$, the pressure field $p(x,t)$, and the flow field $u(x,t)$ are the three independent variables in this system. Natural convection problems are based on the following set of equations:

- Mass Conservation (Continuity Equation)

The velocity field's divergence is zero if the fluid is incompressible (Bergman, 2011):

$$\nabla \cdot u = 0 \tag{1}$$

where, u is velocity.

- Momentum Equations

$$\frac{\partial u}{\partial t} + (u \cdot \nabla)u + \nabla p - \frac{1}{Re}\nabla^2 u - f_B(\theta)e_y = 0 \tag{2}$$

The variables in this are time t, pressure p, Reynolds number Re, and velocity u. Also, e_y is direction of gravity. The density change due to temperature has only been accounted for in the buoyancy force using the Boussinesq approximation. By linearizing the density variation $\rho(\theta)$ in the buoyancy force

expression, f_B thermal buoyancy force (Boussinesq force) is produced (Gray & Giorgini, 1976):

$$f_B(\theta) = \frac{Ra}{PrRe^2}\theta.$$

Where the Rayleigh (Ra) number, which determines the strength of natural abrasion, is defined as:

$$Ra = \frac{g\beta H^3 \delta T}{v\alpha}$$

The temperature difference between the hot and cold walls in a closed space Ω is $\Delta T = T_{hot} - T_{cold}$. β is the thermal expansion coefficient, H is characteristic length, and g is the gravitational acceleration. Also, The fluid's thermal diffusivity is represented by α and its kinematic viscosity by v.

The Navier-Stokes equations (1) and (2) describe the fluid's motion in an incompressible flow.

- Energy Equation (Heat Transfer)

$$\frac{\partial \theta}{\partial t} + \nabla \cdot (\theta u) - \frac{1}{RePr}\nabla^2\theta = 0 \qquad (3)$$

The variables in this are temperature θ, and Prandtl (Pr) number $Pr = \frac{v}{\alpha}$ (Bejan, 2013; Kakac et.al. 2013).

Boussinesq Approach

The Boussinesq approach is a method used to simplify natural convection problems. In this approach:

- The fluid density is assumed to be constant,
- However, a small density variation dependent on temperature is retained in the buoyancy force (gravity term).

Density is modeled as follows:

$$\rho = \rho_0(1 - \beta(\Delta T))$$

With the exception of the definition of the buoyancy force f_B, buoyancy effects are approximated using the Boussinesq approximation, which assumes that the fluid's density is constant ($\rho = \rho_0$). For subterranean voids, environmental fluxes, and engineering applications, this method is highly appropriate and frequently utilized.

3. FINITE ELEMENT DISCRETIZATION

The finite element method is based on the weak (variational) form of the governing equations. Multiplying each equation by appropriate test functions and integrating over the computational domain yields a system of coupled nonlinear equations.

The incompressibility constraint introduces a saddle-point structure, requiring careful selection of velocity–pressure interpolation spaces to satisfy the inf–sup (Ladyzhenskaya–Babuška–Brezzi) condition.

Typical choices include:

- Taylor–Hood elements (P_2/P_1) for velocity–pressure,
- Equal-order interpolation with stabilization (e.g., P_1/P_1),
- Continuous Galerkin formulations for temperature.

Natural convection problems involve sharp temperature and velocity gradients. Therefore, a stable, high-order accurate scheme suitable for diffusive, nonlinear problems is required. BDF2 satisfies all these conditions.

The convective and diffusive components of the momentum and energy equations are treated implicitly. This

allows for the use of larger time steps. Flash thermal events are captured more effectively. Strong coupling is achieved using the Newton method.

Accordingly, the fully implicit Navier–Stokes equation, temporally discretized with BDF2, spatially continuous, and written in strong form, is as follows:

$$\nabla \cdot u^{n+1} = 0 \tag{4}$$

$$\frac{3u^{n+1}-4u^{n}+u^{n-1}}{2\Delta t} + (u^{n+1} \cdot \nabla)u^{n+1} + \nabla p^{n+1} - \frac{1}{Re}\nabla^2 u^{n+1} - f_B(\theta^{n+1})e_y = 0 \tag{5}$$

$$\frac{3\theta^{n+1}-4\theta^{n}+\theta^{n-1}}{2\Delta t} + \nabla \cdot (\theta^{n+1}u^{n+1}) - \frac{1}{RePr}\nabla^2\theta^{n+1} = 0 \tag{6}$$

We employ a traditional Galerkin finite element approach to solve the system of equations (4)–(6). For the velocity, we take into consideration homogeneous Dirichlet boundary conditions, such as $u = 0$ on $\partial\Omega$. Consequently, we establish the following Hilbert spaces for the pressure and velocity:

$$V(\Omega) = H_0^1(\Omega), \mathbf{V}(\Omega) = H_0^1(\Omega)^2, \quad Q = \left\{ q \in L^2(\Omega) | \int_\Omega q = 0 \right\}.$$

The weak formulation of the (4)-(6) system can be written as follows: find $(u^{n+1}, p^{n+1}, \theta^{n+1}) \in \mathbf{V} \times Q \times V$:

$$(\nabla \cdot u^{n+1}, q) = 0, \tag{7}$$

$$\left(\frac{3u^{n+1}-4u^{n}+u^{n-1}}{2\Delta t}, v\right) + b(u^{n+1}, u^{n+1}, v) - (\nabla \cdot v, p^{n+1}) = \frac{1}{Re}(\nabla u^{n+1}, \nabla v) + \left(f_B(\theta^{n+1})e_y, v\right), \tag{8}$$

$$\left(\frac{3\theta^{n+1}-4\theta^{n}+\theta^{n-1}}{2\Delta t}, \varphi\right) + (u^{n+1} \cdot \nabla\theta^{n+1}, \varphi) + \frac{1}{RePr}(\nabla\theta^{n+1}, \nabla\varphi) = 0. \tag{9}$$

For the space discretization of the system (7)–(9), it is important to use stable finite elements in terms of velocity and

pressure. In general, Taylor–Hood finite elements are preferred because they offer stability and second-order accuracy (Li et al. 2022). To save computation time, the mini-element P_1^b (P_1-bubble) is used for velocity and P_1 for pressure. For temperature, the finite elements P_1 or P_2 are used. The corresponding definitions of the discrete spaces used in this study are as follows: P_1^b ($\mathbf{V}_h$ space) for velocity, P_1 (Q_h space) for pressure, and P_1 or P_2 (V_h space) for temperature.

$$\mathbf{V}_h = \{\mathbf{v} \in H^1(\Omega)^2 | \forall \kappa \in T_h\};$$

$$V_h = Q_h = \{v \in H^1(\Omega) | \forall \kappa \in T_h\}$$

where the characteristic mesh size is denoted by h.

Implicit time separation has led to the derivation of the nonlinear system of equations (7)–(9). To apply the Newton method, this system is written in the form $F(w) = 0$, where $w = (u^{n+1}, p^{n+1}, \theta^{n+1}) \in \mathbf{V} \times Q \times V$ is the variable; here, $F: \mathbf{V} \times Q \times V \to \mathbf{V} \times Q \times V$ is a differentiable transformation. The initial estimate is taken as $w_0 = (u^n, p^n, \theta^n)$ (the solution at time t_n), and the Newton series $w_k = (u_k, p_k, \theta_k)$ is formed by solving for each inner iteration k. If it is defined as $(u_w, p_w, \theta_w) = w_k - w_{k+1}$ and after differentiating equations (7)–(9), equation system can be written explicitly written as:

$$(\nabla \cdot u_w, q) - (\nabla \cdot u_k, q) = 0 \tag{10}$$

$$\left(\frac{3(u_w - u_k) - 4u^n + u^{n-1}}{2\Delta t}, v\right) + b(u_w, u_k, v) + b(u_k, u_w, v) - b(u_k, u_k, v) - (\nabla \cdot v, p_w) + (\nabla \cdot v, p_k) - \left(f_B(\theta_w)e_y, v\right) = \frac{1}{Re}(\nabla u_w, \nabla v) - \frac{1}{Re}(\nabla u_k, \nabla v) - \left(f_B(\theta_k)e_y, v\right), \tag{11}$$

$$\left(\frac{3(\theta_w - \theta_k) - 4\theta^n + \theta^{n-1}}{2\Delta t}, \varphi\right) + (u_w \cdot \nabla\theta_k, \varphi) + (u_k \cdot \nabla\theta_w, \varphi) - (u_k \cdot \nabla\theta_k, \varphi) + \frac{1}{RePr}(\nabla\theta_w, \nabla\varphi) = \frac{1}{RePr}(\nabla\theta_k, \nabla\varphi). \tag{12}$$

4. NUMERICAL STUDIES

In the study by Edde et al. (2025), the objective is to apply the numerical method developed for the investigated numerical model to a realistic underground cavity geometry and to examine the physical characteristics of natural convection.

The simulations were conducted for five different Rayleigh numbers in the range of 10^5–10^9. The results indicate that, as the Rayleigh number increases, natural convection within the cavity becomes significantly stronger, with velocity magnitudes and temperature gradients intensifying particularly in the well region.

While the three-dimensional simulations exhibit qualitative similarities with the two-dimensional results, they also demonstrate that the flow acquires a more irregular and inherently three-dimensional character. In this case, the temperature field becomes more homogeneous within the cavity, and the Nusselt numbers computed at the surface remain lower compared to the two-dimensional case. Nevertheless, the heat fluxes formed at the well mouth indicate that the surface temperature anomalies are of a magnitude detectable by remote sensing methods.

According to this study, two- and three-dimensional numerical simulations performed using a realistic geometry reveal that natural convection in underground cavities is the primary physical mechanism responsible for transporting thermal signals from the cavity to the surface through the well. These findings strengthen the physical basis of cavity detection approaches based on thermal infrared measurements.

Oztop et al. (2019) numerically investigated three-dimensional natural convection flow in a cubic cavity with partial openings on the upper and lower surfaces. In their study, the Navier–Stokes and energy equations were solved under the Boussinesq approximation, and the effects of the Rayleigh

number and opening configurations on flow structures and heat transfer were analyzed. In addition, the thermodynamic performance of the system was evaluated through entropy generation and irreversibility analysis, demonstrating that the location and size of the openings significantly affect both flow organization and heat transfer efficiency. In this respect, the study provides an important reference for modeling systems with surface-opening cavities by elucidating the role of geometric openings in natural convection (Oztop et al., 2019).

Rakotondrandisa, Sadaka, and Danaila (2020) developed a finite element–based numerical toolbox for solving solid–liquid phase change problems coupled with natural convection. In this work, the energy equation and the Navier–Stokes equations were fully coupled, and the enthalpy method was employed to model melting and solidification processes. The developed numerical framework was validated in both two- and three-dimensional configurations, and the interaction between the evolution of the phase boundary and natural convection currents was demonstrated in detail. This study occupies an important place in the literature by providing a flexible and reliable FEM infrastructure for natural convection problems involving complex heat transfer processes (Rakotondrandisa et al., 2020).

Sadaka et al. (2020) advanced this approach further by developing parallel finite element codes for two- and three-dimensional natural convection phase change problems. In the study, parallel computing strategies were implemented to efficiently resolve complex flow structures arising at high Rayleigh numbers, and scalability analyses were performed. The developed codes provide both accuracy and computational efficiency for large-scale and computationally demanding problems. In this regard, the study offers a powerful computational framework for three-dimensional numerical

simulations of underground cavities or engineering systems dominated by natural convection (Sadaka et al., 2020).

Together, these studies strengthen the theoretical and computational foundations of the numerical methodology used in Edde et al. (2025), particularly by providing the necessary computational framework for the reliable simulation of strong convective flows in complex geometries. Therefore, this body of literature forms a complementary whole along the axes of geometric complexity (Oztop et al., 2019; Edde et al., 2025) and advanced numerical infrastructure and scalability (Rakotondrandisa et al., 2020; Sadaka et al., 2020).

Table 1. Summary of Related Numerical Studies on Natural Convection

Reference	Physical Problem	Geometry / Configuration	Dimension	Numerical Method	Main Contribution
Oztop et al. (2019)	Natural convection, heat transfer, entropy generation	Cubic cavity with partial openings at the top and bottom walls	3D	Finite volume method; Navier–Stokes and energy equations	Quantified the influence of opening location and size on flow structures, heat transfer, and thermodynamic irreversibility
Rakotondrandisa et al. (2020)	Natural convection coupled with solid–liquid phase change	General cavity configurations	2D–3D	Finite element method with enthalpy formulation	Developed and validated a FEM toolbox for simulating phase-change systems with natural convection
Sadaka et al. (2020)	Natural convection with phase change	Large-scale 2D and 3D configurations	2D–3D	Parallel finite element method	Introduced scalable parallel FEM codes enabling efficient simulation at high Rayleigh numbers
Edde et al. (2025)	Natural convection and heat transfer	Underground cavity connected to the surface by a vertical well	3D	Finite element method	Investigated the impact of surface connection and well geometry on three-dimensional natural convection patterns

5. CONCLUSION

In this chapter, a comprehensive theoretical and numerical framework for the finite element simulation of three-dimensional natural convection problems governed by the incompressible Navier–Stokes and energy equations under the Boussinesq approximation has been presented. Rather than introducing a new numerical method, the primary objective has been to clarify the mathematical foundations, modeling assumptions, and numerical strategies that are commonly adopted in reliable and robust three-dimensional simulations of buoyancy-driven flows.

The strong nonlinear coupling between fluid motion and heat transfer inherent in natural convection has been highlighted as a central challenge, particularly in three-dimensional configurations and at moderate to high Rayleigh numbers. In this context, the selection of stable mixed finite element spaces satisfying the Ladyzhenskaya–Babuška–Brezzi condition for the velocity–pressure pair, together with appropriate continuous Galerkin discretizations for the temperature field, has been emphasized as a key requirement for numerical stability and accuracy. The use of a fully implicit second-order backward differentiation formula (BDF2) for time integration has been shown to provide favorable stability properties, allowing the resolution of thin thermal boundary layers and strong convective effects. Furthermore, Newton-based nonlinear solution strategies play a critical role in efficiently handling the strong coupling and nonlinearity of the governing equations.

The review of representative numerical studies from the literature demonstrates that three-dimensional effects are often decisive in natural convection problems and cannot, in general, be adequately captured by two-dimensional models. In applications involving complex geometries, such as underground cavities, enclosures with surface openings, or engineering

systems with geometric irregularities, three-dimensional simulations reveal more intricate flow structures and different heat transfer characteristics compared to their two-dimensional counterparts. These studies also underline the importance of scalable and parallel finite element implementations for addressing large-scale problems and high-Rayleigh-number regimes in a computationally efficient manner.

In conclusion, the finite element framework outlined in this chapter provides a solid and flexible foundation for the numerical investigation of three-dimensional natural convection phenomena. The discussed modeling and discretization choices are broadly applicable to a wide range of engineering, environmental, and geophysical problems. Future research directions include the incorporation of more advanced physical models, such as variable-density formulations beyond the Boussinesq approximation, turbulence modeling, phase-change effects, and adaptive mesh refinement, which would further enhance the predictive capability of finite element simulations for complex natural convection systems.

REFERENCES

Bejan, A. (2013). Convection heat transfer. John wiley & sons.

Bergman, T. L. (2011). Fundamentals of heat and mass transfer. John Wiley & Sons.

Donea, J., & Huerta, A. (2003). Finite element methods for flow problems. John Wiley & Sons.

Edde, G., Sadaka, G., Antoine, R., & Danaila, I. (2025). Three-dimensional numerical modeling of natural convection in underground cavities connected to the surface by a well. Computational Geosciences, 29(2), 1-28.

Gray, D. D., & Giorgini, A. (1976). The validity of the Boussinesq approximation for liquids and gases. International Journal of Heat and Mass Transfer, 19(5), 545-551.

Guo, X., & Shang, Y. (2025). Local and parallel two-grid discretization algorithms for natural convection flows. Numerical Algorithms, 1-35.

Hasan, A., Ali, M. M., Hossain, S., Siam, N. H., Rony, A., & Shohan, A. A. (2025). A comprehensive review on natural convection in various shaped enclosures by FEM: Engineering applications. South African Journal of Chemical Engineering, 54, 308-334.

Kakac, S., Yener, Y., & Pramuanjaroenkij, A. (2013). Convective heat transfer. CRC press.

Lee, H. G., & Kim, J. (2012). A comparison study of the Boussinesq and the variable density models on buoyancy-driven flows. Journal of Engineering Mathematics, 75(1), 15-27.

Li, H., Kondoh, T., Jolivet, P., Furuta, K., Yamada, T., Zhu, B., ... & Nishiwaki, S. (2022). Optimum design and thermal

modeling for 2D and 3D natural convection problems incorporating level set-based topology optimization with body-fitted mesh. International Journal for Numerical Methods in Engineering, 123(9), 1954-1990.

Mayeli, P., & Sheard, G. J. (2021). A centrifugal buoyancy formulation for Boussinesq-type natural convection flows applied to the annulus cavity problem. International Journal for Numerical Methods in Fluids, 93(3), 683-702.

Mayeli, P., & Sheard, G. J. (2021). Buoyancy-driven flows beyond the Boussinesq approximation: A brief review. International Communications in Heat and Mass Transfer, 125, 105316.

Oztop, H. F., A. Almeshaal, M., Kolsi, L., Rashidi, M. M., & E. Ali, M. (2019). Natural convection and irreversibility evaluation in a cubic cavity with partial opening in both top and bottom sides. Entropy, 21(2), 116.

Pordanjani, A. H., Aghakhani, S., Afrand, M., Sharifpur, M., Meyer, J. P., Xu, H., ... & Cheraghian, G. (2021). Nanofluids: Physical phenomena, applications in thermal systems and the environment effects-a critical review. Journal of Cleaner Production, 320, 128573.

Rakotondrandisa, A., Sadaka, G., & Danaila, I. (2020). A finite-element toolbox for the simulation of solid–liquid phase-change systems with natural convection. Computer Physics Communications, 253, 107188.

Sadaka, G., Rakotondrandisa, A., Tournier, P. H., Luddens, F., Lothodé, C., & Danaila, I. (2020). Parallel finite-element codes for the simulation of two-dimensional and three-dimensional solid–liquid phase-change systems with natural convection. Computer Physics Communications, 257, 107492.

Shang, Y. (2024). A parallel finite element discretization scheme for the natural convection equations. Journal of Scientific Computing, 100(2), 56.

Szewc, K., Pozorski, J., & Taniere, A. (2011). Modeling of natural convection with smoothed particle hydrodynamics: non-Boussinesq formulation. International Journal of Heat and Mass Transfer, 54(23-24), 4807-4816.

ON A CLASS OF PERFECT NUMERICAL SEMIGROUPS

Sedat İLHAN[1]

1. INTRODUCTION

Numerical semigroups are fundamental algebraic structures used in fields such as determining the structure of error correction codes in coding theory, solving frobenius-type problems in number theory, investigating curve singularities in algebraic geometry, analyzing monoid and generator structures in combinatorics, and defining discrete structures in some cryptographic and statistical models.

Let ¥ and ¢ be the sets of non negative integers and integers, respectively. If it is satisfied following conditions then the subset K of ¥ is a numerical semigroup :

(1) $0 \hat{\imath} K$,

(2) $k_1 + k_2 \hat{\imath} K$, *for all* $k_1, k_2 \hat{\imath} K$,

(3) $Card(¥ \backslash K) < ¥$ (Û $\gcd(K) = 1$).

Here, $\gcd(K)$ is greatest common divisor the elements of K .

Let K be a numerical semigroup, then we define following numbers:

$f(K) = \max(¢ \backslash K)$ is called Frobenius number of K ,

[1] Prof. Dr. Dicle Üniversitesi, Fen Fakültesi, Matematik Bölümü, ORCID: 0000-0002-6608-8848.

$q(K) = \min\{k \in K : k > 0\}$ is called multiplicity of K, and

$d(K) = Card(\{0,1,2,..., f(K)\} \cap K)$ is called determine number of K.

If K is a numerical semigroup such that $K = < z_1, z_2, ..., z_q >$,

then we write that $K = < z_1, z_2, ..., z_q > = \{k_0 = 0, k_1, k_2, ..., k_{d-1}, k_d = f(K) + 1, \rightarrow ...\}$ where $k_v < k_{v+1}$, $d = d(K)$ and $v = 1,2,..., d = d(K)$. Here, the arrow means: if $x > f(K) + 1$ then $x \in K$.

If $b \in \mathbb{N}$ and $b \notin K$, then b is called gap of K. We denote the set of all gaps of K, by $B(K)$, i.e, $B(K) = \mathbb{N} \setminus K$, and the $g(K) = Card(B(K))$ is called genus of K. Also, it is known that $g(K) = f(K) + 1 - d(K)$ (for details see Froberg, 1987;Rosales,2009;Çelik 2020; Assi,2020).

If $b \in B(K)$ and $2b, 3b \in K$, then b is called fundamental gap of K. We denote the set of all fundamental gaps of K, by $U(K)$, that is, $U(K) = \{b \in B(K) : 2b, 3b \in K\}$. Also, the element u is called special gap of K if $u \in \mathbb{N} \setminus K$, $2u \in K$ and $u + r \in K, \forall r \in K \setminus \{0\}$. We denote the set of all special gaps of K, by $T(K)$, i.e.

$T(K) = \{u \in \mathbb{N} \setminus K : 2x \in S, u + r \in K, \forall r \in K \setminus \{0\}\}$ (Rosales, 2005 ; Rosales,2009; Assi,2020).

If $d \in \mathbb{N} \setminus K$ and $d + v \in K, \forall v \in K \setminus \{0\}$ then d is called Pseudo Frobenius number of K. We denote the set of all Pseudo Frobenius numbers of K, by $m(K)$, that is, $m(K) = \{d \in \mathbb{N} \setminus K : d + v \in K, \forall v \in K \setminus \{0\}\}$

(Delgado, 2010; Rosales, 2009; Assi 2020). Let $K = < z_1, z_2, ..., z_q > = \{k_0 = 0, k_1, k_2, ..., k_{d-1}, k_d = f(K) + 1, \circledR ...\}$ be a numerical semigroup. Then for $j \geq 0$, we define the following sets:

$$K_j = \{k \in K : k \geq k_j\} \text{ and } K(j) = \{n \in \mathbb{N} : n + K_j \subseteq K\}.$$

It is clear that $K(j)$ is a numerical semigroup, and we obtain the following chain

$$K_d \subseteq K_{d-1} \subseteq ... \subseteq K_1 \subseteq K_0 = K = K(0) \subseteq K(1) \subseteq ... \subseteq K(d-1) \subseteq K(d) = \mathbb{N}.$$

In this case, the number $c(K) = Card(K(1) \backslash K)$ is called the type of K (D'anna, 1998).

Let K be a numerical semigroup, then K is called symmetric numerical semigroup if $f(K) - g \notin K$, for all $g \notin \mathbb{Z} \backslash K$. It is well known that $K = < z_1, z_2 >$ is symmetric numerical semigroup, and if K is a symmetric numerical semigroup then $d(K) = g(K) = \frac{f(K)+1}{2}$ (Rosales, 1996; Assi, 2020, Çelik,2023). Also, it is known that K is a symmetric numerical semigroup if and only if $c(K) = 1$ (Rosales, 1996; Rosales 2009) .

Let K be a numerical semigroup, then $d \in B(K)$ is a isolated gaps of K if $d-1, d+1 \notin K$ .The set of all isolated gaps of K is denoted by $I(K)$, that is $I(K) = \{d \in B(K) : d-1, d+1 \notin K\}$. A numerical semigroup K is called perfect if $I(K) = \emptyset$ (for details see Moreno,2019; Harold, 2022).

If K is a numerical semigroup such that $K = < z_1, z_2, ..., z_q >$, then the numerical semigroup

$L(K) = \langle z_1, z_2 - z_1, z_3 - z_1, ..., a_q - z_1 \rangle$ is called Lipman numerical semigroup of K, and it is known that

$L_0(K) = K \subseteq L_1(K) = L(L_0(K)) \subseteq L_2 = L(L_1(K)) \subseteq ... \subseteq L_u \subseteq ... \subseteq$.

Let K be a numerical semigroup, then K is Arf if $z_1 + z_2 - z_3 \in K$, for all $z_1, z_2, z_3 \in K$ such that $z_1 \geq z_2 \geq z_3$. In this case, the set $T = \bigcup_{K \subseteq V} V$ is Arf numerical semigroup, where V is Arf numerical semigroup. Thus, ¥ is an Arf numerical semigroup, and the smallest Arf numerical semigroup containing a numerical semigroup K is called the Arf closure of K, and it is denoted by $Arf(K)$. That is, we write $Arf(K) = T$ (Rosales,2004; İlhan, 2017; Angeles, 2020).

In this study, we will give some results about some fundamental concepts of a class of Perfect numerical semigroups K_a such that $K_a = < 2a - 1, 2a, 2a + 1 >$ where $a > 1$ and $a \in$ ¥.

2. MAIN RESULTS

Theorem 2.1. Let $K_a = < 2a - 1, 2a, 2a + 1 >$ be a numerical semigroup where $a > 1$ and $a \in$ ¥. Then, K_a is a perfect numerical semigroup.

Proof. Let $K_a = < 2a - 1, 2a, 2a + 1 >$ be a numerical semigroup where $a > 1$ and $a \in$ ¥. Then, we write $K_a = < 2a - 1, 2a, 2a + 1 > =$

$\{0, 2a - 1, 2a, 2a + 1, 4a - 2, 4a - 1, 4a, 4a + 1, 4a + 2, ..., 2a^2 - 3a - 2, 2a^2 - 3a + 1, \textregistered ...\}$.

So, we obtain $I(K_a) = \{d \in B(K_a) : d - 1, d + 1\} = \text{Æ}$ since

$B(S_a) = \{1, 2, 3, ..., 2a - 2, 2a + 2, 2a + 3, ..., 4a - 3, 2a^2 - 3a - 1, 2a^2 - 3a\}$.

Thus, we find that K_a is a perfect numerical semigroup.

Proposition 2.2. Let $K_a = < 2a-1, 2a, 2a+1 >$ be a numerical semigroup where $a > 1$ and $a \in \mathbb{N}$. Then, we have

(a) $f(K_a) = a(2a-3)$

(b) $d(K_a) = (a-1)^2$

(c) $g(K_a) = a(a-1)$.

Proof. Let $K_a = < 2a-1, 2a, 2a+1 >$ be a numerical semigroup where $a > 1$ and $a \in \mathbb{N}$. Then, we have

(a) $f(K_a) = a^2 - 3a = a(2a-3)$ from definition Frobenius number of $K_a = < 2a-1, 2a, 2a+1 > =$

$\{0, 2a-1, 2a, 2a+1, 4a-2, 4a-1, 4a, 4a+1, 4a+2, ..., 2a^2-3a-2, 2a^2-3a+1, \ldots\}$.

(c) $g(K_a) = Card(B(K_a)) = a(a-1)$ from the set of all gaps of K_a is $B(K_a) = \{1, 2, 3, ..., 2a-2, 2a+2, 2a+3, ..., 4a-3, 2a^2-3a-1, 2a^2-3a\}$.

(b) $d(K_a) = f(K_a) + 1 - g(K_a)$

$= a(2a-3) + 1 - a(a-1) = a^2 - 2a + 1 = (a-1)^2$.

Corollary 2.3. Let $K_a = < 2a-1, 2a, 2a+1 >$ be a numerical semigroup where $a > 1$ and $a \in \mathbb{N}$. Then, the type of K_a is $c(K_a) = 2$.

Proof. Let $K_a = < 2a-1, 2a, 2a+1 >$ be a numerical semigroup where $a > 1$ and $a \in \mathbb{N}$. Then, $K_a = < 2a-1, 2a, 2a+1 > =$

$\{0, 2a-1, 2a, 2a+1, 4a-2, 4a-1, 4a, 4a+1, 4a+2, ..., 2a^2-3a-2, 2a^2-3a+1, \ldots\}$.

Thus, we write $(K_a)_1 = \{k \in K_a : k \geq k_1 = 2a-1\}$

$= \{2a-1, 2a, 2a+1, 4a-2, 4a-1, 4a, 4a+1, 4a+2, ..., 2a^2-3a-2, 2a^2-3a+1, \ldots\}$

and $K_a(1) = \{n \in \mathbb{N} : n + (K_a)_1 \in K_a\} = \{0, 2a-1, \ldots\}$. Thus, we obtain $c(K_a) = Card(K_a(1) \backslash K)$

$$= Card(\{2a^2-3a, 2a^2-3a-1\}) = 2.$$

Proposition 2.4.(Angeles, 2020) Let K be a numerical semigroup and $c(K) = 2$.

Then, $m(K) = \{f(K)-1, f(K)\} \cup \{f(K)-1\} \subset K$.

Proposition 2.5. Let $K_a = \langle 2a-1, 2a, 2a+1 \rangle$ be a numerical semigroup where $a > 1$ and $a \in \mathbb{N}$. Then, we have $m(K_a) = \{f(K_a)-1, f(K_a)\}$.

Proof. Let $K_a = \langle 2a-1, 2a, 2a+1 \rangle$ be a numerical semigroup where $a > 1$ and $a \in \mathbb{N}$.

Then $f(K_a)-1 = a(2a-3)-1 = 2a^2-3a-1 \notin K_a$ since

$B(K_a) = \{1, 2, 3, \ldots, 2a-2, 2a+2, 2a+3, \ldots, 4a-3, 2a^2-3a-1, 2a^2-3a\}$.

Thus, we find $m(K_a) = \{f(K_a)-1, f(K_a)\}$ from Proposition 2.4.

Proposition 2.6. (Assi, 2020). Let $K_a = \langle 2a-1, 2a, 2a+1 \rangle$ be a numerical semigroup where $a > 1$ and $a \in \mathbb{N}$. Then $c(K_a) = Card(m(K_3))$.

Theorem 2.7. (İlhan, 2017). Let K be a numerical semigroup and let $q_j = q(L_j)$ where L_j is the j th term of the Lipman sequence of semigroups of K for each $j \geq 0$. Let, $f(Arf(K)) = f^{(b)}, d(Arf(K) = d^{(b)}$. Then $d^{(b)} = l(K) = l$ and we have,

$Arf(K) = \{k_0^{(b)} = 0, k_1^{(b)}, k_2^{(b)}, ..., k_{l-1}^{(b)}, k_l^{(b)} = f^{(b)} + 1, \ldots\}$ where,

$k_1^{(b)} = q_0 = q(K)$,
$k_2^{(a)} = q_0 + q_1^{(b)}, ..., q_{l-1}^{(b)} = q_0 + q_1 + q_2 + ... + q_{l-2}$,
$k_l^{(b)} = q_0 + q_1 + q_2 + ... + q_{l-2} + q_{l-1}$

and $f^{(b)} = q_0 + q_1 + q_2 + ... + q_{l-2} + q_{l-1} - 1$.

Theorem 2.8. Let $K_a = < 2a-1, 2a, 2a+1 >$ be a numerical semigroup where $a > 1$ and $a \in \mathbb{N}$. Then, we have $Arf(K_a) = \{0, 2a-1, \ldots\}$.

Proof. Let $K_a = < 2a-1, 2a, 2a+1 >$ be a numerical semigroup where $a > 1$ and $a \in \mathbb{N}$.

Then, we obtain $Arf(K_a) = \{0, 2a-1, \ldots\}$ since $L_0(K_a) = K_a$; $q_0 = 2a-2$, and $L_1(K_a) = < 2a-1, 1, 2 > = < 1 > = \mathbb{N}$.

Proposition 2.9. Let $K_a = < 2a-1, 2a, 2a+1 >$ be a numerical semigroup where $a > 1$ and $a \in \mathbb{N}$. Then, we have

(a) $f(Arf(K_a)) = 2a-2$

(b) $d(Arf(K_a)) = 1$

(c) $g(Arf(K_a)) = 2a-2$.

Proof. Let $K_a = < 2a-1, 2a, 2a+1 >$ be a numerical semigroup where $a > 1$ and $a \in \mathbb{N}$. Then, it is clear that

(a) $f(Arf(K_a)) = 2a-2$ and (b) $d(Arf(K_a)) = 1$ from definitions of Frobenius number and determine number.

Also, we obtain

(c) $g(Arf(K_a)) = f(Arf(K_a)) + 1 - d(Arf(K_a)) = 2a-2$.

Proposition 2.10. Let $K_a = < 2a-1, 2a, 2a+1 >$ be a numerical semigroup where $a > 1$ and $a \in \mathbb{N}$. Then, we have $m(Arf(K_a)) = B(Arf(K_a))$.

Proof. Let $K_a = < 2a-1, 2a, 2a+1 >$ be a numerical semigroup where $a > 1$ and $a \in \mathbb{N}$.Then, we write $Arf(K_a) = \{0, 2a-1, \ldots\}$ and

$B(Arf(K_a)) = \{1, 2, 3, \ldots, 2a-2\}$. Thus,we obtain

$$m(Arf(K_a)) = \{x \in B(Arf(K_a)) : x + h \in Arf(K_a), \forall h \in Arf(K_a), h \neq 0\}$$

$$= \{1, 2, 3, \ldots, 2a-2\} = B(Arf(K_a)).$$

Corollary 2.11. Let $K_a = < 2a-1, 2a, 2a+1 >$ be a numerical semigroup where $a > 1$ and $a \in \mathbb{N}$. Then $c(Arf(K_a)) = 2a-2$.

Proof. Let $K_a = < 2a-1, 2a, 2a+1 >$ be a numerical semigroup where $a > 1$ and $a \in \mathbb{N}$.Thenwe write $c(Arf(K_a)) = Card(m(Arf(K_a))) = 2a-2$ from Proposition 2.6.

Corollary 2.12. Let $K_a = < 2a-1, 2a, 2a+1 >$ be a numerical semigroup where $a > 1$ and $a \in \mathbb{N}$. Then , we have

(a) $f(K_a) = f(Arf(K_a)) + 2a^2 - 5a + 2$

(b) $d(K_a) = (a-1)^2 d(Arf(K_a))$

(c) $g(K_a) = g(Arf(K_a)) + a^2 - 3a + 2$.

Proof. Let $K_a = < 2a-1, 2a, 2a+1 >$ be a numerical semigroup where $a > 1$ and $a \in \mathbb{N}$. Then, we obtain

$f(Arf(K_a)) + 2a^2 - 5a + 2 = 2a - 2 + 2a^2 - 5a + 2 = 2a^2 - 3a = f(S_a)$.

$(a-1)^2 d(Arf(K_a)) = (a-1)^2 = d(K_a)$, and

$g(Arf(K_a)) + a^2 - 3a + 2 = 2a - 2 + a^2 - 3a + 2 = a^2 - a = g(K_a).$

Example 2.13. We put $a = 3$ in the numerical semigroup $K_a = < 2a-1, 2a, 2a+1 >$.

Then, we have $K_3 = \langle 5,6,7 \rangle = \{0,5,6,7,10,\ldots\}$.

In this case, we obtain $q(K_3) = 5$, $f(K_3) = 9$, $d(K_3) = 4$, $B(K_3) = \{1,2,3,4,8,9\}$, and $g(K_3) = Card(B(K_3)) = 6$. Also,

$U(K_3) = \{d \in B(K_3) : 2d, 3d \in K_3\} = \{8,9\}$,

$m(K_3) = \{x \in B(K_3) : x + r \in K_3, \forall r \in K_3 \setminus \{0\}\} = \{8,9\}$ and

$T(S_3) = \{u \in B(K_3) : 2u \in K_3 \text{ and } u + y \in K_3, \forall y \in K_3 \setminus \{0\}\} = \{8,9\}.$

So, $c(K_3) = 2$ since

$(K_3)_1 = \{k \in K : k > k_1 = 5\} = \{5,6,7,10,\ldots\}$ and

$K_3(1) = \{n \in \mathbb{N} : n + (K_3)_1 \subset K\} = \{0,5,6,\ldots\}$, then

$c(K_3) = Card(K_3(1) \setminus K_3) = Card(\{8,9\}) = 2.$

Here, the numerical semigroup

$K_3 = \langle 5,6,7 \rangle = \{0,5,6,7,10,\ldots\}$ is perfect since

$I(K_3) = \{b \in B(K_3) : b-1, b+1 \in K_3\} = \emptyset$. On the other hand,

we write that $Arf(K_3) = \{0,5,\ldots\}$ since

$L_0(K_3) = K_3 = < 5,6,7 >$; $q_0 = 5$ and

$L_1(K_3) = L(L_0(K_3)) = L(< 5,6,7 >) = < 5,1,2 > = < 1 > = \mathbb{N}$; $q_1 = 1$.

Thus, $f(Arf(K_3)) = 4$, $d(Arf(K_3)) = 1$,

$B(Arf(K_3)) = \{1,2,3,4\}$ and

$g(Arf(K_3)) = Card(B(Arf(K_3)) = 4$. Also,

$U(Arf(K_3)) = \{d \in B(Arf(K_3)) : 2d, 3d \in Arf(K_3)\} = \{3,4\}$,

$T(Arf(K_3)) = \{u \in B(Arf(K_3)) : 2u \in Arf(K_3), u + r \in Arf(K_3), "r \in Arf(K_3) \setminus \{0\}\} = \{3,4\}$ and

$m(Arf(K_3)) = \{u \in B(Arf(K_3)) : u + y \in Arf(K_3), "y \in Arf(K_3) \setminus \{0\}\} = \{1,2,3,4\}$,

$c(Arf(K_3)) = Card(m(Arf(K_3))) = 4$. In fact ; we find that

$f(K_3) = 3(2.3 - 3) = 9$, $d(S_3) = (3 - 1)^2 = 4$ and

$g(S_3) = 3(3 - 1) = 6$ from Propotion 2.2. Also,

$m(K_3) = \{f(K_3) - 1, f(K_3)\} = \{8,9\}$ and

$c(K_3) = Card(m(K_3)) = 2$ from Proposition 2.5 and Proposition 2.6., respectively. So, we write

$Arf(K_3) = \{0, 2.3 - 1, \circledR \ldots\} = \{0,5, \circledR \ldots\}$ from Theorem 2.8.

Also, $f(Arf(K_3)) = 2.3 - 2 = 4$, $d(Arf(K_3)) = 1$ and

$g(Arf(K_3)) = 2.3 - 2 = 4$ from Proposition 2.9. On the other hand, $m(Arf(K_3)) = \{1,2,3,4\} = B(Arf(K_3))$ and

$c(Arf(K_3)) = 2.3 - 2 = 4$ from Proposition 2.10 and Proposition 2.11, respectively. Finally, we have

$f(K_3) = f(Arf(K_3)) + 2.9 - 5.3 + 2 = 9$,

$d(K_3) = (3 - 1)^2 d(Arf(K_3)) = 4.1 = 4$ and

$g(K_3) = g(Arf(K_3)) + 3^2 - 3.3 + 2 = 4 + 2 = 6$ from Corollary 2.12.

REFERENCES

[1] Moreno Frais,M.A. and Rosales,J.C.(2019). Perfect numerical semigroups, Turkish Journal of Mathematics, 43, 1742 – 1754.

[2] Harold J. S. (2022). On isolated gaps in numerical semigroups, Turkish Journal of Mathematics, 46, 123 – 129.

[3] Delgado, M., Garcia sanchez,P.A. and Robrez Perez, A.M., (2010).Numerical semigroups with a given set of Pseudo Frobenius numbers, LMS J. Comput. Math.,19(1),186-205.

[4] Froberg, R.,Gotlieb, C., &Haggkvist, R., (1987). On numerical semigroups. *Semigroup Forum*, *35*, 63-68.

[5] Rosales, J. C. (1996). On symmetric numerical semigroups. *Journal of Algebra, 182*(2), 422-434.

[6] Rosales,J.C. (2005). Fundamental gaps of numerical semigroups generated by two elements, Linear Algebra and its Applications, 405, 200-208.

[7] Rosales, J.C. and Garcia-Sanchez, P.A. (2009). Numerical semigroups.New York: Springer 181.

[8] Rosales, J.C., Garcia-Sanchez,P.A., Garcia-Garcia, J.I. and Branco, M.B.(2004). Arf numerical semigroups, Journal of Algebra, 276,3-12.

[9] İlhan S. and Karakaş H.İ. (217). Arf numerical semigroups, Turkish Journal of Mathematics, 41, 1448-1457.

[10] Çelik, A. (2023). A note on the some of class of symmetric numerical semigroups, Adıyaman University Jouenal of Science, 13(1-2),18-27.

[11] D'anna, M.(1998).Type sequencess of numerical semigroups, Semigroup Forum,56,1-31.

[12] Rosales, J.C. and Garcia Sanchez, P.A.(2009). Numerical semigroups, Developments in Mathematics, 20, Springer, Newyork.

[13] Çelik, A., Alakuş, M.S. and İlhan, S.(2020). About some numerical semigroups with embedding dimension three, Al-Quadisiyah Journal of püre sciences, 27(1),82-90.

[14] AngelesMoreno-Frais, M. And Rosales J.C.(2020). Perfect numerical semigroups with embedding dimension three, Publ. Math. Debrecen ,97(1-2),77-84.

[15] Assi, A. , Danna, M. and Garcia Sanchez, P.A.,(2020). Numerical semigroups and Aplications, Springer

MATEMATİKSEL DÜĞÜM VE TOPOLOJİ

Nazmiye ALEMDAR[1]

1. GİRİŞ

Düğüm teorisi, matematikte üç boyutlu kapalı eğrilerin incelendiği bir teoridir. Bir düğümü, matematiksel olarak bir ipin iki ucunun birleştirilmesiyle oluşan kapalı eğri olarak görmek kolay bir yaklaşım olmakla birlikte, teorisi, yani düğüm teorisi, o kadar da basit değildir. Son yıllarda birçok bilim alanında düğüm teorisi ile ilgili çalışmalar yapılmış ve makaleler yazılmıştır. Matematik ve düğüm teorisi arasında vazgeçilmez ve bir o kadar da önemli bir bağlantı vardır; zira matematik, pek çok disiplinde olduğu gibi, düğüm teorisinin doğurduğu problemlerin çözümde temel bir araçtır.

Çok eski zamanlardan beri insanlar düğümlere ihtiyaç duymuştur. Farklı amaçlar için farklı düğüm türleri kullanmıştır. Düğümler ağ örmek, bir şeyleri birbirine bağlamak, kumaş ve hasır örmek, köprüler inşa etmek, tepelere tırmanmak vb. için kullanmıştır. Düğümler kullanılarak güzel dekoratif eşyalar, dikiş ve nakış işleri yapılmaktadır.

Düğümlerin tarihçesi yazının icadından öncesine uzansa da, düğüm teorisinin matematiksel bir disiplin haline gelmesi daha geç bir dönemde gerçekleşmiştir. Matematikçileri bu alanda çalışmaya çeken motivasyon, teorinin kimyada, daha sonra fizikte ve daha yakın zamanda da biyolojide uygulamalarının matematikle açıklanması gerekliliği ile olmuştur.

[1] Doç. Dr., Erciyes Üniversitesi, Fen Fakültesi, Matematik Bölümü, ORCID: 0000-0002-0819-6613.

Düğüm teorisi, genetikten kuantum mekaniğine kadar çeşitli alanlarda var olmuştur. Bilimin kendine özgü sırları olduğu ve düğümlerin bunları çözmek için uygulanan girişimlerden sadece biri olduğu iyi bilinmektedir. Bu çalışmanın amacı düğüm teorisinin temel kavramlarını ve gelişimini örnekleri ile sunmak ve okuyucuya matematik ve topolojinin düğüm teorisi için vazgeçilmez olduğunu anlatmaktır. Bunun için öncelikle düğüm teorisi ile ilgili matematiksel temel tanım ve kavramlar verilecektir. Daha sonra ise düğüm teorisinin tarihsel gelişimi uygulamaları ve teoride matematik ve topolojinin gerekliliği sebepleri ile anlatılacaktır.

2. TEMEL KAVRAMLAR ve TANIMLAR

Bu bölümde verilen temel kavramlar Murasugi (1996) kaynağından alınmıştır.

İp kullanılarak atılabilen en kolay düğümler, el üstü düğümü ve sekiz rakamı düğümüdür.

Şekil 1. El Üstü Düğümü **Şekil 2. Sekiz Düğümü**

İpin iki ucu birbirine yapıştırıldığında bir ilmek oluşur. Bu ilmeğe Matematiksel Düğüm denir. Matematikte aşikar bir düğüm (yani düğümlenmemiş) dolaşık olmayan bir ilmek, üç boyutlu, kapalı ve kendi kendini kesmeyen bir eğridir.

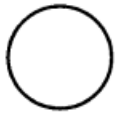

Şekil 3. Aşikar Düğüm

Tanım 1: R^3 de $S^1 = \{(x, y, z): x^2 + y^2 = 1, z = 0\}$ çemberi ile topolojik olarak denk (homeomorfik) olan herhangi bir kümeye düğüm denir. Dolayısıyla düğüm, uzayda bir kapalı eğridir. Başka bir deyişle düğüm, birim çemberin uzaydaki konumudur.

Düğümlerin kendi içinde kesişen noktaları olabilir. Düğüm ya kendi üzerinden ya da altından geçer ki bunlara geçiş denir.

Şekil 4. Bir geçişli düğümler

Şekil 5. İki geçişli düğümler

Düğüm teorisinde, Üç Yapraklı Düğüm (trefoil) en basit, aşikar olmayan düğümdür. Şekil 1 de verilen El Üstü Düğümünün gevşek uçlarının birleştirilmesiyle elde edilir. Bu düğümü kesmeden aşikar düğüm elde etmek mümkün değildir. Şekil 2 de verilen sekiz düğümünün gevşek uçları birleştirildiğinde ise sekizli düğümü elde edilir.

Şekil 6. Üç Yapraklı Düğüm

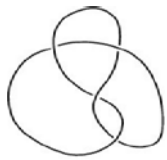

Şekil 7. Sekizli Düğümü

Daha önce belirttiğimiz gibi bir düğüm kapalı bir eğridir. Dolayısıyla bu eğrinin bir başlangıç ve bitiş noktası yoktur. Düğümleri ayırt etmenin bir yolu eğriye bir yön vermektir. Özel olarak, eğri üzerine eklenen bir okla bir düğümün yönü gösterilir.

Şekil 8 de görüldüğü gibi herhangi bir düğüm için olası iki yön vardır.

Şekil 8. Sağ ve Sol Yönlü Üç Yapraklı Düğümler

Birbiri ile kesişmeyen sonlu ve düzenli bir düğüm topluluğuna bağlantı denir. Aşağıdaki şekilde ikişer düğümden oluşan iki bağlantı örneği görülmektedir.

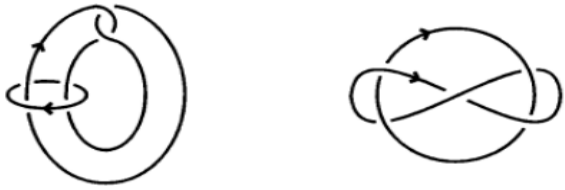

Şekil 9. Bağlantılı Düğümler

Dolaşık bir kapalı ip düğümü, kesmeden kendi içinde çekiştirip hareket ettirilerek deforme edildiğinde ortaya çıkan düğüm tamamen farklı bir düğüm gibi görünür. Ancak deforme edilen bu düğüm, orijinal düğümle aynı kabul edilir. Aşağıdaki şekilde verilen iki düğüm tamamen farklı görünmesine rağmen denk düğümlerdir. Bu düğümler, Perko'nun düğüm çifti olarak adlandırılır.

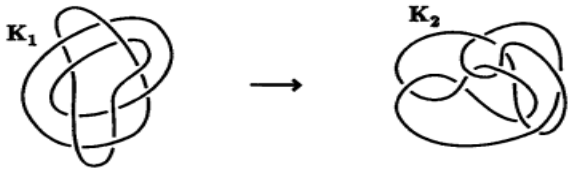

Şekil 10. Perko'nun Düğüm Çifti

Şekil 10 da verilen Perko'nun düğüm çifti yön verilmemiş denk iki düğümdür. Şekil 8 de verilen iki düğüm yönlendirme yapılmadan önce denk iki düğümken yönlü olarak denk değildirler. Yönlü iki düğümün denkliği için aşağıdaki teorem verilmiştir.

Teorem 2: R^3 de K_1 ve K_2 yönlü iki düğüm olsun. Eğer bu iki düğüm arasında yönü koruyan bir homeomorfizm varsa K_1 ve K_2 düğümleri birbirine denktir denir.

İki düğüm denk ise, aynı türden oldukları söylenir.

3. DÜĞÜM TEORİSİNİN TARİHİ GELİŞİMİ, UYGULAMALARI VE TOPOLOJİ

Burada düğüm teorisinin tarihi gelişimi oluşturulurken Silver (2006), Przytycki (1995) ve Sunitha (2016) kaynakları temel olarak kullanılmıştır.

Herhangi bir şekilde ve sayıda iç içe geçmiş düğümlerden oluşan bağlantılar, Antik Roma'da popüler bir motif olarak genellikle evleri ve tapınakları süsleyen mozaiklere eklenirdi. Bunun en iyi örnekleri Kells Kitabı'nda bulunan Kelt düğüm ve bağlantı desenleridir. 7. yüzyılda İrlanda'da ortaya çıkmış ve oradan İskoçya'ya yayılmıştır.

Düğüm kavramına bir matematik konusu olarak ilk atıf, 1771 yılında Fransız matematikçi Theophil Vandermonde'nin yazdığı "Remarques sur les problems de situation" (Konum Problemleri Üzerine Notlar) adlı makalede yapılmıştır. Özellikle örgülerin ve düğümlerin konum geometrisinin konusu olarak ele alındığı bu makalenin ilk paragrafında Vandermonde şöyle yazmıştı: ''Uzaydaki bir iplik parçasının kıvrımları ve dönüşleri ne olursa olsun, boyutlarının hesaplanması için her zaman bir ifade elde edilebilir, ancak bu ifade pratikte pek işe yaramayacaktır. Bir örgü, bir ağ veya bazı düğümler yapan

zanaatkar, ölçüm sorularıyla değil, konum sorularıyla ilgilenecektir: orada gördüğü şey, ipliklerin iç içe geçme biçimidir''.

Günümüzde Düğüm Teorisi olarak adlandırılan matematiksel düğüm teorisi, Alman matematikçi Carl Friedrich Gauss'un (1777-1855) düğümlerin tablolaştırılması için bir yöntem geliştirdiği 19. yüzyıla kadar uzanmaktadır. Dunnington (1955) ve Stäckel kaynaklarında: "Gauss'a ait belgeler arasında bulunan en eski notlardan biri, 1794 tarihli bir kağıttır. Başlığında "Düğüm koleksiyonu" yazan bu kağıt, yanlarında İngilizce isimleri yazılı on üç adet düzgün çizilmiş düğüm resmi içermektedir... Bununla birlikte, düğüm resimleri içeren iki ek kağıt parçası daha vardır. Biri 1819 tarihli; diğeri ise çok daha sonraki bir tarihe aittir..." şeklindeki ifadenin varlığından bahsedilmektedir. Bu ise Gauus tarafından çizilen düğümlerin bulunduğu belgelerin hala kaybolmadığı anlamına gelir. Şekil 11 de 1794 yılından kalma kağıtta bulunan Gauss'un çizdiği 10. düğüm olan iç içe geçme düğümü verilmiştir.

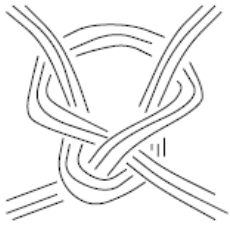

Şekil 11. Gauss'un İç İçe Geçme Düğümü

Bir duvar ustasının oğlu ve döneminin en büyük matematikçisi olan Johann Carl Friedrich Gauss, bağlantılar hakkında aşikar olmayan bir gerçeği keşfeden ilk kişiydi. Gauss, düğüm kavramını elektrodinamik alanındaki çalışmalarında kullanmıştır. Kapalı bir eğri boyunca bir akım döngüsünün varlığında manyetik kutup üzerinde ne kadar iş yapıldığını bilmek istemiştir. Birbirini kesmeyen iki döngüyü ele almıştır. 1833'te,

günümüzde "Gauss bağlantı sayısı" olarak adlandırılan "birbirine dolanma" sayısının bir integralle hesaplanabileceğini göstermiştir. 1876'da O. Boeddicker ise belli bir bağlamda bağlantı sayısının, ikinci eğrinin birinci eğri tarafından sınırlanan bir yüzeyle kesişme noktalarının sayısı olduğunu gözlemlemiştir.

1847 yılı, düğüm teorisi (aynı zamanda graf teorisi ve topoloji) için çok önemli bir yıldır. Gustav Robert Kirchoff (1824-1887) elektrik devreleri üzerine temel makalesini yayınlamıştır. Kirchhoff (1947) makalesi düğüm teorisi ile ilişkilidir ancak bu ilişki yaklaşık yüz yıl sonra keşfedilmiştir (örneğin, bir devrenin Kirchhoff karmaşıklığı, devre tarafından belirlenen düğümün veya bağlantının determinantına karşılık gelir).

Gauss'un, düğümler üzerine çalışmalarından etkilenen öğrencisi Johann Benedict Listing de (1808-1882) düğümlerle ilgilenmiştir. Listing, konumun geometrisini tanımlamak için Yunanca topos (yer) ve logos (akıl) kelimelerinin birleşimi olan topoloji kelimesine türeten kişidir. "Topoloji" terimini ilk kez kullandığı "Vorstudien zur Topologie" adlı çalışmasında matematiksel düğümler ve bunların sınıflandırılması üzerine bir tartışmaya yer vermiştir. Özellikle, düğümlerin kiralitesiyle, yani bir düğüm ile onun ayna görüntüsü arasındaki denklik ilişkisiyle ilgilenmiştir. Sağ Elli Üç Yapraklı Düğüm ile Sol Elli Üç Yapraklı Düğümün denk olmadığını (birbirine dönüştürülemediğini) ifade eden ilk kişidir. Buna karşılık, Listing düğümü olarak da bilinen Sekizli Düğümün akiral; yani kendi ayna görüntüsüne denk olduğunu belirtmiştir.

(a) **(b)**

Şekil 12. (a) Sağ Elli ve (b)Sol Elli Üç Yapraklı Düğümler

1860'larda ünlü İngiliz fizikçi Sir William Thomson (1824-1907) (daha sonra Lord Kelvin olarak bilinecek), fizikçi Herman von Helmholtz'un (1821-1894) girdap hareketi üzerine yaptığı çalışmalardan ve Peter Gurthrie Tait'in (1831-1901) girdap duman halkaları üretme gösterisinden ilham almıştır. Tait, Alman bilim insanı Hermann von Helmholtz'un bir makalesinden, ideal bir akışkandaki girdap halkasının kararlı ve kalıcı olacağını öğrenmiştir. Hava ideal bir akışkan olmamasına rağmen Tait yaklaşık bir model oluşturmuştur. Tahta bir kutunun bir ucuna büyük bir delik açmıştır ve diğer ucunu sıkıca gerilmiş bir havluyla değiştirmiştir. Kutunun içine güçlü bir amonyak çözeltisi serpmiştir ve üzerine yemek tuzu dökülmüş sülfürik asit içeren bir kap yerleştirmiştir. Tait yedi yıl sonra bir konferansta, havluyu yere vurduğunda, girdap halkaları ortaya çıktığını ve şiddetle titreştiklerini, sanki katı kauçuk halkalarmış gibi olduklarını açıklamıştır. Tait bunların kararlılığına hayran kalmıştır. Yuvarlak bir delik yerine eliptik veya kare bir delik kullanılsaydı, girdap şekli sallanıp titreşerek dairesel bir şekil alırdı. Tait, Thomson'ın girdap halkaları kavramını 1874'te yayınlanan bir dizi konferansta açıklamıştır. Girdap Atomları Teorisi (Theory of Vortex Atoms); Sir William Thomson tarafından 19. yüzyılda ortaya atılan, atomların eterdeki (o dönemde varsayılan bir ortam) kararlı girdap halkaları (vortex rings) olduğu fikrine dayanan hipotezdir. Bu teori, elementlerin farklı özelliklerini, bu girdapların farklı düğümlü yapılarıyla açıklamayı amaçlamıştır. Girdap halkalarının etkileşimlerini, bir çay kaşığını bir fincan çayın yüzeyinde gezdirmenin etkileriyle karşılaştırmıştır. William Thomson'a göre tüm madde atomları- zorunlu olarak sonsuz olmalıdır, yani uçları herhangi bir sayıda kıvrım veya düğümlenmenin en sonunda birleşmiş olmalıdır.

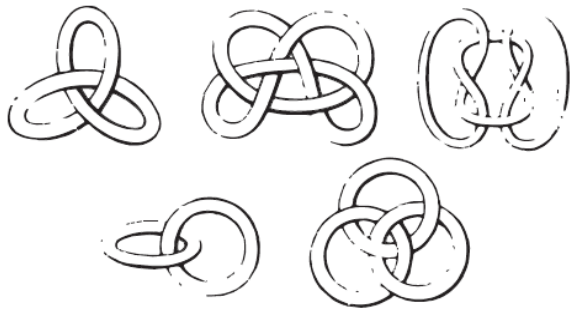

Şekil 13. William Thomson'a (Kelvin) ait 1867 tarihli düğümler ve bağlantılar

Modern düğüm teorisinin kökeni dört fizikçiyle ilişkilendirilebilir: Hermann von Helmholtz, William Thomson (Lord Kelvin), Maxwell ve Peter Guthrie Tait.

James Clerk Maxwell (1831-1879) ile Tait ilk kez Edinburgh Akademisi'nde öğrenciyken tanışmışlardı. Daha sonra meslektaş olarak, iki arkadaş neredeyse her gün yeni yarım penilik kartpostallarla yazışmışlardır. Knott (1911) ve Lomonaco (1996), Maxwell'in 13 Kasım 1867 tarihinde Tait'e yazdığı bir mektuptan bahsetmektedir; bu mektuptan, Maxwell'in düğümler hakkındaki fikirlerini arkadaşıyla paylaştığı anlaşılmaktadır. Maxwell'in düğümlere ve topolojiye olan derin ilgisi, muhtemelen Thomson'ın girdap-atom teorisinden ve Tait'in etkisinden kaynaklanmıştır. James Clerk Maxwell, elektrik ve manyetizma üzerine yaptığı çalışmalarında, özellikle yeni yayımlanan Gauss'un derlenmiş eserlerinden esinlenerek, düğümler ve bağlantılar hakkında bazı teorik yaklaşımlar geliştirmiştir. Üstten ve alttan geçişleri belirten düğüm diyagramları oluşturmuştur. 3 Reidemeister hareketini tanımlamıştır. Maxwell, iki düğümün bağlantı sayısının fiziksel bir önemi olduğunu açıklamıştır. Bir düğümden elektrik akımı geçtiğinde manyetik alan oluşturduğunu söylemiştir. Bağlantı sayısı, esasen ikinci düğümün yolu boyunca hareket eden yüklü bir parçacığın yaptığı iştir demiştir. Maxwell, bağlantı sayısını

Gauss'un daha önce keşfettiği bir çift katlı integral olarak ifade etmiştir. Ayrıca, ayrılamayan ancak Gauss integral değeri sıfıra eşit olan Şekil 14 de verilen iki kapalı eğriden oluşan bağlantıyı tanımlamıştır.

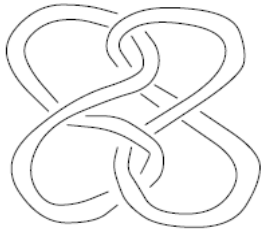

Şekil 14. Maxwell'e ait bağlantı

Atom teorisinin girdap modeli, düğümlerin sınıflandırılmasını gerektiriyordu. Fizikçi Peter Gurthrie Tait, 1867'de düğümlerin ilk tablosunu oluşturmaya başlamıştır. Tait; Rahip Thomas Penyngton Kirkman (1806-1895) ile iş birliği içinde ve Charles Newton Little'dan bağımsız olarak, düğümleri numaralandırma problemi üzerinde önemli bir ilerleme kaydetmiştir. Bu sayede 1900 yılına gelindiğinde, on geçişli düğümlere kadar olan (asal) düğüm tabloları Tait (1877), Kirkman (1885), Little (1885), Little (1889) kaynaklarında yayınlamıştır. Bu tablolar, Haseman'ın (1918) doktora teziyle kısmen genişletilmiştir. 11 geçiş sayısına kadar olan düğümlerin numaralandırılması ise Conway (1969) da verilmiştir. 13 geçişe kadar olan düğümler, Dowker ve Thistlethwaite (1983) ve Thistlethwaite (1985) de numaralandırılmıştır. Tait, düğüm tabloları oluşturabilmek amacıyla Tait Varsayımları olarak adlandırılan üç temel ilke ortaya koymuştur. Bu varsayımların tamamı yakın zamanda çözüme kavuşturulmuştur.

Düğüm teorisindeki en temel problem, denk olmayan düğümleri birbirinden ayırt edebilmektir. Jules Henri Poincaré (1854-1912), Poincaré (1895) 'Analysis Situs' isimli makalesinde cebirsel topolojinin temellerini atana kadar basit iki düğüm olan Aşikar Düğüm ile Üç Yapraklı Düğümün birbirinden ayırt

edilmesi mümkün olmamıştır. Heinrich Tietze (1880-1964) ise Aşikar Düğümü, Üç Yapraklı Düğümden ayırt etmek için düğüm grubu olarak adlandırılan bir düğümün R^3 içindeki dış yüzeyinin temel grubunu kullanmıştır (Tietze, 1908). Temel grup, esasen Poincaré (1895) makalesinde tanıtılmıştır. Buradan anlaşılacağı üzere düğüm teorisindeki en temel problem olan denk olmayan düğümleri ayırt etmek için matematiğin konum geometrisi ile ilgilenilen alanı topoloji ve cebir ile topolojinin birlikte çalışıldığı alan cebirsel topoloji kullanılmıştır.

Kiralite kavramı, Düğüm Teorisi ile kimya arasındaki en güçlü köprüdür. Düğüm teorisinde bir düğüm, eğer sürekli bir deformasyonla (parçaları kesip yapıştırmadan sadece esnetip bükerek) kendi ayna görüntüsüne dönüştürülemiyorsa topolojik olarak kiral kabul edilir.

Kimyasal bağları aynı olan ancak topolojik yapıları (düğümlenme veya halkalanma biçimleri) farklı olan moleküllere topolojik stereoizomerler denir. Kimyagerler, topolojik stereoizomer çiftlerini sentezleyebilmek için bir düğümün kiral mi yoksa akiral mi olduğunu bilmelidir. Sol-elli kiral bir molekül, sağ-elli muadilinden farklı fiziksel veya kimyasal özellikler sergileyebilir. Bu özellik farkı, kiralite çalışmalarını kimya biliminde kritik bir konuma taşımaktadır. Bir kimyager, laboratuvarda düğümlü bir molekül sentezlediğinde, bunun hangi el yönünde kiral olduğunu belirlemek için Jones Polinomu gibi matematiksel araçlara ihtiyaç duyar. Bu da matematik ve topolojinin düğümlü bir molekülün kiralitesini belirlemede kullanıldığını göstermektedir.

Genetik bilimindeki en önemli kırılma noktalarından biri, 1950'li yıllarda James Watson ve Francis Crick'in DNA'nın çift sarmallı yapısını keşfetmesiyle yaşanmıştır. Bu yapısal model, DNA replikasyonunun mekanizmasının aydınlatılmasına olanak sağlamıştır. Watson ve Crick'in bu modeli, DNA'nın iki uzun

polimer zincirinden oluştuğunu ve bu zincirlerin birbirine tamamlayıcı baz eşleşmeleriyle bağlandığını göstermiştir: Adenin (A) her zaman Timin (T), Guanin (G) ise her zaman Sitozin (C) ile eşleşir. Bu yapı, DNA replikasyonunun (eşlenmesinin) temel mekanizmasını da ortaya çıkarmıştır. Bu bağlar, baz istiflenmesi etkileşimleriyle birlikte DNA zincirini bir arada tutmaktadır. Sarmalın iki kolu bir fermuar gibi açıldığında, her bir kol yeni sentezlenecek olan zincir için bir kalıp görevi görür. Baz eşleşme kuralı sayesinde, orijinal dizilim tam doğrulukla kopyalanabilir.

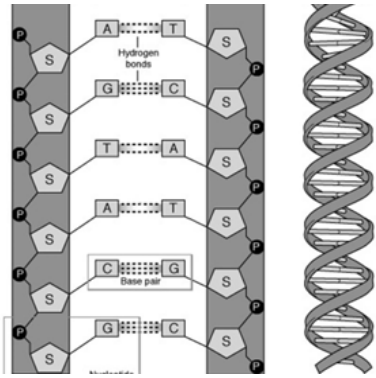

Şekil 15. DNA'nın birincil ve ikincil yapısı

DNA'nın çift sarmal yapısı ile Düğüm Teorisi arasındaki ilişki, modern moleküler biyolojinin en büyüleyici konularından biridir. DNA, hücre çekirdeğine sığabilmek için sıkı bir şekilde paketlenmiş durumdadır. Bu paketlenme ve replikasyon (eşlenme) süreci sırasında DNA zincirlerinin düğümlenmesi ve birbirine dolanması kaçınılmazdır.

Liu ve Davis (1981) çalışmasında ilk kez laboratuvar ortamında düğümlenmiş DNA moleküllerini izole etmişlerdir. Deneysel olarak DNA düğümlerini ve bağlantılarını ayrıştırmanın veya analiz etmenin iki yolu bulunmaktadır: elektron mikroskobu veya elektroforetik göç (Krasnow et al., 1983; Trigueros et al., 2001; Zechiedrich & Crisona, 1989).

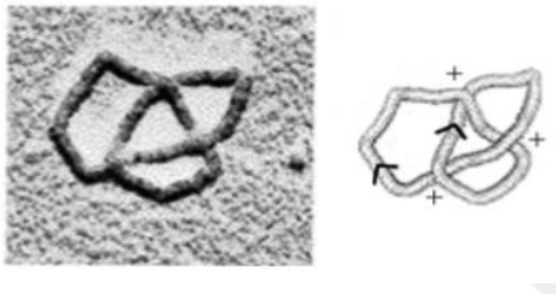

Şekil 16. Düğümlenmiş DNA'nın elektron mikroskop görüntüsü

DNA, hücre çekirdeği içerisinde oldukça yoğun (kompakt) bir biçimde muhafaza edilmektedir. Halkasal bir DNA'nın süper-sarmal, düğümlenmiş ve bağlantılı olmak üzere üç topolojik temel formu vardır. Replikasyon, verilen bir DNA molekülünün kopyalanması sürecidir. DNA kopyalanırken sarmal açıldığında, fermuarın ön kısmında aşırı bir burulma (süper kıvrılma) oluşur. Eğer bu gerilim çözülmezse DNA zinciri kopabilir veya kopyalama durabilir. Watson ve Crick'in keşfettiği çift sarmal, matematiksel olarak iki kapalı halkanın birbirine dolanması (bağlantı) gibidir. Hücrelerimizde Topoizomeraz adı verilen özel enzimler yani doğal düğüm çözücüler bulunur. Bu enzimler, DNA zincirini keserler sonra dolanmış olan diğer zinciri bu kesiğin içinden geçirirler ve son olarak kesiği tekrar yapıştırırlar. Bu reaksiyon sonunda, nükleotid dizilimi ve temel bağlar (fosfodiester bağları) değişmez ki bu Düğüm Teorisi'ndeki "Reidemeister Hamleleri"ne (düğümü bozmadan yapılan temel hareketler) biyolojik bir örnektir. Ancak bu halkaların birbirinden ayrılması için topolojik bir değişim gerekir. Buck (2009), Demidov (2002), Ketron ve Osheroff (2014) vb. birçok çalışmada DNA topolojisi çalışılmıştır.

Topolojik enzimoloji, enzimlerin (özellikle topoizomeraz ve rekombinazların) DNA'nın düğümlenme veya bağlantılı olma durumunu nasıl değiştirdiğini inceleyen disiplinler arası bir daldır.

Bilim insanları, DNA'nın topolojik formunu inceleyerek hangi enzimin nasıl çalıştığını anlarlar. Bu yaklaşımla, enzimleri doğrudan gözlemlemek yerine, onların DNA üzerinde bıraktığı "topolojik imzaları" (oluşturdukları düğüm ve halka türlerini) inceleyerek çalışma mekanizmaları çözülür. Örneğin, bir deney tüpündeki DNA'nın elektron mikroskobu altındaki görüntüsünde bir Üç Yapraklı Düğüm oluşmuşsa, bu durum belirli enzimlerin o bölgede işlem yaptığını kanıtlar. Eğer düğüm çözülmezse hücre bölünemez ve ölür. Birçok kanser ilacı ve antibiyotik, tam olarak bu süreci hedef alır; yani topoizomeraz enzimlerini durdurarak kanserli hücrenin DNA düğümlerini çözmesini engeller ve hücrenin kendi düğümlerinde boğulmasını dolayısıyla yok olmasını sağlar.

DNA düğümleri ile ilgili çalışmalarda matematik ve topolojinin gerekliliği açıkça görülmektedir.

4. SONUÇ

Bu çalışma; düğüm teorisinin tarihi gelişim sürecinde matematik ve topoloji kullanılmasına neden gerek duyulduğunu, bu alandaki çalışmaların güncelliğini/önemini, teorinin ele aldığı temel kavramları, konunun tarihsel süreçteki yavaş gelişimini ve disiplinler arası alanlardaki uygulamalarını inceleyen bir literatür taraması niteliğindedir.

KAYNAKÇA

Boeddicker, O. (1876a). *Beitrag zur Theorien des Winkels* (Doktora tezi). Göttingen Üniversitesi, Almanya.

Boeddicker, O. (1876b). *Erweiterung der Gausschen Theorie der Verschlingungen*. Stuttgart, Almanya.

Buck, D. (2009). DNA topology. *Proceedings of Symposia in Applied Mathematics, 66*, 47–79.

Conway, J. H. (1969). An enumeration of knots and links. J. Leech (Ed.), *Computational problems in abstract algebra* içinde (ss. 329–358). Oxford, İngiltere: Pergamon Press.

Demidov, V. (2002). On proteins, DNA and topology. *Trends in Biotechnology, 20*(6), 234.

Dowker, C. H., & Thistlethwaite, M. B. (1983). Classification of knot projections. *Topology and Its Applications*, *16*(1), 19–31.

Dunnington, G. W. (1955). *Carl Friedrich Gauss: Titan of science*. New York, NY: Hafner Publishing Co.

Haseman, M. G. (1918). On knots, with a census of the amphicheirals with twelve crossings. *Transactions of the Royal Society of Edinburgh, 52*(11), 235–255.

Ketron, A. C., & Osheroff, N. (2014). DNA topology and topoisomerases. *Molecular Life Sciences* içinde (ss. 1–19). New York, NY: Springer.

Kirchhoff, G. R. (1847). Über die Auflösung der Gleichungen, auf welche man bei der Untersuchung der linearen Verteilung galvanischer Ströme geführt wird. *Annalen der Physik und Chemie*, *148*(12), 497–508.

Kirkman, T. P. (1885). The enumeration, description and construction of knots with fewer than ten crossings.

Transactions of the Royal Society of Edinburgh, 32, 281–309.

Knott, C. G. (1911). *Life and scientific work of Peter Guthrie Tait*. Cambridge, İngiltere: Cambridge University Press.

Krasnow, M. A., Stasiak, A., Spengler, S. J., Dean, F., Koller, T., & Cozzarelli, N. R. (1983). Determination of the absolute handedness of knots and catenanes of DNA. *Nature, 304*(5926), 559–560.

Little, C. N. (1885). On knots, with a census for order ten. *Transactions of the Connecticut Academy of Arts and Sciences, 18*, 374–378.

Little, C. N. (1899). Non-alternate knots. *Transactions of the Royal Society of Edinburgh, 39*(3), 771–778.

Liu, L. F., & Davis, J. L. (1981). Novel topologically knotted DNA from bacteriophage P4 capsids: Studies with topoisomerases. *Nucleic Acids Research, 9*(16), 3979–3989.

Lomonaco, S. L. (1996). The modern legacies of Thomson's atomic vortex theory in classical electrodynamics. *Proceedings of Symposia in Applied Mathematics, 51*, 145–166.

Murasugi, K. (1996). *Knot theory and its applications*. Boston, MA: Birkhäuser.

Poincaré, H. (1895). Analysis situs. *Journal de l'École Polytechnique, 1*, 1–121.

Przytycki, J. H. (1995). *Knot theory from Vandermonde to Jones*. George Washington University. https://arxiv.org/abs/math/0703096

Silver, D. S. (2006). Knot theory's odd origins. *American Scientist, 94*(2), 158–165.

Stäckel, P. (t.y.). Gauss als Geometer. *Gauss' collected works* içinde (Cilt 10).

Sunitha, K. G. (2016). *Knot theory* (Final Project Report No. F.MRP / 12th Plan / 14–15 / KLCA 025). Ottapalam, Hindistan: N. S. S. College, Department of Mathematics.

Tait, P. G. (1898–1900). *On knots I, II, III*. *Scientific papers* içinde. Cambridge, İngiltere: Cambridge University Press. (Orijinal çalışma 1877'de yayımlanmıştır)

Thistlethwaite, M. B. (1985). Knot tabulations and related topics. I. M. James & E. H. Kronheimer (Ed.), *Aspects of topology* içinde (ss. 1–76). Cambridge, İngiltere: Cambridge University Press.

Tietze, H. (1908). Über die topologischen Invarianten mehrdimensionaler Mannigfaltigkeiten. *Monatshefte für Mathematik und Physik*, *19*(1), 1–118.

Trigueros, S., Arsuaga, J., Vazquez, M. E., Sumners, D. W., & Roca, J. (2001). Novel display of knotted DNA molecules by two-dimensional gel electrophoresis. *Nucleic Acids Research*, *29*(13), e67.

Zechiedrich, E. L., & Crisona, N. J. (1989). Coating DNA with RecA protein to distinguish DNA path by electron microscopy. M. Bjornsti & N. Osheroff (Ed.), *Methods in molecular biology: DNA topoisomerase protocols* içinde (Cilt 1, ss. 99–108). Totowa, NJ: Humana Press.

PARAMETER ESTIMATION OF UNIT-TEISSIER DISTRIBUTION UNDER DIFFERENT SAMPLING SCHEMES

Hasan Hüseyin GÜL[1]

1. GİRİŞ

Sampling designs have long been employed as an effective tool to reduce the cost and effort associated with data collection, particularly in studies where full observation of all units is impractical. Among these designs, simple random sampling (SRS) remains the most commonly used approach due to its simplicity. However, in many applications the precision of estimators obtained from SRS may be improved if additional information about the relative ordering of units is available.

Ranked set sampling (RSS) represents one such approach in which auxiliary ranking information is incorporated into the sampling process. The method was first introduced by McIntyre (1952) in the context of agricultural studies, where measuring pasture yield was costly but visual ranking of plots could be performed with little effort. Since then, the theoretical properties of RSS have been investigated extensively, and it has been shown that estimators based on RSS can achieve higher efficiency than those based on SRS without increasing the number of measured observations (Takahasi and Wakimoto, 1968; Dell and Clutter, 1972).

The RSS procedure relies on a structured selection mechanism. Instead of measuring all sampled units, several SRS

[1] Doç. Dr., Giresun Üniversitesi, Fen-Edebiyat Fakültesi, Veri Bilimi ve Analitiği, ORCID: 0000-0001-9905-8605.

of equal size are drawn from the population, and the units within each sample are ordered using judgmental criteria or auxiliary variables. Only one unit from each ranked sample is then selected for actual measurement, and the procedure is repeated over multiple cycles to obtain the desired sample size. This strategy allows ranking information to be exploited while keeping measurement costs fixed.

Motivated by these properties, a wide range of modifications of RSS have been proposed in the literature to address practical issues such as ranking errors and sample wastage. These extensions have been applied to parameter estimation problems for various probability distributions, including the Kumaraswamy distribution (Hussian, 2014), the exponential distribution (Samuh and Qtait, 2015), and the Rayleigh-type models (Dey et al., 2016; Esemen and Gürler, 2018), among others. The growing interest in RSS-based estimation highlights its usefulness as an alternative sampling framework in both theoretical and applied studies.Khamnei et al. (2022) focused on the exponentiated Pareto distribution, and Shaaban (2023) studied parameter estimation for the inverted topp–Leone distribution under different RSS variants. Gul (2023) examined the Lomax distribution under RSS using genetic algorithm. Additional related contributions can be found in weighted exponential distribution by Deng and Chen (2024), transmuted inverse Rayleigh distribution by Al-Omari et al. (2025), exponential-Poisson distribution by Chen et al. (2025), Birnbaum-Saunders distribution by Zhang et al. (2025), lognormal distribution by Tiwari et al. (2025) and Gompertz distribution by Gul and Kocer (2025).

In addition to the classical RSS framework, several modified designs have been proposed in the literature to improve efficiency and robustness against ranking errors. Among these, extreme ranked set sampling (ERSS), introduced by Samawi et

al. (1996). Other notable extensions include median ranked set sampling proposed by Muttlak (1997), double ranked set sampling developed by Al-Saleh and Al-Kadiri (2000), and multi-stage ranked set sampling introduced by Al-Saleh and Al-Omari (2002). Furthermore, ranked set sampling has been adapted to incorporate auxiliary or concomitant information, leading to designs such as two-layer ranked set sampling (Chen and Shen, 2003). Additional variants, including moving extreme ranked set sampling (Al-Saleh and Al-Hadrami, 2003) and L-ranked set sampling based on L-statistics (Al-Naseer, 2007), have also been proposed as effective alternatives within the ranked set sampling family. More recently, folded ranked set sampling (FRSS) was introduced by Bani-Mustafa et al. (2011) with the aim of reducing the wastage of sampling units while maintaining high estimation efficiency. By combining information from both lower and upper ranked observations within each cycle, FRSS provides a more balanced utilization of ranked units.

In the folded RSS design, a total of $[(m+1)/2]$ random samples, each of size m are initially drawn from the population. Within each sample, the units are ordered according to the variable of interest using inexpensive ranking procedures such as visual judgment or auxiliary information. Under the FRSS scheme, the selection of units for actual measurement is carried out symmetrically from both ends of the ranked sets. Specifically, the smallest and largest units are measured from the first ranked sample, followed by the second smallest and the $(m-1)$th units from the second sample. This alternating selection pattern continues in a folded fashion until all required ranks are exhausted. Repeating this process over multiple cycles yields a folded ranked set sample of the predetermined size.

The main objective of this work is to investigate the MLE of the unknown parameter of the Unit-Teissier (UT) distribution under different sampling strategies, namely SRS, RSS and FRSS.

The UT distribution is a bounded model obtained from the classical Teissier distribution, which was originally proposed by Georges Teissier to describe mortality behavior in animal populations driven by aging effects. Let X denote a random variable following the Unit–Teissier distribution with parameter θ The corresponding probability density and distribution functions are given by Equations (1) and (2), respectively

$$f(x) = \theta\left(x^{\theta} - 1\right)x^{-(\theta+1)}e^{-x^{-\theta}} + 1, \qquad x\varepsilon(0,1) \tag{1}$$

$$F(x) = x^{\theta}e^{-x^{-\theta}} + 1. \tag{2}$$

To examine the impact of the sampling design on estimation accuracy, a detailed Monte Carlo simulation study is conducted. The performance of the maximum likelihood estimator is evaluated using bias and mean squared error for different combinations of sample sizes and parameter values. Furthermore, a real data example is analyzed to demonstrate the applicability of the proposed estimation procedures and to highlight the comparative performance of SRS, RSS, and FRSS in practice.

2. PARAMETER ESTIMATION

This section presents the MLE of the UT distribution parameter under different sampling designs. The estimation procedures for SRS, RSS and FRSS are discussed in the subsections that follow.

2.1. MLE BASED ON SRS

Consider an independent sample $X_1, X_2, \ldots, X_n$ from the UT distribution with probability density function presented in Eq. (1). The resulting likelihood function for the parameter θ takes the form

$$L(\theta; x) = \theta^n \prod_{i=1}^{n} x_i^{-(\theta+1)} \prod_{i=1}^{n} \left(x_i^{-\theta} - 1\right) e^{-\sum_{i=1}^{n}\left(x_i^{-\theta}-1\right)} \quad (3)$$

and the log likelihood function is

$$l(\theta) = nln(\theta) - (\theta + 1) \sum_{i=1}^{n} \ln(x_i) + \sum_{i=1}^{n} \ln\left(x_i^{-\theta} - 1\right) - \sum_{i=1}^{n}\left(x_i^{-\theta} - 1\right) \quad (4)$$

Then the MLE of θ, say $\hat{\theta}$, is obtained by maximizing $l(\theta)$ with respect to θ. The likelihood equation of θ is given by

$$\frac{dl}{d\theta} = \frac{n}{\theta} - \sum_{i=1}^{n} \ln(x_i) - \sum_{i=1}^{n} \frac{x_i^{-\theta} \log(x_i)}{x_i^{-\theta}-1} + \sum_{i=1}^{n} x_i^{-\theta} \ln(x_i) \quad (5)$$

These equations do not admit closed-form solutions and therefore must be solved using numerical optimization techniques.

2.2. MLE BASED ON RSS

Let $X_{(i:m)j}, i = 1, \dots, m\,; j = 1, \dots, r$ be a RSS from UT distribution with sample size $n=mr$ where m is the set size and r is the number of cycles. We denote $X_{(i:m)j}$ by X_{ij}. Then, the pdf of X_{ij} is given by

$$y\left(x_{ij}\,;\,\theta\right) = \frac{m!}{(i-1)!(m-i)!} f\left(x_{ij};\,\theta\right)\left(F\left(x_{ij};\,\theta\right)\right)^{i-1} \times \left(1 - F\left(x_{ij};\,\theta\right)\right)^{m-i} \quad (6)$$

where $f\left(x_{ij};\,\theta\right)$ is the pdf and $F\left(x_{ij};\,\theta\right)$ is the cumulative distribution function of X. The likelihood function of RSS is given by

$$L(\theta;\,\mathrm{x}) = \prod_{j=1}^{r} \prod_{i=1}^{m} y\left(x_{ij}\,;\,\theta\right) =$$
$$C_1{}^{mr} \theta^{mr} \prod_{j=1}^{r} \prod_{i=1}^{m} \left(x_{ij}^{-(\theta+1)}\left(x_{ij}^{-\theta} - 1\right) e^{-\sum_{i=1}^{n}\left(x_{ij}^{-\theta}-1\right)} + 1\right) \times$$
$$\left(x_{ij}^{-\theta} e^{-x_{ij}^{-\theta}} + 1\right)^{(i-1)} \left(x_{ij}^{-\theta} e^{-x_{ij}^{-\theta}}\right)^{(m-i)} \quad (7)$$

where $C_1 = m!/(m-i)!\,(i-1)!$. The log-likelihood function is

$$l(\theta) = mr\ln(C_1) + mr\ln(\theta) - (\theta+1)\sum_{j=1}^{r}\sum_{i=1}^{m} ln\left(x_{ij}\right) + \sum_{j=1}^{r}\sum_{i=1}^{m} ln\left(x_{ij}^{-\theta}-1\right) - \sum_{j=1}^{r}\sum_{i=1}^{m}\left(x_{ij}^{-\theta}-1\right) + mr - \theta\sum_{j=1}^{r}\sum_{i=1}^{m}(i-1)ln\left(x_{ij}\right) - \sum_{j=1}^{r}\sum_{i=1}^{m}(i-1)x_{ij}^{-\theta} + \sum_{j=1}^{r}\sum_{i=1}^{m}(i-1)mr - \theta\sum_{j=1}^{r}\sum_{i=1}^{m}(m-i)ln\left(x_{ij}\right) - \sum_{j=1}^{r}\sum_{i=1}^{m}(m-i)\left(x_{ij}^{-\theta}\right). \quad (8)$$

The likelihood equation of θ is given by

$$\frac{\partial l}{\partial\theta} = \frac{mr}{\theta} - \sum_{j=1}^{r}\sum_{i=1}^{m} ln\left(x_{ij}\right) + \sum_{j=1}^{r}\sum_{i=1}^{m}\frac{x_{ij}^{-\theta}\ln(x_i)}{x_{ij}^{-\theta}-1} - \sum_{j=1}^{r}\sum_{i=1}^{m} x_{ij}^{-\theta}\ln\left(x_{ij}\right) - \sum_{j=1}^{r}\sum_{i=1}^{m}(i-1)ln\left(x_{ij}\right) - \sum_{j=1}^{r}\sum_{i=1}^{m}(i-1)x_{ij}^{-\theta}\ln\left(x_{ij}\right) - \sum_{j=1}^{r}\sum_{i=1}^{m}(m-i)ln\left(x_{ij}\right) - \sum_{j=1}^{r}\sum_{i=1}^{m}(m-i)x_{ij}^{-\theta}\ln\left(x_{ij}\right) = 0. \quad (9)$$

2.3. MLE BASED ON FRSS

The FRSS sample can be constructed as $X = \left\{X_{(i)j}, i = 1,2,\dots,\frac{m+1}{2}; j = 1,\dots,r\right\} \cup \left\{X_{(m-i+1)j}, i = 1,2,\dots,\frac{m+1}{2}; j = 1,\dots,r\right\}$. Based on this sampling scheme, the likelihood function for the UT distribution is expressed as follows:

$$L_f(\lambda,\beta;x) = \prod_{j=1}^{r}\prod_{i=1}^{\frac{m+1}{2}} C_2 f\left(x_{ij};\lambda,\beta\right)\left[F\left(x_{ij};\lambda,\beta\right)\right]^{i-1}\left[1 - F\left(x_{ij};\lambda,\beta\right)\right]^{m-i} \times \prod_{j=1}^{r}\prod_{\substack{i=1\\ i<m-i+1}}^{\frac{m+1}{2}} C_2 f\left(x_{ij(m-i+1)};\lambda,\beta\right)\left[F\left(x_{ij(m-i+1)};\lambda,\beta\right)\right]^{m-i} \times \left[1 - F\left(x_{ij(m-i+1)};\lambda,\beta\right)\right]^{i-1} \quad (10)$$

$$= {C_3}^{mr}\theta^{mr}\prod_{j=1}^{r}\prod_{i=1}^{\frac{m+1}{2}}\left(x_{ij}^{-(\theta+1)}\left(x_{ij}^{-\theta}-1\right)e^{-\sum_{i=1}^{n}\left(x_{ij}^{-\theta}-1\right)} + 1\right)\left(x_{ij}^{-\theta}e^{-x_{ij}^{-\theta}}+1\right)^{(i-1)}\left(x_{ij}^{-\theta}e^{-x_{ij}^{-\theta}}\right)^{(m-i)} \times \prod_{j=1}^{r}\prod_{\substack{i=1\\ i<m-i+1}}^{\frac{m+1}{2}}\left(x_{ij(m-i+1)}^{-(\theta+1)}\left(x_{ij(m-i+1)}^{-\theta}-\right.\right.$$

$$1\Big)e^{-\sum_{i=1}^{n}\left(x_{ij(m-i+1)}^{-\theta}-1\right)}+1\Big)\times\Big(x_{ij(m-i+1)}^{-\theta}e^{-x_{ij(m-i+1)}^{-\theta}}+$$
$$1\Big)^{(m-i)}\left(x_{ij(m-i+1)}^{-\theta}e^{-x_{ij(m-i+1)}^{-\theta}}\right)^{(i-1)} \qquad (11)$$

where $C_3=(C_2)^2=\left(\frac{m!}{(i-1)!(m-i)!}\right)^2$. The log-likelihood function is then given by

$$l(\theta)=mr\ln(C_3)+mr\ln(\theta)-(\theta+1)\sum_{j=1}^{r}\sum_{i=1}^{\frac{m+1}{2}}ln\big(x_{ij}\big)+$$
$$\sum_{j=1}^{r}\sum_{i=1}^{\frac{m+1}{2}}ln\big(x_{ij}^{-\theta}-1\big)-\sum_{j=1}^{r}\sum_{i=1}^{\frac{m+1}{2}}\big(x_{ij}^{-\theta}-1\big)+mr-$$
$$\theta\sum_{j=1}^{r}\sum_{i=1}^{\frac{m+1}{2}}(i-1)ln\big(x_{ij}\big)-\sum_{j=1}^{r}\sum_{i=1}^{\frac{m+1}{2}}(i-1)x_{ij}^{-\theta}+$$
$$\sum_{j=1}^{r}\sum_{i=1}^{\frac{m+1}{2}}(i-1)mr-\theta\sum_{j=1}^{r}\sum_{i=1}^{\frac{m+1}{2}}(m-i)ln\big(x_{ij}\big)-$$
$$\sum_{j=1}^{r}\sum_{i=1}^{\frac{m+1}{2}}(m-i)\big(x_{ij}^{-\theta}\big)-(\theta+$$
$$1)\sum_{j=1}^{r}\sum_{\substack{i=1\\ i<m-i+1}}^{\frac{m+1}{2}}ln\big(x_{ij(m-i+1)}\big)+$$
$$\sum_{j=1}^{r}\sum_{\substack{i=1\\ i<m-i+1}}^{\frac{m+1}{2}}ln\big(x_{ij(m-i+1)}^{-\theta}-1\big)-$$
$$\sum_{j=1}^{r}\sum_{\substack{i=1\\ i<m-i+1}}^{\frac{m+1}{2}}\big(x_{ij(m-i+1)}^{-\theta}-1\big)+mr-\theta\sum_{j=1}^{r}\sum_{\substack{i=1\\ i<m-i+1}}^{\frac{m+1}{2}}(i-$$
$$1)ln\big(x_{ij(m-i+1)}\big)-\sum_{j=1}^{r}\sum_{\substack{i=1\\ i<m-i+1}}^{\frac{m+1}{2}}(i-1)x_{ij(m-i+1)}^{-\theta}+$$
$$\sum_{j=1}^{r}\sum_{\substack{i=1\\ i<m-i+1}}^{\frac{m+1}{2}}(i-1)mr-\theta\sum_{j=1}^{r}\sum_{\substack{i=1\\ i<m-i+1}}^{\frac{m+1}{2}}(m-$$
$$i)ln\big(x_{ij(m-i+1)}\big)-\sum_{j=1}^{r}\sum_{\substack{i=1\\ i<m-i+1}}^{\frac{m+1}{2}}(m-i)\big(x_{ij(m-i+1)}^{-\theta}\big). \qquad (11)$$

The likelihood equation of θ is given by

$$\frac{\partial l}{\partial\theta}=\frac{mr}{\theta}-\sum_{j=1}^{r}\sum_{i=1}^{\frac{m+1}{2}}ln\big(x_{ij}\big)+\sum_{j=1}^{r}\sum_{i=1}^{\frac{m+1}{2}}\frac{x_{ij}^{-\theta}\ln(x_i)}{x_{ij}^{-\theta}-1}-$$
$$\sum_{j=1}^{r}\sum_{i=1}^{\frac{m+1}{2}}x_{ij}^{-\theta}\ln\big(x_{ij}\big)-\sum_{j=1}^{r}\sum_{i=1}^{\frac{m+1}{2}}(i-1)ln\big(x_{ij}\big)-$$

$$\sum_{j=1}^{r}\sum_{i=1}^{\frac{m+1}{2}}(i-1)x_{ij}^{-\theta}\ln\left(x_{ij}\right)-\sum_{j=1}^{r}\sum_{i=1}^{\frac{m+1}{2}}(m-i)ln\left(x_{ij}\right)-$$
$$\sum_{j=1}^{r}\sum_{i=1}^{\frac{m+1}{2}}(m-i)x_{ij}^{-\theta}\ln\left(x_{ij}\right)-$$
$$\sum_{j=1}^{r}\sum_{\substack{i=1\\ i<m-i+1}}^{\frac{m+1}{2}}ln\left(x_{ij(m-i+1)}\right)+$$
$$\sum_{j=1}^{r}\sum_{\substack{i=1\\ i<m-i+1}}^{\frac{m+1}{2}}\frac{x_{ij(m-i+1)}^{-\theta}\ln(x_i)}{x_{ij(m-i+1)}^{-\theta}-1}-$$
$$\sum_{j=1}^{r}\sum_{\substack{i=1\\ i<m-i+1}}^{\frac{m+1}{2}}x_{ij}^{-\theta}\ln\left(x_{ij(m-i+1)}\right)-\sum_{j=1}^{r}\sum_{\substack{i=1\\ i<m-i+1}}^{\frac{m+1}{2}}(m-$$
$$i)ln\left(x_{ij(m-i+1)}\right)-\sum_{j=1}^{r}\sum_{\substack{i=1\\ i<m-i+1}}^{\frac{m+1}{2}}(m-i)x_{ij}^{-\theta}\ln\left(x_{ij(m-i+1)}\right)-$$
$$\sum_{j=1}^{r}\sum_{\substack{i=1\\ i<m-i+1}}^{\frac{m+1}{2}}(i-1)ln\left(x_{ij(m-i+1)}\right)-\sum_{j=1}^{r}\sum_{\substack{i=1\\ i<m-i+1}}^{\frac{m+1}{2}}(i-$$
$$1)x_{ij}^{-\theta}\ln\left(x_{ij(m-i+1)}\right)=0. \qquad (12)$$

Since a closed-form solution is not available, the estimate of θ is obtained by solving the corresponding normal equations.

3. SIMULATION STUDY

Since closed-form expressions for the finite-sample properties of the proposed ML estimators are not available, a Monte Carlo simulation study is performed to assess their performance under different sampling schemes. The study focuses on the estimation of the UT distribution parameter using SRS, RSS and FRSS. The estimators are compared with respect to bias and MSE across a range of sample sizes and parameter configurations. The simulation experiments are carried out in MATLAB with 10,000 replications. The details of the simulation procedure are outlined below.

- SRS of sizes $n = 12, 24, 36, 48$ are generated from the UT distribution. In addition, RSS and FRSS samples are

constructed using different set sizes and numbers of cycles for the same parameter configurations.

- For each generated sample and for each sampling design, the MLE derived in Section 2 is computed to obtain parameter estimates corresponding to the selected sample size.

- The above steps are repeated $N = 10.000$ times. Based on the resulting estimates, the bias and MSE of the estimators are calculated to assess and compare their finite-sample performance.

Table 1. Bias values for the parameter θ.

			$\hat{\theta}_{mle}$		
θ	n	$m;r$	SRS	RSS	FRSS
0.2	12	3;4	0.0095	0.0069	0.0067
		4;3		0.0067	0.0066
		6;2		0.0067	0.0065
	24	3;8	0.0078	0.0064	0.0065
		4;6		0.0063	0.0064
		6;4		0.0063	0.0064
	36	3;12	0.0077	0.0064	0.0064
		4;9		0.0061	0.0063
		6;6		0.0058	0.0061
	48	3;16	0.0075	0.0056	0.0060
		4;12		0.0056	0.0059
		6;8		0.0054	0.0058
0.5	12	3;4	0.0221	0.0175	0.0173
		4;3		0.0168	0.0169
		6;2		0.0167	0.0163
	24	3;8	0.0181	0.0162	0.0160
		4;6		0.0159	0.0161
		6;4		0.0159	0.0160
	36	3;12	0.0177	0.0159	0.0162
		4;9		0.0151	0.0161
		6;6		0.0127	0.0137
	48	3;16	0.0173	0.0149	0.0154
		4;12		0.0142	0.0149
		6;8		0.0141	0.0144
2.0	12	3;4	0.0931	0.0699	0.0666
		4;3		0.0688	0.0671
		6;2		0.0667	0.0661
	24	3;8	0.0765	0.0662	0.0680

		4;6		0.0575	0.0677
		6;4		0.0514	0.0548
		3;12		0.0640	0.0646
	36	4;9	0.0750	0.0535	0.0539
		6;6		0.0543	0.0545
		3;16		0.0611	0.0612
	48	4;12	0.0739	0.0586	0.0595
		6;8		0.0569	0.0580
		3;4		0.1348	0.1345
	12	4;3	0.1759	0.1361	0.1344
		6;2		0.1398	0.1366
		3;8		0.1272	0.1393
	24	4;6	0.1453	0.1277	0.1279
		6;4		0.0997	0.1096
4.0		3;12		0.1273	0.1285
	36	4;9	0.1429	0.1163	0.1274
		6;6		0.1069	0.1272
		3;16		0.1085	0.1231
	48	4;12	0.1416	0.1072	0.1228
		6;8		0.1022	0.1137

Table 2. MSE values for the parameter θ.

				$\hat{\theta}_{mle}$	
θ	n	$m;r$	SRS	RSS	FRSS
		3;4		0.0009	0.0011
	12	4;3	0.0021	0.0008	0.0010
		6;2		0.0008	0.0009
		3;8		0.0007	0.0009
	24	4;6	0.0015	0.0006	0.0008
		6;4		0.0005	0.0008
0.2		3;12		0.0005	0.0007
	36	4;9	0.0009	0.0004	0.0006
		6;6		0.0002	0.0005
		3;16		0.0002	0.0004
	48	4;12	0.0008	0.0001	0.0003
		6;8		0.0001	0.0003
		3;4		0.0015	0.0016
	12	4;3	0.0027	0.0013	0.0016
		6;2		0.0010	0.0011
0.5		3;8		0.0006	0.0007
	24	4;6	0.0015	0.0006	0.0006
		6;4		0.0005	0.0005
	36	3;12	0.0012	0.0005	0.0005

		4;9		0.0005	0.0005
		6;6		0.0005	0.0005
		3;16		0.0004	0.0004
	48	4;12	0.0009	0.0004	0.0004
		6;8		0.0005	0.0005
		3;4		0.0251	0.0272
	12	4;3	0.0447	0.0210	0.0263
		6;2		0.0160	0.0183
		3;8		0.0103	0.0105
	24	4;6	0.0239	0.0090	0.0100
		6;4		0.0082	0.0087
2.0		3;12		0.0076	0.0077
	36	4;9	0.0188	0.0073	0.0077
		6;6		0.0072	0.0074
		3;16		0.0071	0.0072
	48	4;12	0.0154	0.0072	0.0071
		6;8		0.0073	0.0072
		3;4		0.0986	0.1097
	12	4;3	0.1769	0.0803	0.0967
		6;2		0.0622	0.0729
		3;8		0.0399	0.0430
	24	4;6	0.1046	0.0366	0.0411
		6;4		0.0330	0.0342
4.0		3;12		0.0301	0.0320
	36	4;9	0.0932	0.0295	0.0306
		6;6		0.0287	0.0292
		3;16		0.0288	0.0291
	48	4;12	0.0853	0.0286	0.0287
		6;8		0.0289	0.0286

- Across all parameter settings and sample sizes, the ranked set based designs yield clearly improved accuracy relative to SRS. In particular, RSS and FRSS consistently produce smaller absolute biases and markedly lower MSE values than SRS for the same nominal sample size, indicating that incorporating ranking information substantially enhances estimation efficiency under the UT model.

- For each fixed θ both bias and MSE decrease as the sample size increases from $n = 12$ to $n = 48$ reflecting the expected improvement in finite-sample

performance of the MLE. This monotone reduction is especially evident in the MSE values, where the decline is pronounced under SRS and remains visible though at a lower scale under RSS and FRSS, suggesting greater stability of ranked set based estimators even at moderate sample sizes.

- The bias values indicate that both ranked set based sampling designs outperform SRS for all parameter values and sample sizes. Compared with SRS, RSS and FRSS consistently produce smaller bias, confirming the benefit of incorporating ranking information. When RSS and FRSS are compared, RSS generally yields slightly lower bias across most configurations, particularly for small and moderate values of θ. Although the difference between RSS and FRSS is modest, the results suggest that RSS provides the most accurate estimates in terms of bias, while FRSS remains a competitive alternative.
- Compared with FRSS, RSS generally achieves smaller MSE values across most $(m; r)$ configurations, indicating superior overall estimation accuracy when both variance and bias are taken into account. This advantage of RSS is particularly pronounced for larger values of θ where the MSE reduction relative to FRSS becomes more evident. Although FRSS still provides a clear improvement over SRS, the results suggest that RSS offers the most efficient performance in terms of MSE for the MLE of the UT distribution parameter.

4. CONCLUSION

The parameter estimation problem for the UT distribution was studied under SRS and two ranked set based sampling

designs. The comparison focused on the MLE and aimed to evaluate the effect of using ranking information within the sampling process.

The simulation results confirm that incorporating ranking information improves estimation accuracy. In all examined settings, estimators obtained from ranked set based samples exhibit smaller bias and MSE than those based on SRS. The improvement is visible for both small and large sample sizes, indicating that the benefit of ranking is not limited to asymptotic situations.

When the two ranked set based designs are compared, RSS tends to perform better than FRSS in terms of mean squared error. Although FRSS reduces the loss of sampling units and performs well relative to SRS, its estimation accuracy is generally slightly lower than that of RSS, especially for larger parameter values.

In practical applications, these findings suggest that RSS is a suitable choice when estimation accuracy is the main objective. FRSS may still be attractive in situations where operational considerations, such as reducing sample wastage, are important. Further work could explore alternative estimation methods, interval estimation, or other ranked set based designs for the UT distribution and similar bounded models.

REFERENCES

Al-Nasser, A. D. (2007). L unit tesisser: A generalization procedure for robust visual sampling. *Communications in Statistics—Simulation and Computation, 36*(1), 33–43.

Al-Omari, A. I., Benchiha, S. A., & Alomani, G. (2025). Parameter estimation for the transmuted inverse Rayleigh distribution using ranked set sampling: Applications and analysis. *AIMS Mathematics, 10*(7), 16432–16459.

Al-Saleh, M. F., & Al-Hadhrami, S. A. (2003). Estimation of the mean of the exponential distribution using moving extremes ranked set sampling. *Statistical Papers, 44*(3), 367–382.

Al-Saleh, M. F., & Al-Kadiri, M. (2000). Double-ranked set sampling. *Statistics & Probability Letters, 48*, 205–212.

Al-Saleh, M. F., & Al-Omari, A. I. (2002). Multistage ranked set sampling. *Journal of Statistical Planning and Inference, 102*(2), 273–286.

Bani-Mustafa, A., Al-Nasser, A. D., & Aslam, M. (2011). Folded ranked set sampling for asymmetric distributions. *Communications for Statistical Applications and Methods, 18*(1), 147–153.

Chen, M., Chen, W. X., Yang, R., & Zhou, Y. W. (2025). Exponential–Poisson parameters estimation in moving extremes ranked set sampling design. *Acta Mathematicae Applicatae Sinica, English Series, 41*(4), 973–984.

Chen, Z., & Shen, L. (2003). Two-layer ranked set sampling with concomitant variables. *Journal of Statistical Planning and Inference, 115*(1), 45–57.

Deng, C., & Chen, W. (2024). Weighted exponential parameters estimation using maximum ranked set sampling with

unequal samples. *Communications in Statistics—Simulation and Computation*, 1–24. *(Advance online publication)*

Dey, S., Salehi, M., & Ahmadi, J. (2017). Rayleigh distribution revisited via ranked set sampling. *Metron, 75*(1), 69–85.

Esemen, M., & Gürler, S. (2018). Parameter estimation of generalized Rayleigh distribution based on ranked set sample. *Journal of Statistical Computation and Simulation, 88*(4), 615–628.

Gul, H. H. (2023). Parameter estimation of the Lomax distribution using genetic algorithm based on the ranked set samples. *Enterprise Information Systems, 17*(9), 2193153.

Gul, H. H., & Yeniay Koçer, N. (2025). Estimation of the Gompertz distribution's parameters under folded ranked set sampling. *Sigma: Journal of Engineering & Natural Sciences / Mühendislik ve Fen Bilimleri Dergisi, 43*(3).

Hussian, M. A. (2014). Bayesian and maximum likelihood estimation for Kumaraswamy distribution based on ranked set sampling. *American Journal of Mathematics and Statistics, 4*(1), 30–37.

Khamnei, H. J., Meidute-Kavaliauskiene, I., Fathi, M., Valackienė, A., & Ghorbani, S. (2022). Parameter estimation of the exponentiated Pareto distribution using ranked set sampling and simple random sampling. *Axioms, 11*(6), 293.

McIntyre, G. A. (1952). A method of unbiased selective sampling, using ranked sets. *Australian Journal of Agricultural Research, 3*, 385–390.

Muttlak, H. A. (1997). Median ranked set sampling. *Journal of Applied Statistical Science, 6*, 245–255.

Sabry, M. A., & Shaaban, M. (2020). Dependent ranked set sampling designs for parametric estimation with applications. *Annals of Data Science, 7*(2), 357–371.

Samawi, H. M., Ahmed, M. S., & Abu-Dayyeh, W. (1996). Estimating the population mean using extreme ranked set sampling. *Biometrical Journal, 38*(5), 577–586.

Samuh, M. H., & Qtait, A. (2015). Estimation for the parameters of the exponentiated exponential distribution using a median ranked set sampling. *Journal of Modern Applied Statistical Methods, 14*(1), Article 19.

Shaaban, M. (2023). Parameter estimation for inverted Topp–Leone distribution based on different ranked set sampling schemes. *Thailand Statistician, 21*(3), 660–674.

Shaaban, M., & Yahya, M. (2023). Comparison between dependent and independent ranked set sampling designs for parametric estimation with applications. *Annals of Data Science, 10*(1), 167–182.

Teissier, G. (1934). Recherches sur le vieillissement et sur les lois de la mortalité. II. Essai d'interprétation générale des courbes de survie. *Annales de Physiologie et de Physicochimie Biologique, 10*, 260–284.

Tiwari, N., Chandra, G., Bhari, S., & Banerjee, J. (2025). Estimation of location and scale parameters of lognormal distribution using median with extreme ranked set sampling. *Sankhya B, 87*(1), 76–102.

Zhang, J., Chen, W., & Yang, R. (2025). Birnbaum–Saunders parameters estimation using simple random sampling and ranked set sampling. *Communications in Statistics—Simulation and Computation, 54*(9), 3624–3643.

TÜRKİYE VE DÜNYADA

MATEMATİK

yaz
yayınları

YAZ Yayınları
M.İhtisas OSB Mah. 4A Cad. No:3/3
İscehisar / AFYONKARAHİSAR
Tel : (0 531) 880 92 99
yazyayinlari@gmail.com • www.yazyayinlari.com